UNIVERSITÀ DEGLI STUDI DI MILANO
SCUOLA DI DOTTORATO
TERRA, AMBIENTE E BIODIVERSITÀ

Dottorato di Ricerca in Scienze della Terra
Ciclo XXIII

Groundwater vulnerability assessment using statistical methods

Ph.D. Thesis

Alessandro Sorichetta
Matricola R07615

Tutori
Dott. Marco Masetti
Prof. Giovanni P. Beretta

Anno Accademico
2009-2010

Coordinatore
Prof. Stefano Poli

Acknowledgements

First, I want to thank Mel for always bearing, supporting and helping me, she is my life and none of this would have been possible without her.
I am very grateful to Marco Masetti for being always available with his constant support and inspiring guidance all throughout my Ph.D. studies, for all the friendly and very fruitful discussions, and especially for allowing me to formulate my own ideas yet providing me with insightful comments and constructive criticisms.
I also want to express my sincere gratitude to Professor Giovanni Pietro Beretta for what he taught me, for his endless encouragement, suggestions, and contagious enthusiasm.
Mostly I want to deeply thank both of them for giving me the opportunity to work with them, for their confidence in me and for everything they have done for me.
A special thank goes to Simone Sterlacchini and Andrea Taramelli for all they did when I arrived in Milan and for their contribution to my scientific activities.
Thanks also to Cristiano Ballabio, Andrea Chahoud, Marco Marcaccio, Marianna Bonfanti, Matteo Pozzi, and Jan Blahut for their precious contribution to this Thesis.
Next thanks go to Tiziana Apuani, Professor Gianpaolo Giani, Alessio Conforto, Andrea Merri, Daniele Pedretti, Corrado Camera, Federica Ferrari and Alberto Francioli.
I owe a lot to Yuri Gorokhovich, Deborah Balk, Leonardo “Nano” Seeber and Son Nghiem.
Others people I wish to thank are Chris Small, Mark Becker, Greg Yetman, Bridget Anderson, Hans Bosh, Saleh Ghani, Cecilia McHugh, Marie-Helene “Milene” Cormier, Jim Cochran, Roger Buck, Mike Steckler, Jon Barbour, Monia Santini, Ezio Crestaz, Anna Spinaci and Roberto Capancioni.
The last thank goes to all my friends I have around the world and to the ones I grow up with at home in Montegiorgio.
The very last and greatest thank goes to my family, especially my parents Enzo and Rita, and to Mel's family for their love, their support, and everything they did for us over the years.

Contents

Chapter 1
Introduction

On July 28, 2010 the United Nations General Assembly, with 122 votes in favor to none against and 41 abstentions, adopted a historical resolution recognizing access to clean water and sanitation as a human right (UN, 2010a). The passed text on "The human right to water and sanitation" (UN, 2010b) clearly states that: "The General Assembly, (omissis) Deeply concerned that approximately 884 million people lack access to safe drinking water and that more than 2.6 billion do not have access to basic sanitation, and alarmed that approximately 1.5 million children under 5 years of age die (omissis) each year as a result of water- and sanitation-related diseases, Acknowledging the importance of equitable, safe and clean drinking water and sanitation as an integral component of the realization of all human rights, (omissis) Bearing in mind the commitment made by the international community to fully achieve the Millennium Development Goals, and stressing, in that context, the resolve of Heads of State and Government, as expressed in the United Nations Millennium Declaration, to halve, by 2015, the proportion of people unable to reach or afford safe drinking water, and to halve the proportion of people without access to basic sanitation, as agreed in the Plan of Implementation of the World Summit on Sustainable Development ("Johannesburg Plan of Implementation"),

- Declares the right to safe and clean drinking water and sanitation as a human right that is essential for the full enjoyment of life and all human rights;
- Calls upon States and international organizations to provide financial resources, capacity-building and technology transfer, through international assistance and cooperation, in particular to developing countries, in order to scale up efforts to provide safe, clean, accessible and affordable drinking water and sanitation for all;
- (omissis)."

Freshwater represents about 2.5% of all water on earth and is mostly trapped in glaciers and snow packs, leaving only 0.77% of it available for being used (Shiklomanov, 1993). Groundwater accounts for about 98% of the available freshwater (about 0.76% of all water on earth) whereas the remaining 2% is present as surface water (i.e., streams and lakes) and

distributed in the soil and atmosphere (Shiklomanov, 1997). Thus, not surprisingly, in many regions of the world groundwater represents the main, if not the only, source of drinking water, especially where surface water resources are limited and/or contaminated to some degree (WHO, 2006). Some of these regions however are rapidly depleting their aquifers, consuming groundwater faster than it is naturally replenished (Postel, 1993), and population growth is expected to stress water availability even more in the near future (Shiklomanov, 1999), especially in underdeveloped and developing countries where most of the people already being unable to access safe drinking water are located (Bidlack et al., 2004). To further complicate this matter, it has to be considered that all aquifers are vulnerable to contamination to some degree (NRC, 1993) and that, once groundwater is contaminated, its remediation is very challenging, costly, time-consuming, and sometimes even unfeasible (e.g., USEPA, 1990).

In such context, it is clear the importance of developing and adopting, at national and international level, an integrated water resources management approach (GWP, 2000) in which groundwater quality protection must be one of the first aspects to be considered in order to tackle the problem of global freshwater scarcity (WHO, 2004 and previous editions).

To effectively and properly protect groundwater, it is crucial being able to identify areas where groundwater may be most vulnerable to contamination and translate this information into vulnerability maps that can be used by potential end-users, such as land and water-resources managers, to prevent or minimize harmful impacts on groundwater quality (Arthur et al., 2007). To this end, various methods, based on different approaches and using diverse input parameters, have been developed to perform groundwater vulnerability assessment. However, in order to be considered effective tools to be used in environmental planning and management, the end-products of such methods (i.e., groundwater vulnerability maps) must be scientifically sound, meaningful and reliable. In fact, a groundwater vulnerability map must allow taking scientifically defensible decision to protect groundwater resources, must represent the study area through a limited number of vulnerability classes consenting to meet policy and management objectives, and must depict the actual spatial distribution of the contamination in the study area (Focazio et al., 2002).

To this regard, the use of statistical methods to assess groundwater vulnerability represents a reasonable compromise, among model complexity and costs, in order to produce scientifically defensible end-products (Focazio et al., 2002). Indeed, statistical methods provide the possibility, over various spatial scales, ranging from catchment (e.g., Worral and Kolpin, 2003) to sub-national (e.g., Arthur et al, 2007) and national (e.g., Nolan, 2001), to objectively identify the

factors influencing the vulnerability in the study area and to quantify the uncertainty inherent in the assessment. Nevertheless, it has to be highlighted that the meaningfulness of their outputs is not always straightforward and that additional interpretation is often required to obtain functional (reclassified) vulnerability maps (Focazio et al., 2002), which reliability need to be careful addressed before being used in environmental planning and management. Thus, as also stated by Fabbri and Chung (2008), at present the research effort in this field should primarily be aimed not at implementing new statistical modeling techniques but rather at evaluating the robustness of the already available ones and the reliability of their end-products (i.e., reclassified groundwater vulnerability maps).

1.1 Purpose of this study

Mostly using the Weights of Evidence (WofE) modeling technique, the main purpose of this study was to define its strength as exploratory and predictive tool and address more general issues associated with the use of statistical methods, modeling binary-response variables, for assessing groundwater vulnerability.
In particular, this study allowed to:

- evaluate the robustness of the WofE modeling technique in accurately assessing groundwater vulnerability and its strength in appropriately selecting the explanatory variables (i.e., predictor factors) to be used in the statistical analysis;
- develop an objective semi-guided procedure to generalize the evidential themes (representing the selected explanatory variables) to be used as inputs in the WofE model;
- suggest a suitable method to reclassify statistical model outputs (initially expressed as relative probability maps) in order to obtain meaningful groundwater vulnerability maps (henceforth referred as “reclassified maps”);
- observe that even reclassified maps being apparently similar in terms of predictive power can exhibit poor agreement in terms of predicted vulnerability spatial pattern;
- suggest a series of validation techniques that can be used to estimate the reliability of the reclassified maps;

- evaluate the effect of using different threshold values, to distinguish between positive and negative evidences of contamination, on the predicted vulnerability spatial pattern and on the importance of each considered predictor factor in influencing groundwater vulnerability;
- identify limits and drawbacks of statistical methods, highlighting possible new challenges.

1.2 Study areas

The WofE modeling technique was used for assessing groundwater vulnerability to nitrate contamination in two study areas characterized by very different hydrogeological settings and land use conditions, both located in Italy within the Po Plain area (Fig. 1.1), classified as a Nitrate Vulnerable Zone by the European Union since 1991 (EU, 1991):

- the porous shallow unconfined aquifer located in the Province of Milan (panel A on the left in Fig. 1.1), Lombardia Region;
- the porous shallow mixed (confined-unconfined) aquifer located within the Province of Piacenza (panel B on the right in Fig 1.1), Emilia-Romagna Region.

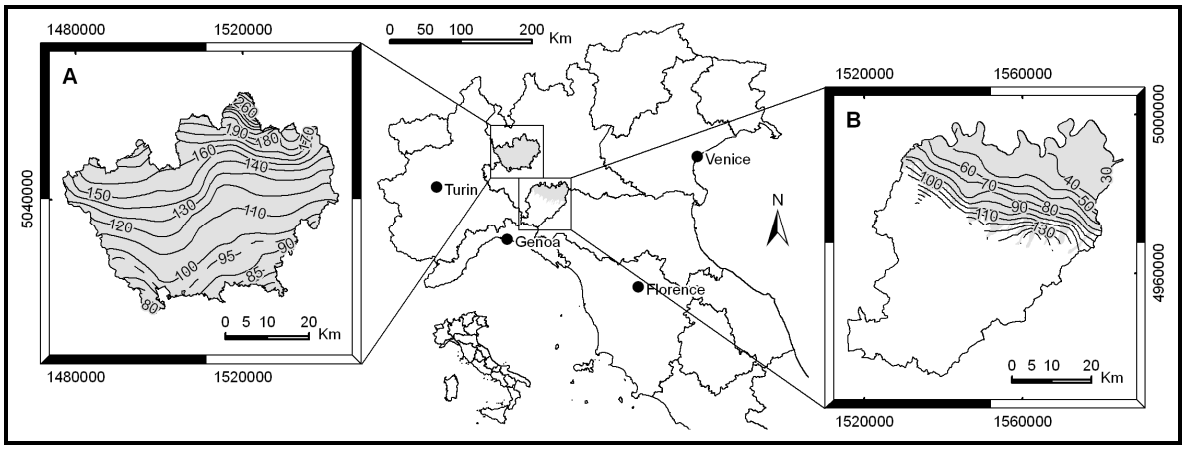

Figure 1.1 – Location and piezometric levels of the two porous shallow aquifers (light grey areas) considered in this study.

Chapter 2
Groundwater vulnerability

The term “vulnerability” indicates the degree to which a system is likely to experience harm due to perturbation or stress. Vulnerability can be conceptualized in different ways in different fields, or even within the same field (Füssel, 2007), and can be identified for a given system exposed to a specific hazard or to a group of hazards (Brooks, 2003).

When considering an aquifer system exposed to a potential source of contamination, the concept of vulnerability has to be derived from the assumption that soil and aquifer characteristics may provide some degree of protection, especially against sources located on the land surface (WHO, 2006).

Although the concept of groundwater vulnerability is obviously central in assessing the relative ease with which troublesome concentrations of contaminants could reach groundwater (Worrall and Besien, 2005), at present there is no single standardized definition for it (Liggett and Talwar, 2009). Indeed, hydrogeologists have failed to reach a consensus concerning the definitions of groundwater vulnerability and consequently also to provide a reference term for groundwater vulnerability assessment (Gogu and Dassargues, 2000). Furthermore, within the scientific community, there is still an on-going debate about whether groundwater vulnerability should be considered as an intrinsic property of the aquifer, being only a function of its chemical and physical characteristics, or whether it should be considered also as a function of contaminant properties (Liggett and Talwar, 2009). To this regard, however, it has to be pointed out that, at present, the general concept of groundwater vulnerability entailing the two notions of intrinsic and specific vulnerability is widely recognized and considered useful by most hydrogeologists.

Nevertheless, it is important to be aware that a clear distinction between intrinsic and specific vulnerability is not always possible (NRC, 1993), and that, even when explicitly referring to either one or the other, several different definitions exist.

2.1 Definitions of groundwater vulnerability

One of the first definitions of groundwater/aquifer vulnerability that can be found in the literature is the one from Albinet and Margat (1970) that described it as “the penetrating and spreading abilities of the pollutants in aquifers according to the nature of the surface layers and the hydrogeological conditions”.

Since then, the concept of groundwater vulnerability has considerably evolved (Popescu et al, 2008) and many other definitions have been proposed.

Civita (1987) defined the intrinsic (i.e., natural) aquifer vulnerability to contamination as “the specific susceptibility of aquifer systems, in their parts, geometric and hydrodynamic settings, to receive and diffuse fluid and/or hydro-vectored contaminants, the impact of which, on the groundwater quality, is a function of space and time”.

Foster (1987) defined aquifer pollution vulnerability as “the intrinsic characteristic which determine the sensitivity of various parts of an aquifer to begin adversely affected by a contaminant load”.

The US Environmental Protection Agency (1993) first distinguished between aquifer sensitivity and groundwater vulnerability, respectively as independent and dependent on land-use and contaminant properties. Accordingly, aquifer sensitivity was defined as “the relative ease with which a contaminant (in this case a pesticide) applied on or near the land surface can migrate to the aquifer of interest as a function of the intrinsic characteristics of the geological materials of interest, any overlying unsaturated zone”; groundwater vulnerability as “the relative ease with which a contaminant (in this case a pesticide) applied on or near the land surface can migrate to the aquifer of interest under a given set of agronomic management practices, pesticide characteristics and hydrogeologic sensitivity conditions”.

The US Committee on Techniques for Assessing Ground Water Vulnerability (NRC, 1993) acknowledged that “vulnerability assessments may or may not account for different behaviors of different contaminants” and, exclusively referring to contamination resulting from non-point sources and/or areally distributed point sources of pollution, defined groundwater vulnerability to contamination as ”the tendency or likelihood for contaminants to reach a specified position in the groundwater system after introduction at some location above the upper most aquifer”.

Vrba and Zoporozec (1994) explicitly introduced the concepts of “relative, non measurable and dimensionless” in the definition of groundwater vulnerability identified as an “intrinsic property

of a groundwater system, depending on the sensitivity of that system to human and/or natural impacts". Consequently, intrinsic vulnerability was defined as a "relative, non measurable and dimensionless property of the groundwater cover, determined by its thickness, the lithologic properties of the vadose zone, the aquifer properties and the recharge"; specific vulnerability as "the vulnerability of groundwater to certain pollutants taking into account land use practices".

Most recently, the working group of the European COST Action 620 (EU, 2003), in an effort to develop "an improved and consistent European approach for the protection of karst groundwater", agreed that "the intrinsic vulnerability of groundwater to contaminants takes into account the geological, hydrological and hydrogeological characteristics of an area, but is independent of the nature of the contaminants and the contamination scenario", while "the specific vulnerability takes into account the properties of a particular contaminant or group of contaminants and its (their) relationship(s) to the various aspects of the intrinsic vulnerability of the area". Hence, the terminology proposed by the European COST Action 620 (EU, 2003) simply identifies what has to be considered when referring to intrinsic and specific vulnerability; without indicating the possibility of a quantitative assessment (Voigt et al., 2004) or including the concepts of "relative, non measurable and dimensionless" introduced in the definition by Vrba and Zoporozec (1994) and earlier discussed by the NRC (1993).

At this point, it is obvious that groundwater vulnerability represents an ambiguous concept (Stigter, 2006; Frind, et al., 2006) that probably cannot be easily defined in a unique and rigorous way (Daly et al., 2002).

Thus, from a practical point of view, in absence of a standard and unanimously accepted definition, when performing a groundwater vulnerability assessment it is extremely important to:

- carefully establish the objectives that must be achieved;
- explicitly refer to the definition of groundwater vulnerability to be used;
- select the proper assessment method according to the established objectives and the adopted definition.

This has to be done in order to avoid misunderstandings in the interpretation of the results and a consequently improper use of them.

2.2 Groundwater vulnerability assessment methods

Bearing in mind that groundwater vulnerability is not a physical property measurable in the field (NRC, 1993) and that "some areas are more vulnerable to groundwater contamination than others" (Vrba and Zaporozec, 1994), according to Gogu and Dassargues (2000) vulnerable areas can be divided in:

- naturally vulnerable areas where neither the soil/subsoil nor the bedrock provide an adequate protection against groundwater contamination (e.g., recharge areas of shallow aquifer);
- well-protection zones where contaminant can quickly reach and mix with the pumped groundwater;
- potential problem areas (e.g., areas being close or coincident to/with non-point or aerially distributed point sources of contamination).

Considering the type of parameters being used to assess groundwater/aquifer vulnerability to contamination, three main approaches can be identified (Gogu and Dassargues, 2000):

- an approach accounting only for soil and vadose zone properties without considering any transport process within the saturated zone (in this case, the assessment is clearly limited to the relative probability that troublesome concentrations of contaminants reach the saturated zone);
- an approach in which groundwater flow and contaminant transport processes within the saturated zone are considered to some extent (mostly used to delineate well-protection zones);
- an approach accounting for soil, vadose zone, saturated zone, and contaminant properties.

Then, all groundwater/aquifer vulnerability assessment methods, based on the above described approaches, can be divided in two major groups (Focazio et al., 2002; Arthur et al., 2007):

- subjective methods (also referred as knowledge-driven models);
- objective methods (also referred data-driven models).

2.2.1 Subjective methods

Subjective methods include overlay and index methods and hybrid methods producing subjective categorization of the vulnerability. Overlay and index methods can be divided in two main categories (Gogu and Dassargues 2000):

- Hydrological Complex and Settings methods (HCS);
- Parametric System methods (including Matrix System, Rating System, and Point Count System Models).

2.2.1.1 HCS methods

HCS methods are generally used to assess groundwater/aquifer vulnerability at spatial scale ranging from medium (e.g., Ferrara, 1990) to broad (e.g., Margat, 1968). Such methods are primarily based on the identification of homogeneous zones in terms of being characterized by similar hydrogeological, hydrographical and/or geomorphological settings. The degree of vulnerability of each homogeneous zone is then qualitatively evaluated considering the relative importance of each setting in influencing groundwater vulnerability.
An example of HCS method is the GNDCI-CNR basic method (Civita, 1987) that provides a qualitative description of the main hydrogeological settings that can be found in Italy, along with their corresponding degree of intrinsic vulnerability. Lithological, structural, piezometric and hydrodynamic indexes were used to identify the main hydrogeological settings later characterized by the main factors controlling groundwater vulnerability (e.g., depth to groundwater, porosity, fracturing index, karst index, linkage between stream and aquifer). At this point, taking into account the dynamics and the frequency of groundwater contamination in Italy and abroad, a different degree of vulnerability distributed over six classes, ranging from null/very low to extremely high, was assigned to each hydrogeological setting previously identified.

2.2.1.2 Parametric System methods

Parametric system methods include Matrix System (MS), Rating System (RS), and Point Count System Models (PCSM). All these methods are based on quite similar procedures that, relying on expert judgment, allow assessing the degree of vulnerability of zones that can be considered homogeneous in terms of unique combinations of classes of different parameters.

In general, the parameters to be used are subjectively selected, arranged in classes and somehow rated in an effort to reflect their importance in controlling groundwater vulnerability in the study area.

Matrix System methods take into account a restricted and carefully selected number of parameters being arranged into classes, rated and then combined following diverse strategies specifically developed for local case studies (e.g., Gossens and Van Damme, 1987; Carter et al., 1987).

Rating System methods take into account a variable numbers of parameters (depending on the considered method) being arranged into properly predefined classes, rated using a fixed range of values divided according to the variation interval of the considered parameter, and then combined in a predefined way in order to obtain vulnerability indexes corresponding to different degrees of vulnerability.

The GOD and AVI method are two examples of RS methods, both based on the assumption of considering a generic contaminant.

The GOD method (Foster, 1987) takes into account three parameters: the groundwater occurrence, the depth to groundwater, and the lithology of the overlying layers (considered only in the case of unconfined aquifer). Parameter are arranged into classes, rated and combined according to the scheme in Figure 2.1 in order to calculate, for each homogeneous zone, the vulnerability index expressing the corresponding degree of vulnerability.

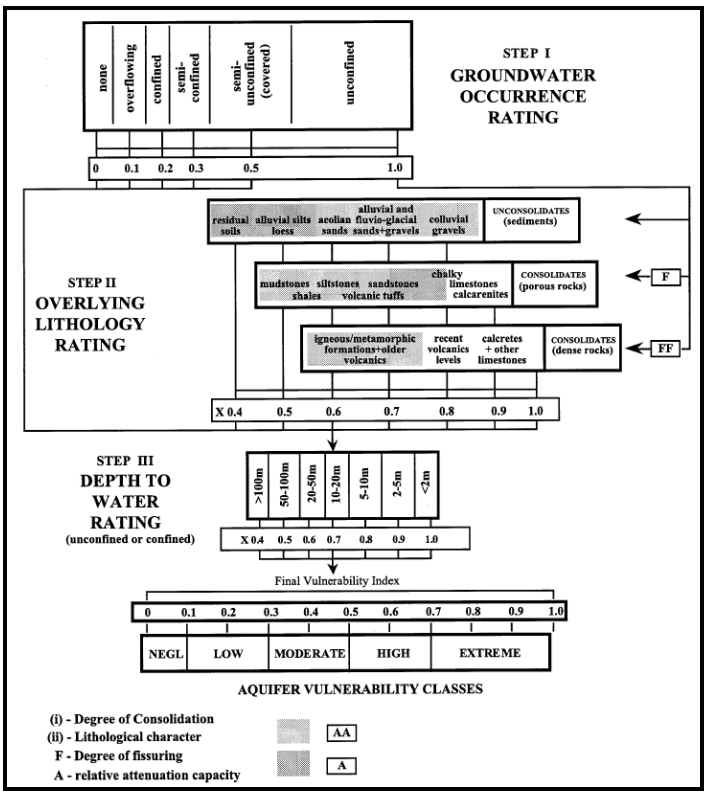

Figure 2.1 – The GOD method scheme (from Foster, 1987).

The AVI method (Van Stempvoort et al., 1993) takes into account only two parameters: the thickness and the estimated hydraulic conductivity of each sedimentary layer above the saturated zone.

The two parameters are used to calculate the hydraulic resistance, c, for each homogeneous zone as:

$$c = \sum_{i=1}^{n} (d_i / k_i) \qquad (2.1)$$

where d_i and k_i are respectively the thickness and the hydraulic conductivity of the layer i.

The hydraulic resistance, c, is then related to a qualitative aquifer vulnerability index by a relationship table allowing to obtain different AVI zones, each one characterized by a different degree of vulnerability.

Point Count System Models (also known as Parameter Weighting and Rating methods) are RS methods that introduce the use of weight factors, usually referred as weight strings, to correctly reflect the relative importance of each considered parameter in controlling groundwater vulnerability with respect to specific land use practices and/or hydrogeological conditions.

The DRASTIC method (Aller et al., 1987), developed by the US EPA, is the worldwide most used method to assess groundwater vulnerability at various scale, ranging from national (Kellogg et al., 1997) to township (Shukla et al., 2000). The DRASTIC method assumes that the contaminant is applied on the surface, that is introduced in the aquifer system by precipitation and that has the mobility of the water. It takes into account seven parameters: Depth to water, net Recharge, Aquifer media, Soil media, Topography, Impact of vadose zone media, and Hydraulic Conductivity of the aquifer. To each class of each considered parameter is assigned a rate ranging from 1 to 10 following predefined schemes such as the one in Table 2.1.

Class	Rating	Typical Rating
Massive Shale	1-3	2
Metamorphic/Igneous	2-5	3
Weathered Metamorphic/Igneous	3-5	4
Glacial Till	4-6	5
Bedded Sandstone, Limestone and Shale Sequences	5-9	6
Massive Sandstone	4-9	6
Massive Limestone	4-9	6
Sand and Gravel	4-9	8
Basalt	2-10	9
Karst Limestone	9-10	10
DRASTIC Weight 3 – PESTICIDE DRASTIC Weight 3		

Table 2.1 – Ranges and rating for the parameter aquifer media (modified from Aller et al., 1987).

The DRASTIC method provides two weight strings, one to be used for general conditions and another for intensive cultivated areas (generally referred as PESTICIDE DRASTIC; Table 2.1).

For each homogeneous zone the DRASTIC vulnerability index, Di, is computed as:

$$D_i = \sum_{j=1}^{7} (W_j / R_j) \qquad (2.2)$$

where Wj is the weighting factor for the parameter j and Rj is the rating value for the parameter j.

The DRASTIC index, D_i, ranging from 23 to 226, is then usually divided in intervals, each one corresponding to a different degree of vulnerability. Several modifications of the original DRASTIC method, such as fuzzy DRASTIC (Shouyu and Guangtao, 2003) and visual DRASTIC (Bojorquez-Tapia et al., 2009), have been proposed by different authors, mainly in order to obtain improved results.

The SINTACS method (Civita, 1994) considers seven parameters: Depth to groundwater (Soggiacenza), effective infiltration (Infiltrazione), unsaturated zone attenuation capacity (Non saturo), soil/overburden attenuation capacity (Tipologia della copertura), hydrogeologic characteristics of the aquifer (Aquifero), hydraulic Conductivity range of the aquifer (Conducibilità), and hydrologic role of the topographic slope (Superficie topografica). To each class of each considered parameter is assigned a rate ranging from 1 to 10 following predefined schemes such as the one in Figure 2.2.

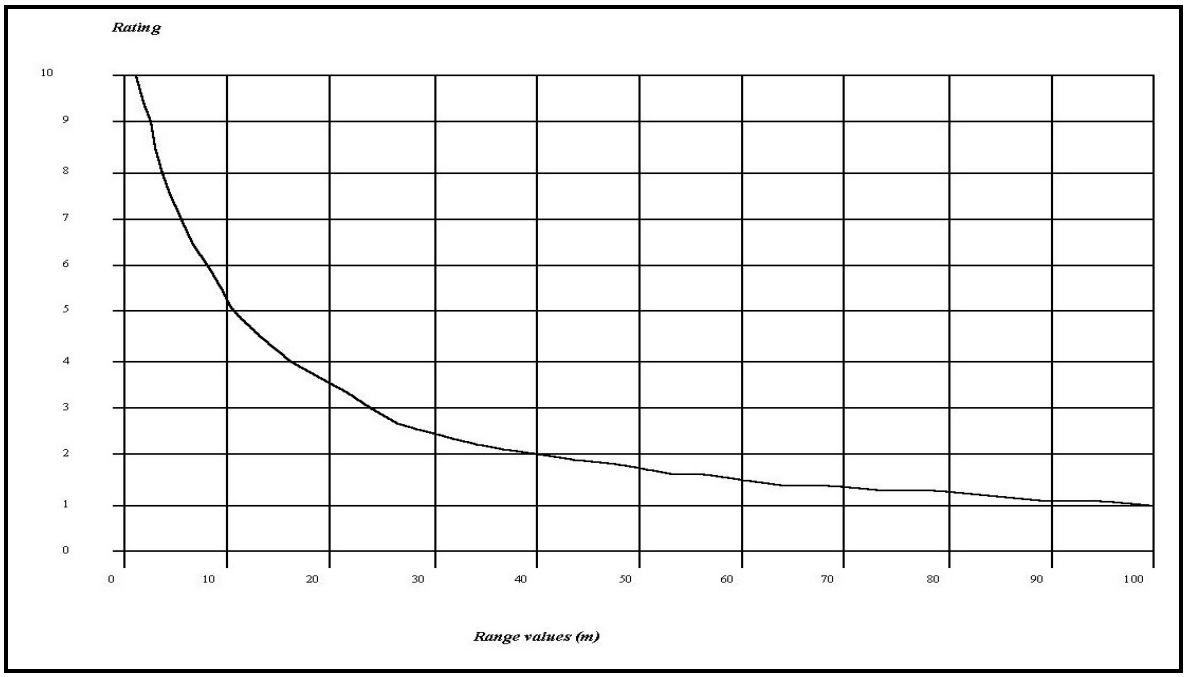

Figure 2.2 – Ranges and rating for Depth to water (from Civita and De Maio, 2004).

The SINTACS method provides five different weight strings, which can be used in series or in parallel, for a specific hydrogeological and land use condition/situation, allowing considering the

different influence of each parameter in five different hydrogeological and land use situations. For each homogeneous zone the SINTACS vulnerability index, I_v, is computed as:

$$D_i = \sum (P_{(1,7)} \times W_{1,n}) \quad (2.3)$$

where $P_{(1,7)}$ is the rating of each parameter, $W_{(1,n)}$ is the associated weight, and *n* is the number of weight strings used.

The SINTACS index, ranging from 26 to 260, is then divided in 6 intervals, each one corresponding to a different degree of vulnerability (Civita, 1994) varying from null/very low to extremely high.

The EPIK method (Doerfliger and Zwahlen, 1997) was specifically developed to assess groundwater vulnerability in karst hydrogeological contexts. It considers four parameters: Epikarst, Protective cover, Infiltration conditions and Karst network development. To each class of each considered parameter is assigned a rate and a predefined weight string is used to balance their importance.

The EPIK vulnerability index, *Fp*, is computed as:

$$F_p = (3 \times E_i) + (1 \times P_j) + (3 \times I_k) + (2 \times K_l) \quad (2.4)$$

where E_i is the rating value for the epikarst parameter, P_j is the rating value for the protective cover parameter, I_k is the rating value for the infiltration condition parameter, and K_i is the rating value for the karst network development parameter.

The EPIK index, ranging from 9 to 34, is then divided in 3 intervals each one corresponding to a different degree of vulnerability (high, medium and low); a forth degree, corresponding to very low vulnerability, is identified by the presence of a soil protective cover of thick detrital having very low hydraulic conductivity and a minimum thickness of 8 meters.

2.2.1.3 Subjective hybrid methods

Subjective hybrid methods combine different components of Overlay and Indexing methods and statistical and physically process-based methods in order to produce subjective, usually project-specific, categorization of the vulnerability.
An example of subjective hybrid methods is “the Italian combined approach” method (Civita and De Maio, 2004) that combine the SINTACS (Civita, 1994) and the GNDCI-CNR basic method (Civita, 1987) in order to cover vast areas where the SINTACS alone cannot be used due to lack of data.

2.2.2 Objective methods

Objective methods produce objective, normally site specific, categorizations of groundwater vulnerability and include:

- physically processed-based methods;
- statistical methods;
- hybrid methods (mostly physically processed-based methods that include statistical components to model complex physical and chemical processes).

2.2.2.1 Physically process-based methods

Physically process-based methods either simulate or consider one or many physical and chemical processes of groundwater flow and the fate and transport of potential associated contaminants in order to somehow assess groundwater vulnerability (Focazio et al., 2002).
Thus, they comprise the use of both deterministic process-simulation models and physically-based techniques such as direct field observations of environmental tracers and/or isotopic analyses, mostly used to determine source and age of groundwater (e.g., Coplen et al., 1999).
Deterministic models include analytical and/or numerical solutions of mathematical equations that are usually solved through computer programs such as SEEP, MODFLOW and/or SWAT.

Physically process-based methods are typically applied at small scales, mostly to define well-protection zones, rather than to assess groundwater vulnerability at broader scales (Frind et al., 2006).

2.2.2.2 Statistical methods

Statistical methods range from the use of simple descriptive statistics (e.g., Welch et al., 2000) to more complex techniques, such as regression (e.g., Eckardt and Stackelberg, 1995) and conditional probability analyses (e.g., Alberti et al, 2001; Worral and Besian, 2005; Masetti et al., 2009), allowing to objectively determine the importance of each predictor factors in influencing/controlling the vulnerability.

Statistical methods correlate, at various spatial scale, contaminant occurrences within a given study area with intrinsic properties of the aquifer system and potential sources of contamination in an attempt to predict contaminant concentrations (e.g., Gardner and Vogel, 2005) or probabilities of contamination, with respect to one (e.g., Tesoriero and Voss, 1997) or more thresholds (Muller et al., 1997; Greene et al., 2004; Masetti et al., 2009).

When enough water quality data are available, Logistic Regression analysis (Hosmer and Lameshow, 1989) is the most common statistical method used for assessing groundwater vulnerability in terms of probability of contamination occurrences.

The basic assumption is that the natural logarithm of the odds ratio is linearly related to the considered explanatory variables (Afifi and Clark, 1984). Thus, once identified the statistically significant explanatory variables ($p<0.05$), probability P that contaminant concentration exceed a given threshold, expressed as the log of its odds ratio, ($P/1–P$), can be computed as:

$$\log(P/(1-P)) = b_0 + \sum_{i=1}^{n} b_i X_i \qquad (2.5)$$

where b_0 is a scalar parameter (intercept), b_i is a statistically derived coefficient (slope) and X_i is the value of the i explanatory variable.

2.2.3 Discussion

Aquifer/groundwater vulnerability can be assessed using different methods ranging from simple, qualitative, and relatively inexpensive to rigorous, quantitative, and costly approaches. The best method to be chosen for assessing vulnerability should be a function of the spatial scale, cost (data availability), time, scientific defensibility, and acceptable uncertainty in relation to the requirements of the end-user.

However, groundwater vulnerability assessment should maintain objectivity with an appropriate level of complexity and an acceptable uncertainty. Moreover, objective methods should be preferred because, being based on ground data and not on expert opinion, help to scientifically defend end-user decisions (Focazio et al., 2002).

At present, overlay and index methods are the methods most commonly used to assess groundwater/aquifer vulnerability mostly because they are relatively easy to implement and require a limited amount of data. Despite almost every year a new method of such type is developed and proposed (Popescu et al, 2008), their results can be questioned because they rely more on expert opinion than on actual hydrogeological process (Frind et al., 2006). Moreover, overlay and index methods present a number of proved significant flaws as showed, among others, by Rosen (1994), Rupert, (2001) and Stigetr et al. (2001). Indeed, final vulnerability maps obtained using such methods showed large discrepancies between predicted vulnerability pattern and the actual spatial distribution of the contamination. Also, Gogu et al. (2003) and Frind and Martin (2004) showed that using different index and overlay methods on the same study area dramatically dissimilar results are obtained.

One of the main limitations is that even using weight strings to balance the importance of each parameter in controlling the vulnerability, the rating score to be assigned to each class of each parameter and thus their correlation with the vulnerability is pre-constituted, regardless of specific contaminants or hydrogeological conditions of the study area.

For example, while increasing depth to water is considered to inhibit contamination and thus in all the index and overlay method described above the rating score increase with decreasing of the depth to water, using different statistical methods, Nolan (2001) and Masetti et al. (2007) found that in shallow aquifer, both in US and in Milan, nitrate contamination is positively correlated with increasing of depth to water. Although counterintuitive, such correlation can be explained in the case of nitrate contamination, by the fact that, as showed in Figure 2.3, other organisms could outcompete the nitrifying organisms in the shallower part of the aquifer.

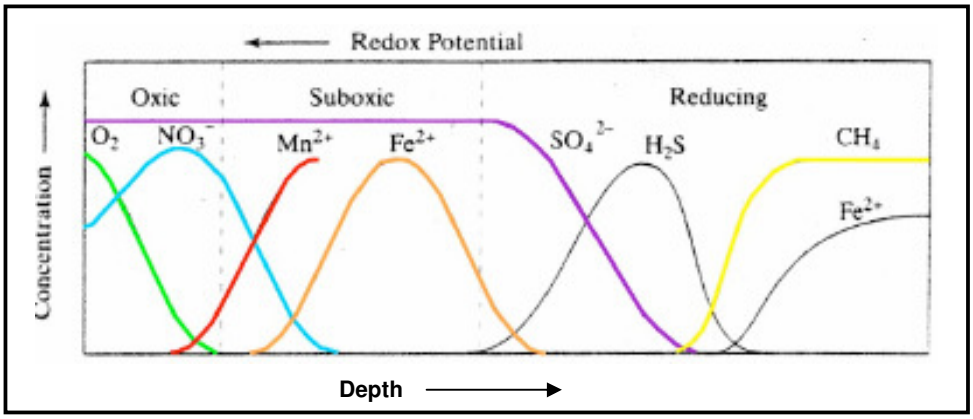

Figure 2.3 – Changes in concentration of redox parameters (modified from Appello and Postma, 1996).

Another explanation could be that shallow depth to water creates anoxic condition and thus promote denitrification (Nolan, 1999).

Thus, in terms of scientifically defensibility, both physically process-based and statistical method should be preferred.

However, although physically process-based are able to provide the most accurate representation of interacting physical and chemical processes controlling groundwater vulnerability, they are very complex to use and their use is limited at small scale. Furthermore, it has to be considered that results of physically process-based methods rely on model assumption, that such methods produce reliable results only when a large amount of data is available and that even in this case uncertainty of the results is very difficult to determine (Focazio et al., 2002). Moreover, physically process-based methods even if extremely useful to highlight the most important factors controlling groundwater vulnerability (e.g., Holtschlag and Luukkonen, 1997) they can account only for one or few processes controlling it (Focazio et al., 2002).

In conclusion, when comparing statistical methods to both subjective and physically process-based methods, the formers present several advantages that can be summarized as follow:

- statistical methods are based on field observations (and thus, neither on expert/professional judgment nor on model assumptions);
- can be successfully used to assess groundwater vulnerability over various spatial scales ranging from catchment to national;
- allow to objectively identify the most appropriated explanatory variables controlling groundwater vulnerability in the study area;

- can easily combine multiple information derived from multiple sources of information and different in type, accuracy, and survey scale;
- are developed in a probabilistic framework allowing to evaluate the uncertainty of the results;
- can be easily updated as new information become available;
- allow to readily test the results against further observations;
- allow to test the consistency of the assumptions made in building the conceptual model;
- ultimately, help land and water-resources managers to defend their decisions.

Nevertheless, even when using statistical methods care must be always taken in the selection of the parameters to be used and in testing and interpreting the results. Indeed, assumption and simplification of the conceptual model or inadequate description of the hydrogeological system (i.e., of the considered parameters) could greatly affect the reliability of the results and thus of the final (i.e. reclassified) groundwater vulnerability maps.

To this regard, it is important to draw attention to the fact that the best way to evaluate the reliability of a groundwater vulnerability map, is not to analyze the consistency of the results obtained using different methods as suggested in Stigter et al. (2006), but rather to validate them against field observations (i.e., concentrations of a given contaminant, or group of contaminants, measured in the field).

2.3 Use of groundwater vulnerability maps

The first attempt to produce groundwater vulnerability map was made in France by Margat (1968), with the intention to show where contamination was more likely to occur as a function of different hydrogeological settings.

Both the NCR (1993) and Vrba and Zaporozec (1994) demonstrate the useful role of groundwater vulnerability maps in protecting groundwater. Indeed, although vulnerability maps represent the vulnerability as a relative value and not in terms of an absolute value, when reliable, they are able to provide key information allowing planning land use and human activities in general as an integral part of an overall environmental policy including groundwater protection.

The importance of groundwater vulnerability maps was then implicitly reaffirmed by the water framework directive of the European Union (EU, 2000) requiring to characterize catchments areas in order to evaluate "to what extent the groundwater bodies are used and the risk is as high that they not fulfill the targets for each individual groundwater body in accordance with article 4 (environmental targets)".

In this context however, it has to be highlighted that groundwater vulnerability maps are intended for identify and thus reduce the number of situations needing a deeper investigation and never should be used to substitute or avoid specific site analysis.

Chapter 3
The Bayes' Theorem and Weights of Evidence (WofE)

Bayes' Theorem, named after Reverend Thomas Bayes (1702–1761), describes how new information can be used to update probability estimates (Bayes, 1763).

As a logical consequence of the product rule of probability, Bayes' Theorem assumes that, given two events A and B, the probability of the two events happening is equal to the conditional probability that the event A happens given that the event B has already happened (henceforth just conditional probability of A given B) multiplied by the unconditional probability that the event B happens (henceforth just unconditional probability of B) and to the conditional probability of B given A multiplied by the unconditional probability of A.

Mathematically, the probability of A and B both happening, $P\{A \cap B\}$, can be written as:

$$P\{A \cap B\} = P\{A|B\} \times P\{B\} = P\{B|A\} \times P\{A\} \tag{3.1}$$

where $P\{A|B\}$ is the conditional probability of A given B, $P\{B\}$ is the unconditional probability of B, $P\{B|A\}$ is the conditional probability of B given A and $P\{A\}$ is the unconditional probability of A.

Thus, considering the event A, the conditional (or posterior) probability of A given B can be expressed as a function of a new evidence, $P\{B|A\}$, and of a previous knowledge, $P\{A\}$, and can be written as:

$$P\{A|B\} = P\{B|A\} \times P\{A\}/P\{B\} \tag{3.2}$$

where $P\{B|A\}$ is called the likelihood, $P\{A\}$ is the prior probability of A and $P\{B\} \neq 0$ acts as a normalizing constant.

Nowadays, various methods based on the Bayes' Theorem are used in many disciplines to combine evidences to test hypotheses. Since early 1970s, Bayes' Theorem was successfully used in quantitative medical diagnosis to combine clinical evidences in order to predict disease or/and

determine genetic predisposition (e.g., Lusted, 1968; Aspinall and Hill, 1983 and subsequent editions; Spiegelhalter and Knill-Jones, 1984). Later on, Aspinall (1992) and then Tucker at al. (1997) among others, used modeling procedures based on Bayes' Theorem in ecology for spatial pattern analysis.

Similarly, in geosciences, a Bayesian non-spatial method, mostly relying on expert opinion, was initially applied in mineral exploration to combine geological and geochemical evidences to predict deposit occurrences (e.g., Reboh and Reiter, 1983; McCammon, 1989) and then implemented within a Geographic Information System (GIS) environment in order to combine evidence in map form. More recently, different methods based on the Bayes' Theorem were also used in many other fields of earth and environmental sciences including landslides susceptibility assessment (e.g., Gritzner et al., 2001; Lee et al., 2002) and groundwater vulnerability assessment (e.g., Alberti et al., 2001; Worrall and Basien, 2005).

In particular, if enough survey data are available, the Bayes' Theorem is commonly applied in his log-linear form, data-driven model, known as Weights of Evidence (WofE), in order to objectively estimate the relative importance of multiple evidences in influencing the occurrence of an event (Bonham-Carter, 1994).

3.1 The WofE modeling technique

When using the WofE modeling technique, the importance of each considered evidence (i.e., explanatory variable) in the occurrence of an event, is not arbitrary estimated but objectively determined, within a probabilistic framework, through the calculation of weights representing the existing correlation between the observed events and the considered evidences.

The calculation of the weights is described below considering a raster based approach within a GIS environment.

If $N\{T\}$ is the total numbers of pixels T in a given study area and $N\{A\}$ is the number of pixels containing an occurrence A, the prior (unconditional) probability that a pixel contains an occurrence, $P\{A\}$, can be expressed as the density of $N\{A\}$ in the study area (i.e., the probability that a pixel contains an occurrence based only on the total number of occurrences observed within the study area) and thus can be computed as:

$$P\{A\} = \frac{N\{A\}}{N\{T\}} \tag{3.3}$$

Considering a spatial pattern B, being either present or absent within the study area, it is possible to update the prior probability of A, P{A}, as a function of either $P\{B|A\}$ or $P\{\overline{B} \mid A\}$ depending on if B is either present or absent, respectively.

Indeed, according to the Bayes'Theorem, the posterior probability of A given B, $P\{A \mid B\}$, or of A not given B, $P\{A \mid \overline{B}\}$, can be expressed as:

$$P\{A \mid B\} = \frac{P\{A \cap B\}}{P\{B\}} = P\{A\}\frac{P\{B \mid A\}}{P\{B\}} \tag{3.4}$$

$$P\{A \mid \overline{B}\} = \frac{P\{A \cap \overline{B}\}}{P\{\overline{B}\}} = P\{A\}\frac{P\{\overline{B} \mid A\}}{P\{\overline{B}\}} \tag{3.5}$$

where $P\{B|A\}$ and $P\{\overline{B}|A\}$ are, respectively, the likelihood of a pixel of being and not being within the spatial pattern B when it contains an occurrence (i.e., the conditional probability of B given A and of non-B given A, respectively).

Defining the odds probability as $O = P/(1-P)$, then Equations (3.4) and (3.5) can be written in odds formulation as:

$$O\{A \mid B\} = \mathrm{P}\{\mathrm{A} \mid \mathrm{B}\}/1 - \mathrm{P}\{\mathrm{A} \mid \mathrm{B}\} = \mathrm{P}\{\mathrm{A} \mid \mathrm{B}\}/\mathrm{P}\{\overline{\mathrm{A}} \mid \mathrm{B}\} = O\{A\}\frac{P\{B \mid A\}}{P\{B \mid \overline{A}\}} \tag{3.6}$$

$$O\{A \mid \overline{B}\} = \mathrm{P}\{\mathrm{A} \mid \overline{\mathrm{B}}\}/1 - \mathrm{P}\{\mathrm{A} \mid \overline{\mathrm{B}}\} = \mathrm{P}\{\mathrm{A} \mid \overline{\mathrm{B}}\}/\mathrm{P}\{\overline{\mathrm{A}} \mid \overline{\mathrm{B}}\} = O\{A\}\frac{P\{\overline{B} \mid A\}}{P\{\overline{B} \mid \overline{A}\}} \tag{3.7}$$

where $O\{A \mid B\}$ and $O\{A \mid \overline{B}\}$ are the posterior odds probabilities that a pixel contains an occurrence, respectively, depending on if B is either present or absent (i.e., the conditional odds probabilities of A, respectively, given and not given B), and $O\{A\}$ is the prior odds probability that a pixel contains an occurrence (i.e., the unconditional odds probability of A).

It is now possible to define the positive and negative weight, W^+ and W^-, as:

$$W^+ = \log_e \frac{P\{B \mid A\}}{P\{B \mid \overline{A}\}} \tag{3.8}$$

$$W^- = \log_e \frac{P\{\overline{B} \mid A\}}{P\{\overline{B} \mid \overline{A}\}} \tag{3.9}$$

where $P\{B|A\}$ and $P\{B|\overline{A}\}$ are the probabilities that a pixel is within B, respectively, given that it contains and does not contain an occurrence A, while $P\{\overline{B}|A\}$ and $P\{\overline{B} \mid \overline{A}\}$ are the probabilities of a pixel of not being within B, respectively, given that it contains and does not contain an occurrence A.

Hence, equations (3.6) and (3.7) can be rewritten as:

$$\log_e O\{A \mid B\} = \log_e O\{A\} + W^+ \tag{3.10}$$

$$\log_e O\{A \mid \overline{B}\} = \log_e O\{A\} + W^- \tag{3.11}$$

Considering two spatial patterns, B_1 and B_2, it is thus possible to calculate the posterior probability that a pixel contains an occurrence, given that both spatial patterns are present, as:

$$P\{A \mid B_1 \cap B_2\} = P\{A\} \frac{P\{B_1 \cap B_2 \mid A\}}{P\{B_1 \cap B_2\}} \tag{3.12}$$

Considering that A and $\overline{A}$ are the only two mutual exclusive hypotheses, for the law of total probability, the Equation (3.12) can be also expressed as:

$$P\{A\} \frac{P\{B_1 \cap B_2 \mid A\}}{P\{B_1 \cap B_2\}} = \frac{P\{B_1 \cap B_2 \mid A\}}{P\{B_1 \cap B_2 \cap A\} + P\{B_1 \cap B_2 \cap \overline{A}\}} =$$
$$= \frac{P\{B_1 \cap B_2 \mid A\}}{P\{A\}P\{B_1 \cap B_2 \mid A\} + P\{\overline{A}\}P\{B_1 \cap B_2 \mid \overline{A}\}} \tag{3.13}$$

Assuming that B_1 and B_2 are conditionally independent of each other with respect to A, for the multiplication rule of independent events, the numerator and denominator of Equation (3.12) become respectively:

$$P\{B_1 \cap B_2 \mid A\} = P\{B_1 \mid A\}P\{B_2 \mid A\} \tag{3.14}$$

and

$$P\{B_1 \cap B_2\} = P\{B_1\}P\{B_2\} \tag{3.15}$$

Thus, the Equation (3.12) becomes:

$$P\{A \mid B_1 \cap B_2\} = P\{A\}\frac{P\{B_1 \mid A\}P\{B_2 \mid A\}}{P\{B_1\}P\{B_2\}} \tag{3.16}$$

where $\frac{P\{B_1 \mid A\}}{P\{B_1\}}$ and $\frac{P\{B_2 \mid A\}}{P\{B_2\}}$ are two multiplication factors used to update the prior probability of A, *P{A}*, if B_1 and B_2 are both present.

Thus, depending on if B1 and B2 are both present, both absent, the former present and the latter absent or vice versa, the prior probability that a pixel contains an occurrence A, expressed as the $\log_e O\{A\}$, can be respectively updated as:

$$\log_e O\{A \mid B_1 \cap B_2\} = \log_e O\{A\} + W_1^+ + W_2^+ \tag{3.17}$$

$$\log_e O\{A \mid \overline{B}_1 \cap \overline{B}_2\} = \log_e O\{A\} + W_1^- + W_2^- \tag{3.18}$$

$$\log_e O\{A \mid B_1 \cap \overline{B}_2\} = \log_e O\{A\} + W_1^+ + W_2^- \tag{3.19}$$

$$\log_e O\{A \mid \overline{B}_1 \cap B_2\} = \log_e O\{A\} + W_1^- + W_2^+ \tag{3.20}$$

Consequently, considering more than two spatial patterns, B_n, conditionally independent of each other with respect to A, the prior probability that a pixel contains an occurrence A, again expressed as the $\log_e O\{A\}$, can be updated as:

$$\log_e O\{E \mid B_1^m \cap B_2^m \cap B_3^m \ldots B_n^m\} = \log_e O\{A\} + \sum_{j=1}^{n} W_j^m \tag{3.21}$$

where *m* is either a plus (+) or a minus (–) depending on if the prediction spatial pattern, B_n, is either present or absent, respectively.

3.2 Practical aspects of the WofE modeling technique

Thus, the WofE modeling technique can be used to combine diverse spatial data sets in a GIS environment for the purpose of analyzing and describing their interactions and generating predictive models (Bonham-Carter, 1994). WofE can be defined as a data-driven Bayesian method, in a log-linear form, that uses known occurrences of an event (response variables) as training sites (training points) to generate a predictive probability output (response theme) from weighted evidences (evidential themes representing different explanatory variables) influencing the spatial distribution of the occurrences in the study area (Raines, 1999).

An evidential theme is a raster representing a set of continuous or categorical spatial data presumably associated with the location of the occurrences. Ordered evidential themes may have to be generalized prior to carrying out the analysis because of the number and location of the occurrences used as training points (TPs) and the presence of random processes (Arthur et al., 2005). Generalizing an ordered evidential theme means defining the ranges of values that can be grouped into classes having a statistically significant correlation with the TPs.

Hence, TPs are used to calculate the prior probability of occurrence of an event within the study area, the positive and negative weights for all classes of each evidential theme and the posterior probability of occurrence of an event (i.e., the response theme).

Thus, for each given class of each evidential theme, the positive and negative weight, W^+ and W^-, can be, respectively, positive and negative or negative and positive, depending on whether in the given class there are more or fewer TP than would be expected by chance.

The contrast, C, of each class of each evidential theme, calculated as the positive minus the negative weight, represents the overall degree of spatial association between the class itself and the TPs and is a measure of the class usefulness in predicting the location of the TPs (Raines, 1999).

The confidence value (C divided by its standard deviation) corresponds approximately to the statistical levels of significance and provides a useful measure of the significance of the contrast (Raines, 1999).

It is important to highlight that the posterior probability represents the relative probability that a pixel contains an occurrence based on the evidences provided by the evidential themes, meaning that a pixel of a higher posterior probability is more likely to contain an occurrence than a pixel

of a lower one (Raines, 1999). Thus, the posterior probability does not represent the actual probability that a pixel contains an occurrence.

In this study, the WofE modelling technique was applied within the Environmental Systems Research Institute (ESRI) ArcMap 9.2 environment using the Spatial Data Modeller (SDM) software (Sawatzky et al., 2008).

3.3 Application fields of the WofE modeling technique

The Weights of Evidence (Bonham-Carter et al., 1989) has been successfully applied both in geosciences and in many other fields such as archaeology (Duke and Steele, 2010), ecology (Romero-Calcerrada and Luque, 2006), wildfire (Romero-Calcerrada et al., 2008) and epidemiology (Lynen et al., 2007). Applications in geosciences have mainly focused on mineral exploration and resource appraisal (Agterberg et al. 1993; Raines and Mihalasky 2002; Cheng 2004; Corsini et al. 2009), landslide hazard zonation (Lee et al. 2002; Poli and Sterlacchini, 2007; Dahal et al. 2008), and groundwater quality/vulnerability assessment (Alberti et al., 2001; Arthur et al., 2007; Masetti et al., 2007, 2008). Other applications in geosciences include the evaluation of risk of slope failure in open mines (Nelson et al., 2007) and most recently the evaluation of ground subsidence spatial hazard near abandoned underground coal mines (Oh and Lee, 2010).

Chapter 4
Hydrogeological setting

Both areas considered in this study are located in northern Italy within the Po Plain and present very different hydrogeological settings both considering the type of shallow aquifers being present (unconfined in the Province of Milan and mixed within the Province of Piacenza), their thickness and scale.

4.1 Shallow aquifer in the Province of Milan

The first study area covers approximately 2000 km^2 and is coincident with the administrative Province of Milan (Fig. 4.1). From the hydrogeological point of view, the Milan plain is characterized by the presence of several aquifers with various degrees of mutual interaction. Moreover, conditions of superficial recharge are complex because of the presence of an extensive irrigation network and a great number of different soils and land use types.

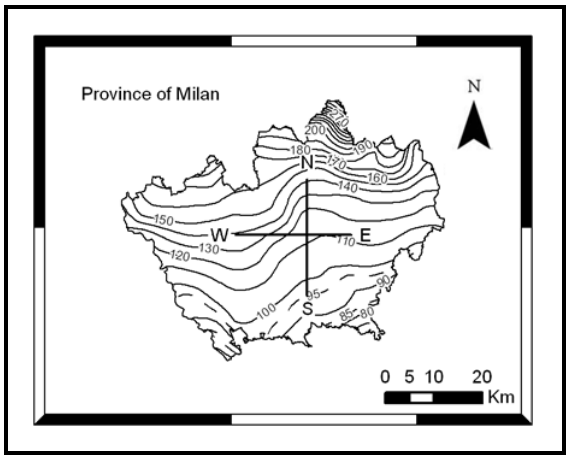

Figure 4.1 – Study area coincident with the Province of Milan, piezometric levels of the shallow aquifer, and location of the hydrogeological sections in Figure 4.4.

The Milan plain subsoil is characterized by Pliocene-Pleistocene sediments that represent considerable groundwater resources. The upper units of this stratigraphic sequence are of alluvial and/or alluvial-glacial origin (constituted by gravels and sands with few interbedded layers of silt and clay) whereas the deeper units are of sea origin (mostly constituted by clay and silt). Toward the end of the Pliocene the Alpine orogenic processes promoted the sea regression and created a delta-lagoon environment where sedimentation was characterized by fine sediments alternated with coarse materials. During Quaternary, the rivers flowing out from the southern borders of the glacial moraines deposited the coarse sediments constituting the upper units of the stratigraphic sequence. In general, the presence of clay and silt in the study area increases not only with the depth but also from north to south due to the fact that the quaternary rivers progressively lost their transport energy southward away from the glacier.

The groundwater flow is generally oriented north-south toward the base level represented by the Po River, while is influenced by the drainage effect of the Ticino and Adda Rivers near the eastern and western boundary of the study area, respectively (Fig 4.1). The groundwater depth decreases from north to south, ranging from values higher than 50 to less than 5 meters (becoming null in correspondence of many natural springs in the south called “fontanili”).

4.1.1 Hydrogeological setting of the study area in the Province of Milan

According to the classification based on the study conducted by the Regione Lombardia and Eni Divisione Agip (2002), four major hydrogeological units, each one delimitated at the bottom by a regional unconformity stratigraphic surface, can be identified in the study area.

Figure 4.2 allow to correlate such four hydrogeological units, denominated Group A, Group B, Group C, and Group D from the shallower to the deeper one, with other classifications derived from previous studies (e.i., Martinis and Mazzarella, 1971; Francani and Pozzi, 1981; Avanzini et al., 1995).

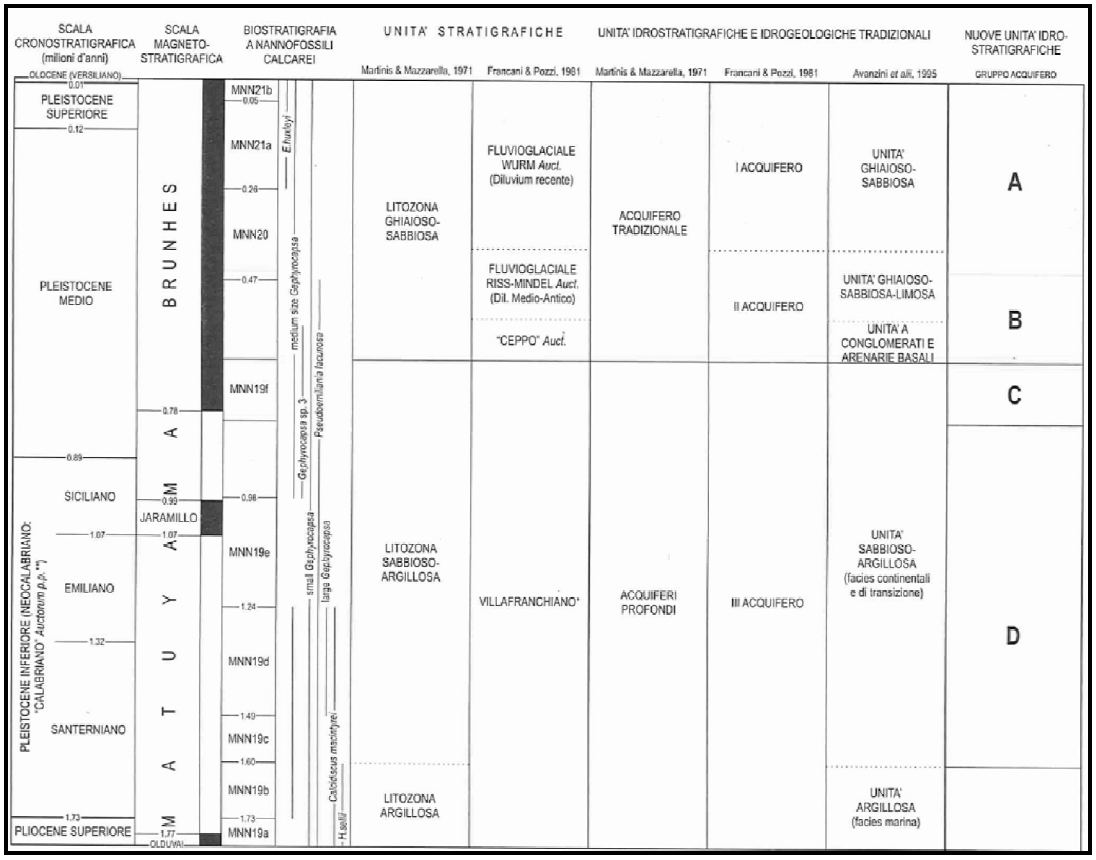

Figure 4.2 – Stratigraphic relationships among the hydrogeological units identified in different studies (from Regione Lombardia and Eni Divisione Agip, 2002).

- The Group A identifies aquifers mainly constituted by medium-to-very-thick layers of polygenic coarse gravel and pebbles, from gray to yellowish-grey, in a medium-to-coarse sandy matrix. Few yellow layers constituted by medium-to-very-coarse (often pebbly) sand are interbedded. The Group A has an average thickness of 60 meters and is characterized by high values of hydraulic conductivity (ranging from 10^{-4} to 10^{-3} m/s) and transmissivity (usually higher than 10^{-2} m^2/s). Just northward the city of Milan two subgroups (A1 and A2) can be distinguished within the Group A, according to the grain size and the stratigraphical position:

  - the Subgroup A1 constituted by coarse and slightly sandy gravel, unconfined all over the study area;
  - the Subgroup A2 constituted by coarse-to-fine sand with interbedded silty layers, semi-confined or confined in the study area.

The Group A is separated from the underlying Group B by a clay-silt layer, of variable thickness and of continuous extension over the study area.

- The Group B identifies aquifers, totally confined in the study area, mainly constituted by gravel and medium-coarse sand in a sandy matrix. Limited to the lower part of the aquifer, very few silty-clay and silty layers, of thickness ranging from few decimeters to few meters, are interbedded. At the bottom of the Group B it is possible to find conglomerates locally slightly cemented and the "Ceppo" (an autochthon kind of conglomerate). The Group B has almost the same average thickness (40-50 meters) of the Group A but, due to the higher presence of clay and silt, it is characterized by lower values of hydraulic conductivity (ranging from 10^{-5} to 10^{-4} m/s) and transmissivity (ranging from 10^{-3} to 10^{-2} m^2/s). Considering the characteristics of the aquifers being part of the Group B three subgroups (B1, B2 and B3) can be distinguished:

  - the subgroup B1 identifying a higher unconfined aquifer;
  - the subgroup B2 identifying a lower confined aquifer;
  - the subgroup B3 constituted by conglomerates.

- The Group C (lower part of the Middle-Pleistocene) is constituted by sediments from marine and transitional environments. Sediments of the continental shelf are constituted by sandy-silty clay and fossiliferous grey clay; sediments of the coastal environment are constituted by fossiliferous, laminate or massive, bioturbated, fine-to-very-fine grey sand, and by medium-to-thick strata of laminate, medium well-sorted grey sand containing organic matter. The Group C is characterized by a variable thickness incresing southward (ranging from 100 meters in the northern part to 1000-1200 meters in the southern one) and low values of both hydraulic conductivity (ranging from 10^{-6} to 10^{-5} m/s) and transmissivity (usually lower than 10^{-3} m^2/s). No subdivisions are identified within the Group C.

- The Group D is represented by facies coarsening upward and is constituted by silty-clay and silt interbedded by thin layers of fine and very fine sand at the base, medium and fine bioturbated grey sand in the middle part, and polygenic grey gravel alternating with sand at the top. As for the Group C, no subdivisions are identified within the Group D.

Below the Group D there are Upper and Middle Pliocene sediments, which top is located at about 700 meters below the sea level, essentially constituted by clay.

As can be inferred also from the hydrogeological sections in Figure 4.3, the subdivision in Aquifer Groups is easier to be identified in the area coincident with the middle and low plain. Indeed, in the high plain and in the area coincident with the hilly zones, characterized mainly by fluvial terraces, the hydrogeologic setting results more complex and some of the Groups described above could not be present everywhere. For example, the Group A may be absent in correspondence of ancient terraces while being present only in the valley of the main rivers.

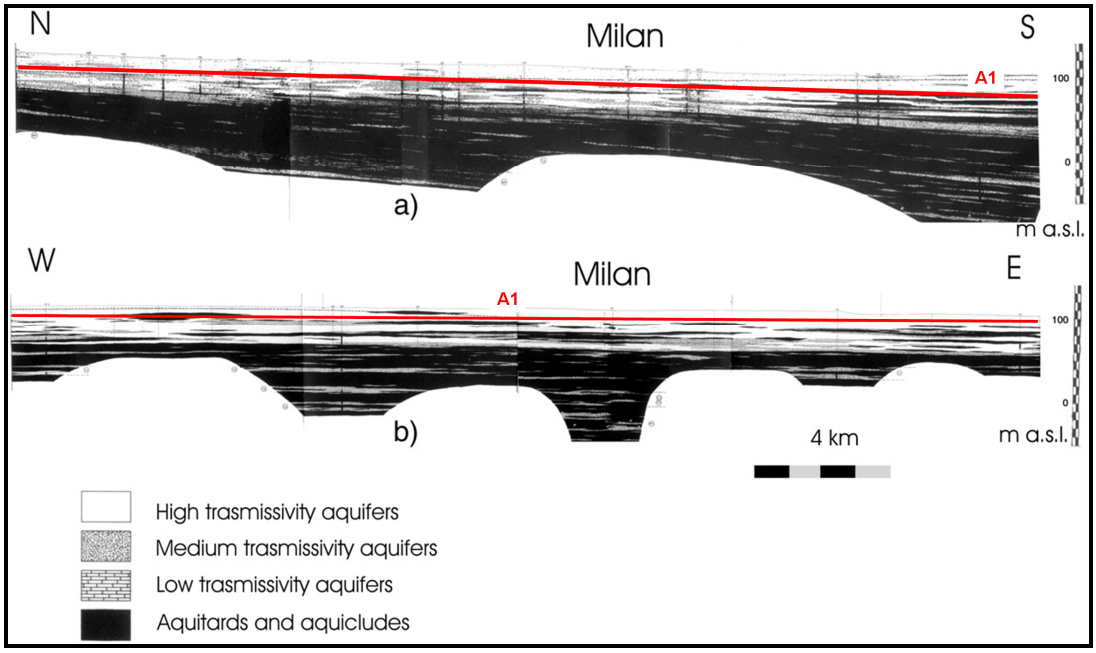

Figure 4.3 – Hydrogeological sections with N-S and W-E direction through the study area in Figure 4.1 (modified from Provincia di Milano and Politecnico di Milano, 1995).

The Subgroup A1 or the corresponding shallow unconfined aquifer in the northern part of the study area (Fig. 4.3) is the portion of aquifer that was used in this study to assess the groundwater vulnerability to nitrate contamination.

4.2 Shallow aquifer within the Province of Piacenza

The second study area is located in a sector of the southern Po Plain close to the Appennine domain an it is located within with the administrative Province of Piacenza and covers approximately 1000 km^2 (Fig. 4.4).

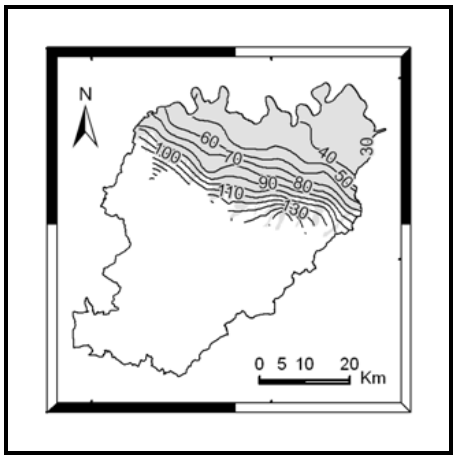

Figure 4.4 – Study area (light-grey) within the Province of Piacenza and piezometric levels of the shallow aquifer.

This area contains in a relative short distance the complete evolution of an alluvial aquifer, from the high energy sedimentary environment close to the hilly recharge sectors to the low energy domain of the Po River.

The groundwater flow is generally oriented south-north toward the base level represented by the Po River, which acts as a completely efficient draining boundary in the southern sector of the area.

4.2.1 Piacenza hydrogeological setting

According to the conceptual model elaborated by Regione Emilia Romagna and Eni divisione Agip (1998), three major overlapping hydrostratigraphic units, each one of thickness up to few hundred meters, can be identified in the study area.

These units, named Aquifer Group A, B and C from the top to the bottom, respectively, can be subdivided into 14 units of lesser rank (Fig. 4.5) with a thickness ranging from few tens to about a hundred meters. The maximum thickness of the entire aquifer is about 600 meters.

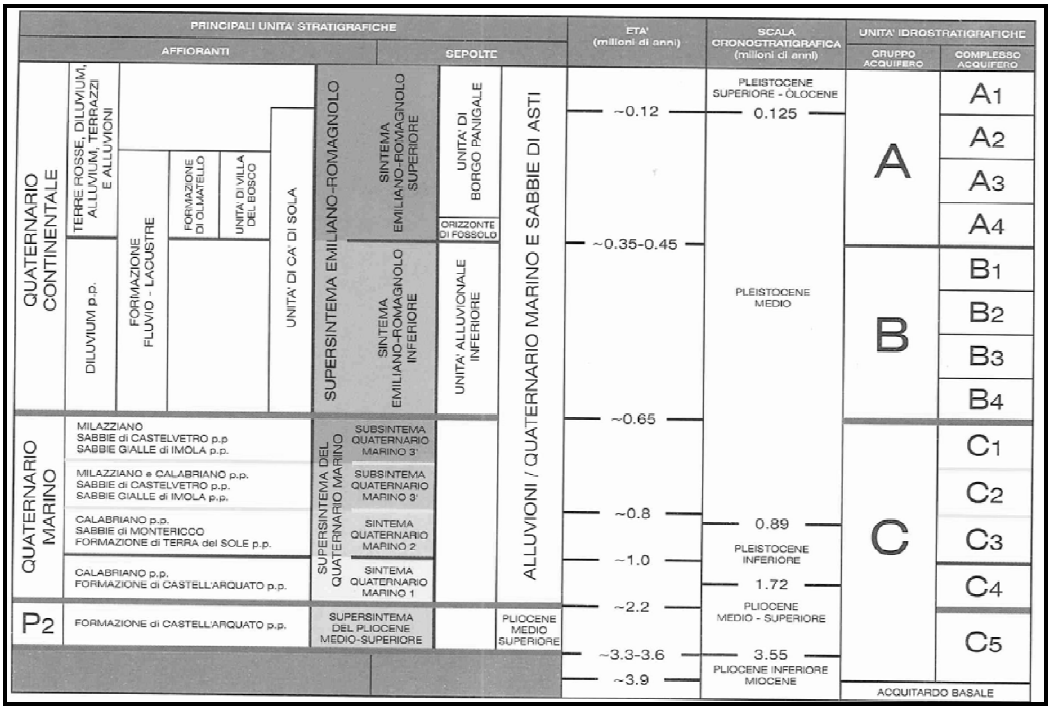

Figure 4.5 – Stratigraphic and hydrogeological setting of the study area in Figure 4.4 (from Regione Emilia Romagna and Eni Divisione Agip, 1998).

- The Aquifer Group A is mainly constituted of alluvial deposits and can be subdivided into four main subunits denominated Aquifer Complexes (A1, A2, A3, and A4). Within each Aquifers Complex, grain sizes fine upwards and it is possible to identify a lower and an upper portion constituted mainly of fine and course sediments, respectively. In addition to the four subunits described above it has to be noted that a fifth subunit, denominated Aquifer Complex A0, can be discontinuously identified above the Aquifer Complex A1. The Aquifer Complex A0, having an average thickness up to 25 meters, is constituted of non-continuous sandy lens and is often connected with the superficial water bodies.
- The Aquifer Group B is mainly constituted of alluvial deposits and can be subdivided into four Aquifer Complexes (B1, B2, B3, and B4).

- The Aquifer Group C is constituted of marine and coastal sediments and can be subdivided in five Aquifer Complexes (C1, C2, C3, C4, and C5).

All Aquifer Groups described above extend through two different hydrogeological domains being, approximately form south to north, the one constituted of multiple Appennine alluvial fans and the one represented by the alluvial Po plain (Fig. 4.6).

Thus, in the southern part of the study area, in correspondence of the Appenine alluvial fans, the sediments are mainly constituted of coarse gravel deposited by the Appenine rivers. In this area, the gravel deposits belonging to the different subunits (i.e., Aquifer Complexes) can be welded together, forming an unconfined single-layer aquifer of thickness ranging from few tens to hundreds of meters. This sector corresponds to the main recharge area of the whole aquifer (interdigitated fans). Otherwise, especially in the distal part of the alluvial fans, the gravel deposits can be distributed in extensive tabular bodies, covered and separated by layers of fine sediments, and thus forming a confined or semi-confined multi-layer aquifer (multi-layered fans). Above the gravel deposits and not connected with them, it is possible to find the unconfined aquifer previously identified as the Aquifer Complex A0. Moving northward, away from the Appennine toward the Po River, the thickness of the layers constituted of fine sediments increases considerably and the gravel deposits are gradually replaced by non-continuous thin sand deposits (which thickness is up to few meters). They become thicker (up to 20-30 meters) and very continuous within the alluvial Po plain (i.e., in the area close to the Po river).

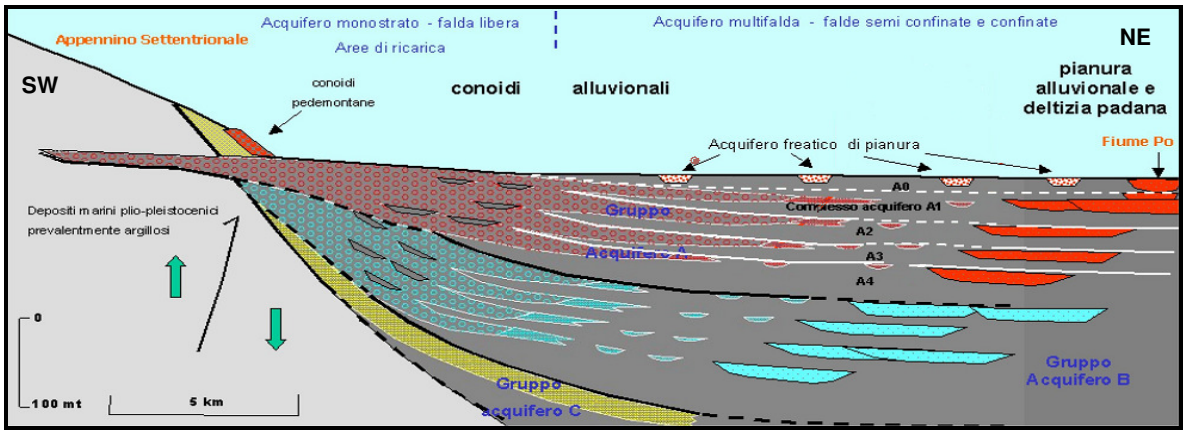

Figure 4.6 – Schematic representation of a hypothetical hydrogeological section with SW-NE direction through the study area in Figure 4.4 (modified from Regione Emilia-Romagna, 2009).

Thus, if not considering the Aquifer Complex A0 and the southernmost area of the floodplain coincident with the apical part of the alluvial interdigitated fans, the aquifer located within the study area can be defined as a confined or semi-confined multilayer aquifer, with each Aquifer Complex having different quantitative and qualitative characteristics. Considering the Aquifer Complex having similar quantitative and qualitative characteristics and referring to the 2000/60/CE and 2000/118/CE Directives, the entire aquifer was divided into two portions, each one subject to a different degree of antrophogenic impacts and representing two different paleogeographic contexts:

- un upper portion constituted by the Aquifer Complexes A1 and A2;
- a lower portion constituted by the Aquifer Complexes A3 and A4 as well as the Aquifer Groups B and C.

The upper aquifer portion identified above (Aquifer Complex A1 and A2) is the one that was used in this study to assess the groundwater vulnerability to nitrate contamination.

Chapter 5
Response and explanatory variables

The choice of using nitrate concentration as the response variable was based on the fact that, from an ideal point of view, when assessing groundwater vulnerability by statistical techniques the indicator of contamination should be ubiquitously present in the study area in relation to homogeneously distributed non-point sources. To this regard, Spalding and Exner (1993) suggested that nitrate may be the most ubiquitous and persistent contaminant in groundwater worldwide and thus a perfect candidate to be used as an environmental indicator of groundwater vulnerability to contamination (Tesoriero and Voss, 1997).

Moreover, it was considered that elevated concentrations of nitrate are usually caused by anthropogenic activities (e.g., domestic sewage disposal, crop fertilization, and animal breeding) extensively present in both study areas.

From the hydrogeological conceptual model of each study area the most important variables thought to being important in controlling nitrate contamination of shallow groundwater were considered for being included in the analysis.

5.1 Response variables

Nitrate contamination of shallow groundwater, both within the Province of Milan and the Province of Piacenza, is monitored by a monitoring network constituted of more than 300 and about 40 wells, respectively.

5.1.1 Monitoring of the shallow aquifer in the Province of Milan

As part of the groundwater monitoring program carried out by the Province of Milan between 2000 and 2002, one shallow-groundwater sample per well was collected in 2000, 2001, early 2002, and late 2002 through four different surveys. Basic descriptive statistics (Table 5.1) reveal that, during the entire considered monitoring period, the nitrate-contamination spatial pattern of

the shallow aquifer (identified as the Subgroup A1 described in Chapter 4, Paragraph 4.1) remained almost unchanged.

Survey	Year	No. of wells	Nitrate concentration					Skewness
			Min	Max	Mean	Median	Std. Dev.	
1	2000	324	0.9	71.0	22.6	21.0	15.0	0.56
2	2001	323	0.8	63.0	22.5	19.5	15.1	0.43
3	Early 2002	307	1.0	70.0	22.4	20.0	15.3	0.36
4	Late 2002	249	1.0	52.0	21.5	20.0	14.1	0.42

Table 5.1– Basic descriptive statistics of water-quality dataset collected in 2000, 2001, early 2002 and late 2002.

The most impacted sector is located in the north-eastern part of the study area (Fig. 5.1), where concentrations exceed 50 mg/l, even if almost the whole northern sector shows values equal to or greater than the guide value of 25 mg/l. Nitrate concentration progressively decreases from north to south where values are consistently lower than 10 mg/l. it is interesting to note how the southward inflexion of the isoconcentration curves located in the correspondence of the city of Milan (light-grey area in Fig. 5.1) represents a local anomaly within the spatial distribution of groundwater nitrate concentration in the study area.

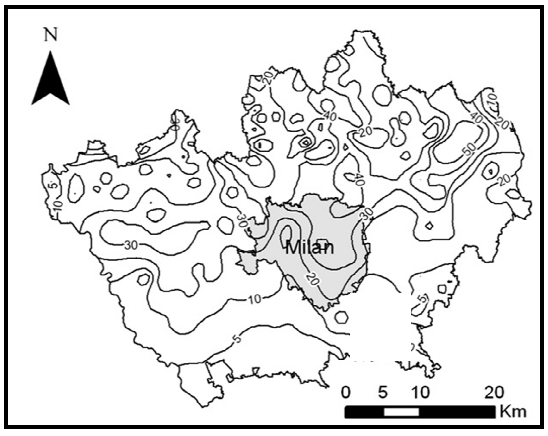

Figure 5.1 – Nitrate distribution in shallow groundwater in the Province of Milan.

5.1.2 Monitoring of the shallow aquifer within the Province of Piacenza

The Emilia-Romagna Region started to qualitatively monitor its aquifer system in 1976 and then quantitatively in 1987 through 62 wells sampled twice per year, 39 of which are used to monitor the upper portion of the aquifer system (identified as the Aquifer Complexes A1 and A2 described in Chapter 4, Paragraph 4.2).

The nitrate distribution in the upper portion of the aquifer remained quite unchanged during the whole monitoring period with the most impacted sectors located in the western part of the study area, in the north-central part around the municipality of Piacenza and in the south-eastern part where concentration greatly exceed 50 mg/l whereas the less impacted sector is coincident with a corridor extending from the south central part to the north-western one where concentration is lower than 15 mg/l (Fig. 5.2).

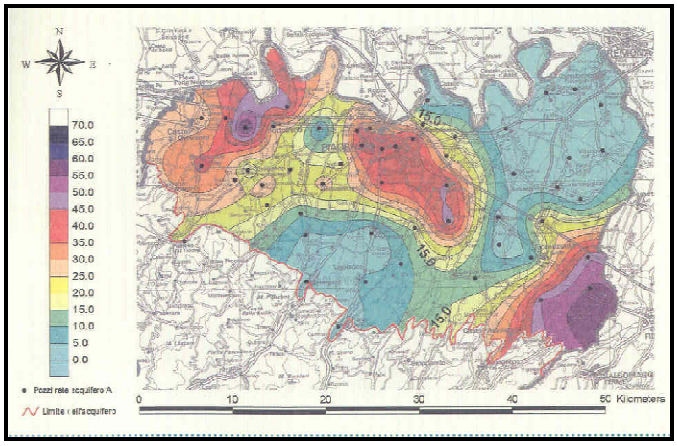

Figure 5.2 – Nitrate distribution in shallow groundwater within the Province of Piacenza (from Regione Emilia-Romagna, ARPA, and Provincia di Piacenza, 2004).

The water-quality data set from the survey carried out in 2008 was used in order to assess the vulnerability of the study area and to compare the assessment with nitrate concentration long term trends evaluated for each monitoring well, using the available time series covering 22 years (Fig. 5.3).

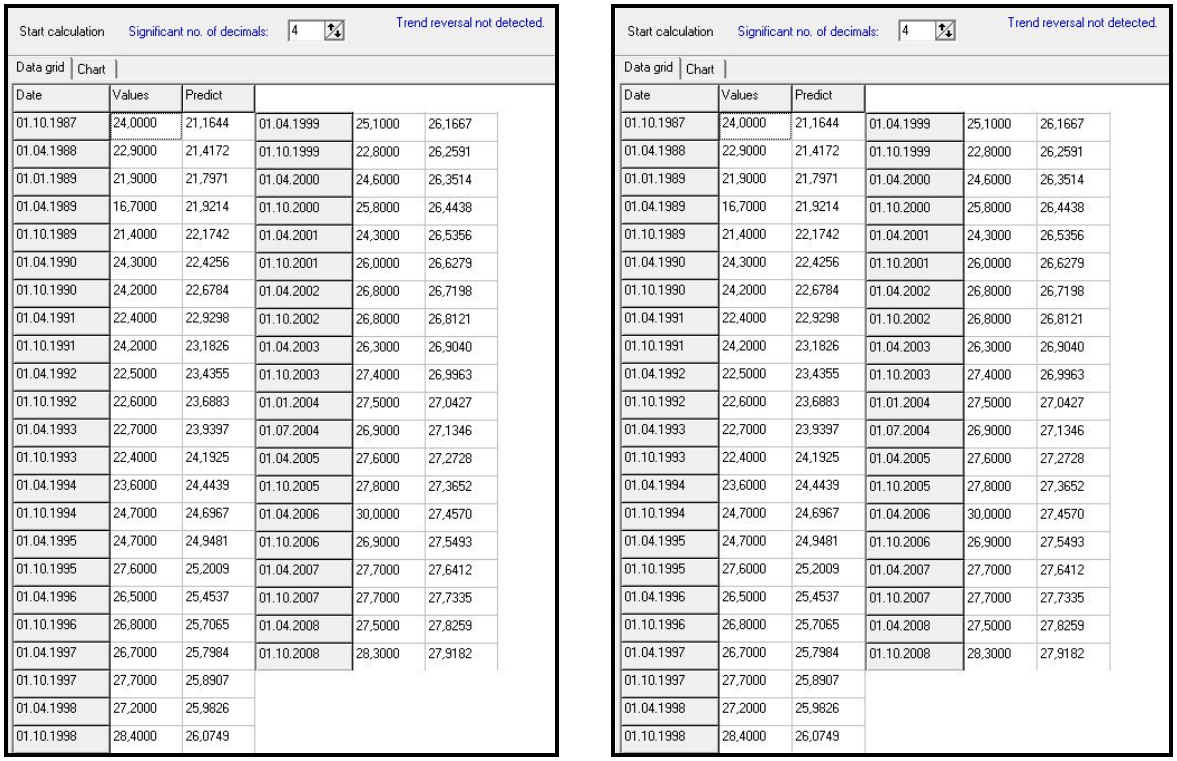

Start calculation Significant no. of decimals: 4 Trend reversal not detected.

Data grid | Chart

Date	Values	Predict			
01.10.1987	24,0000	21,1644	01.04.1999	25,1000	26,1667
01.04.1988	22,9000	21,4172	01.10.1999	22,8000	26,2591
01.01.1989	21,9000	21,7971	01.04.2000	24,6000	26,3514
01.04.1989	16,7000	21,9214	01.10.2000	25,8000	26,4438
01.10.1989	21,4000	22,1742	01.04.2001	24,3000	26,5356
01.04.1990	24,3000	22,4256	01.10.2001	26,0000	26,6279
01.10.1990	24,2000	22,6784	01.04.2002	26,8000	26,7198
01.04.1991	22,4000	22,9298	01.10.2002	26,8000	26,8121
01.10.1991	24,2000	23,1826	01.04.2003	26,3000	26,9040
01.04.1992	22,5000	23,4355	01.10.2003	27,4000	26,9963
01.10.1992	22,6000	23,6883	01.01.2004	27,5000	27,0427
01.04.1993	22,7000	23,9397	01.07.2004	26,9000	27,1346
01.10.1993	22,4000	24,1925	01.04.2005	27,6000	27,2728
01.04.1994	23,6000	24,4439	01.10.2005	27,8000	27,3652
01.10.1994	24,7000	24,6967	01.04.2006	30,0000	27,4570
01.04.1995	24,7000	24,9481	01.10.2006	26,9000	27,5493
01.10.1995	27,6000	25,2009	01.04.2007	27,7000	27,6412
01.04.1996	26,5000	25,4537	01.10.2007	27,7000	27,7335
01.10.1996	26,8000	25,7065	01.04.2008	27,5000	27,8259
01.04.1997	26,7000	25,7984	01.10.2008	28,3000	27,9182
01.10.1997	27,7000	25,8907			
01.04.1998	27,2000	25,9826			
01.10.1998	28,4000	26,0749			

Start calculation Significant no. of decimals: 4 Trend reversal not detected.

Data grid | Chart

Date	Values	Predict			
01.10.1987	24,0000	21,1644	01.04.1999	25,1000	26,1667
01.04.1988	22,9000	21,4172	01.10.1999	22,8000	26,2591
01.01.1989	21,9000	21,7971	01.04.2000	24,6000	26,3514
01.04.1989	16,7000	21,9214	01.10.2000	25,8000	26,4438
01.10.1989	21,4000	22,1742	01.04.2001	24,3000	26,5356
01.04.1990	24,3000	22,4256	01.10.2001	26,0000	26,6279
01.10.1990	24,2000	22,6784	01.04.2002	26,8000	26,7198
01.04.1991	22,4000	22,9298	01.10.2002	26,8000	26,8121
01.10.1991	24,2000	23,1826	01.04.2003	26,3000	26,9040
01.04.1992	22,5000	23,4355	01.10.2003	27,4000	26,9963
01.10.1992	22,6000	23,6883	01.01.2004	27,5000	27,0427
01.04.1993	22,7000	23,9397	01.07.2004	26,9000	27,1346
01.10.1993	22,4000	24,1925	01.04.2005	27,6000	27,2728
01.04.1994	23,6000	24,4439	01.10.2005	27,8000	27,3652
01.10.1994	24,7000	24,6967	01.04.2006	30,0000	27,4570
01.04.1995	24,7000	24,9481	01.10.2006	26,9000	27,5493
01.10.1995	27,6000	25,2009	01.04.2007	27,7000	27,6412
01.04.1996	26,5000	25,4537	01.10.2007	27,7000	27,7335
01.10.1996	26,8000	25,7065	01.04.2008	27,5000	27,8259
01.04.1997	26,7000	25,7984	01.10.2008	28,3000	27,9182
01.10.1997	27,7000	25,8907			
01.04.1998	27,2000	25,9826			
01.10.1998	28,4000	26,0749			

Figure 5.3 – Examples of time series used to evaluate the long term trend of nitrate concentration in two wells used to monitor the upper part of the aquifer system within the Province of Piacenza.

5.2 Explanatory variables

The main sources of nitrate in both study areas are linked to the presence of urban, agricultural and industrial areas.

Raster maps, with a pixel resolution of 50 meters, describing explanatory variables to be used as evidential themes in the WofE model, were derived from multiple sources of information and are different in type, accuracy, and survey scale.

5.2.1 Population density

Population density represents a surrogate of the actual nitrate loading primarily caused by sewer system losses in urban areas (e.g., Tesoriero and Voss 1998; Nolan et al. 2002).

Milan: the population density map at scale 1:25000 for the Province of Milan, referring to 2001, was created using population count data at municipality level from the census database of the Italian National Statistical Institute (Istat, 2001). The higher density is observable within the municipality of Milan (dark grey area in Fig 5.4) and in general in the north-eastern part of the Province.

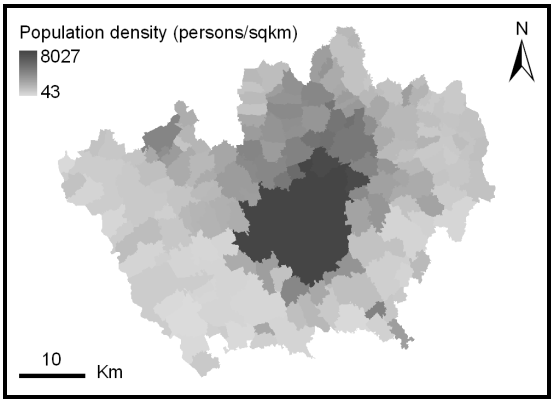

Figure 5.4 – Population density at municipality level within the Province of Milan.

Piacenza: the population density map at scale 1:25000 for the study area located within the Province of Piacenza, referring to 2009, was created using population count data at municipality level the census database of the Italian National Statistical Institute (Istat, 2009). The higher density is observable within the municipality of Piacenza (dark grey area in Fig 5.5) and in general in the eastern part of the Province.

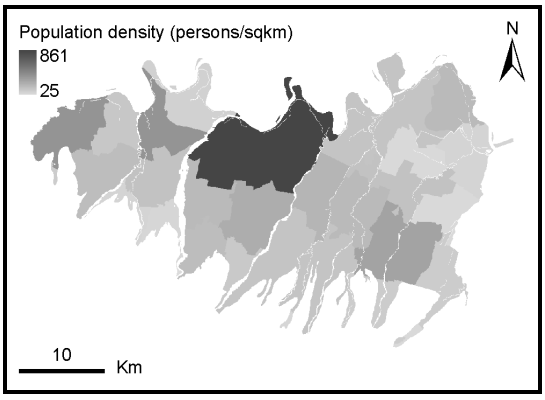

Figure 5.5 – Population density at municipality level in the study area located within the Province of Piacenza.

5.2.2 Nitrogen loading

Nitrate loading accounts for anthropogenic sources of nitrate not related to urban and industrial areas being both the organic and the chemical load correlated with animal breeding and agricultural activities, respectively.

Milan: the nitrogen loading map, at scale 1:25000, for the Province of Milan, referring to 2003, was created using the data prepared by Acutis and Provolo (2003) at municipality level. The higher values of nitrogen load result located in the south-eastern and western part of the study area (Fig. 5.6).

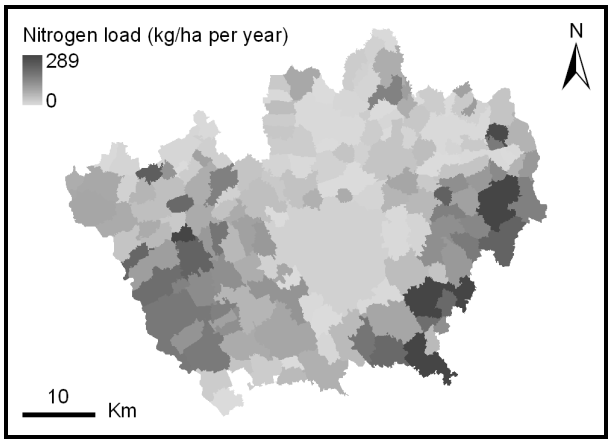

Figure 5.6 – Nitrogen load distribution at Municipality level in the Province of Milan.

Piacenza: the nitrogen loading map for the Province of Piacenza, referring to 2008, was created using the data prepared by the Environmental Agency of (ARPA) Emilia-Romagna Region (2003) at a scale given by the intersection between municipality and catchment areas. The higher values of nitrogen load result located in the north-western part of the study area (Fig. 5.7).

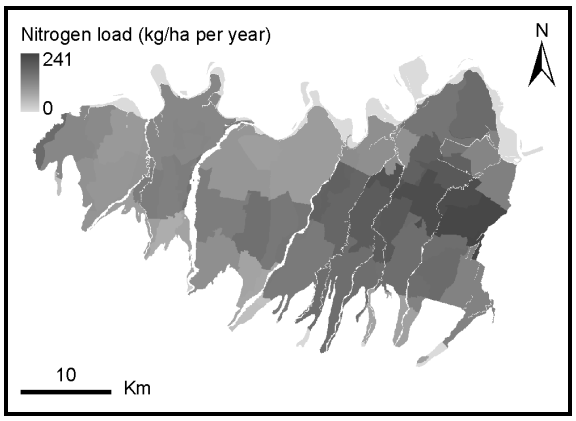

Figure 5.7 – Nitrogen load distribution in the study area within the Province of Piacenza.

5.2.3 Soil protective capacity

The soil protective capacity represents the soil capacity to degrade water-soluble contaminants leaching from the surface.

This explanatory variable was considered only for **Milan:** the map, consisting of three classes representing different degrees of protective capacity, was prepared, at scale 1:25000, by the Regional Agency for Agriculture and Forestry Services, for the whole Po plain and the surrounding hill areas within the Lombardia Province (ERSAF, 2004). It was produced considering the soil filtering and buffering capacity, due to mechanical, biological and microbiological activity.

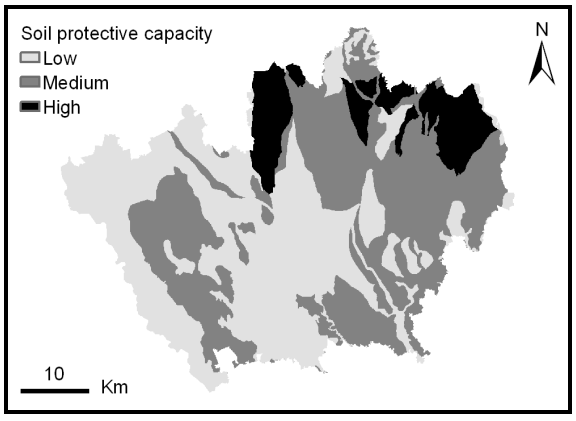

Figure 5.8 – Soil protective capacity in the Province of Milan.

Soils having mostly high and medium protective capacity are mostly present in the north-eastern sector whereas soils having low protective capacity are present in the central, southern and eastern sector (Fig. 5.8).

5.2.4 Groundwater depth

Groundwater depth determine the time of travel of a hydro-vectored contaminants and thus the duration of the attenuation process within the vadose zone.

Milan: the groundwater depth map, referring to 2001, which represents the level of unconfined aquifer identified with the Subgroup A1 (see Chapter 4, Paragraph 4.1), was generated interpolating the piezometric measurements made in 364 wells (about 18 wells per km^2) sampled four times per year and distributed as homogeneously as possible over the study area.

The groundwater depth decreases from north to south over the whole study area, highest values are observable in the north central part whereas the lowest values, even equal to zero, are observable close to the southern border of the Province where are present numerous natural springs (Fig. 5.9).

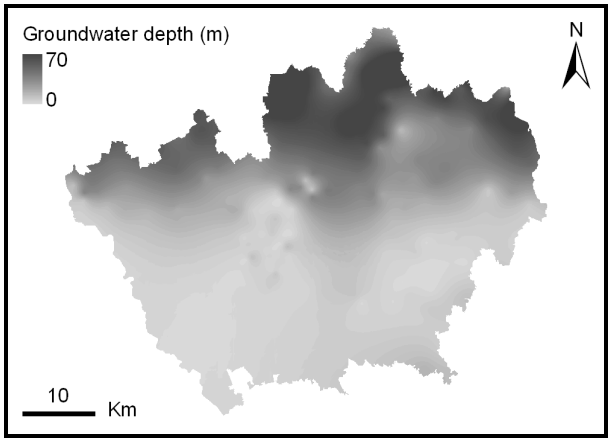

Figure 5.9 – Groundwater depth of the Subgroup Aquifer A1 in the Province of Milan.

Piacenza: the groundwater depth map, which represents the level of the upper portion of the aquifer identified with the Aquifer Complexes A1 and A2, was generated interpolating piezometric measurements made in 40 wells (courtesy of Direzione Tecnica ARPA Emilia-

Romagna), sampled twice per year, and 20 control points representing the elevation of surface water. Groundwater depth is higher in the south-central part of the study area and from there generally decreases eastward, westward and northward.

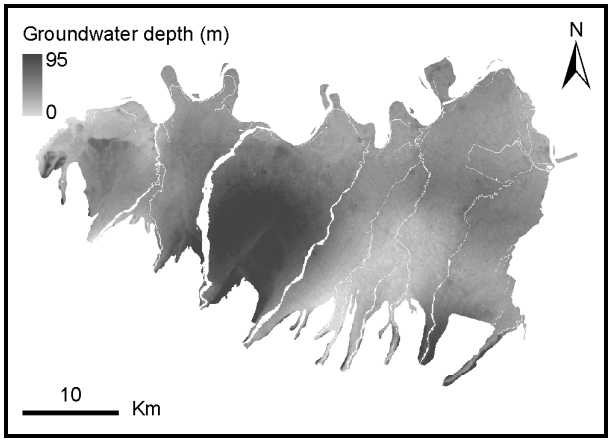

Figure 5.10 – Groundwater depth of the upper part of the aquifer system within the Province of Piacenza.

5.2.5 Unsaturated hydraulic conductivity

Unsaturated hydraulic conductivity represents the capacity of groundwater to move inside the vadose zone and thus the mobility potential of a hydro-vectored contaminant.

This explanatory variable was considered only for **Milan:** the map representing the distribution of the unsaturated hydraulic conductivity in the Province of Milan was generated interpolating experimental data from borehole tests conducted in 606 wells (about 30 wells per km^2) distributed as homogeneously as possible over the study area.

In each well, being the flux through the vadose zone mainly vertical and very sensible to low permeability layers, the following formula has been used:

$$k_{eq} = S \frac{k_1 k_2 k_3 ... k_n}{S_1 k_2 k_3 ... k_n + S_2 k_1 k_3 ... k_n + ... + S_n k_1 k_2 ... k_{n-1}} \qquad (5.1)$$

where S_1 and S_n are, respectively, the thickness of the first and *n_th* layer, S is the total depth, and k_1 and k_n are respectively the hydraulic conductivity of the first and *n-th* layer.

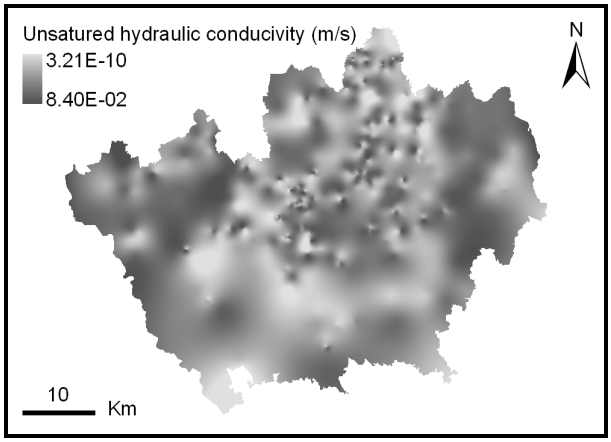

Figure 5.11 – Distribution of the unsaturated hydraulic conductivity in the Province of Milan.

Unsaturated hydraulic conductivity is higher in the north western and north-eastern part of the study area whereas is generally lower in the southern part.

5.2.6 Groundwater velocity

Groundwater velocity is related to the concept of instantaneous dilution occurring when contaminants reach groundwater (Calabrese and Kostecki, 1988).

This explanatory variable was considered only for **Milan:** the groundwater velocity map for the Province of Milan was obtained by interpolating the results of a numerical models, realized with a finite difference code (MODFLOW), that was calibrated and validated on 1200 km^2 within the study area (Alberti et al., 2000).

The obtained groundwater velocity data was aggregated with other available data (for those areas outside the model) and then interpolated in order to obtain a spatial distribution of the analyzed parameter over the entire study area. Two zones of high velocity are located in the central-northern and southern sectors while low values are mainly concentrated in the north-western and south-eastern part of the study area. Difference in velocity can be equally attributed to hydraulic conductivity and hydraulic gradient changes with the last generally higher in the northeastern sector.

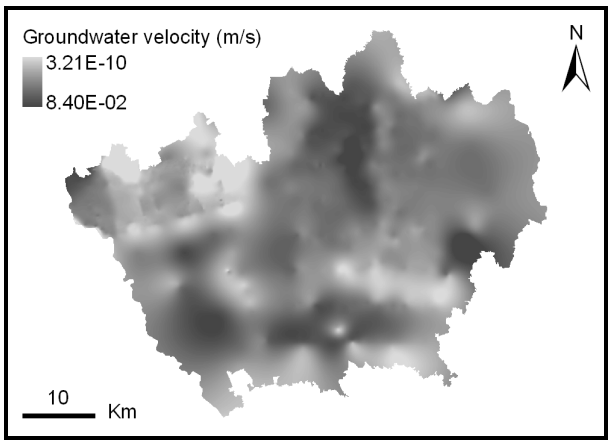

Figure 5.12 – Groundwater velocity within the Province of Milan.

5.2.7 Effective infiltration (irrigation, rainfall and land use)

Effective infiltration is responsible for transporting contaminants in groundwater but also for their dilution, first during the travel through the vadose zone and then within the saturated zone.
Milan: the effective infiltration (*EI*) map for the Province of Milan was generated by combining mean annual irrigation (*I*), rainfall (*R*), and land use through a simple function being:

$$EI=(R + I)* Ci \quad (5.1)$$

where *Ci* represents an infiltration coefficient being a function of the land use (USSCS 1964; Schwab et al. 1993).
Effective infiltration results greatly influenced by the presence of the extensive irrigation net mainly located in the central-southern sector of the study area where indeed the effective infiltration values are the highest (Fig. 5.13).

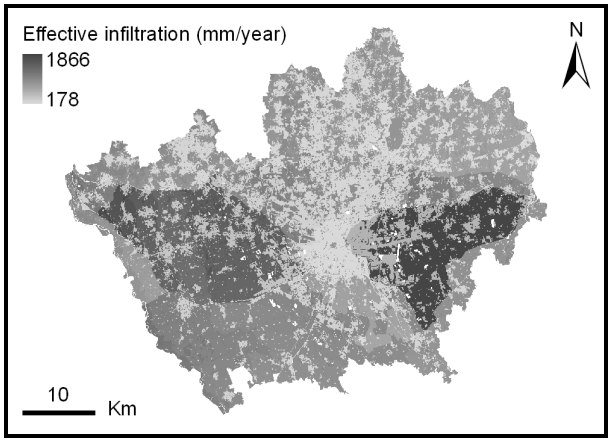

Figure 5.13 – Effective infiltration in the Province of Milan.

The mean annual irrigation map for Milan (Fig. 5.14), at a scale 1:25000, was generated at the Consortium level, by using the average incoming and outgoing discharge values recorded at each flow gauge by each Consortium (Table 5.2).

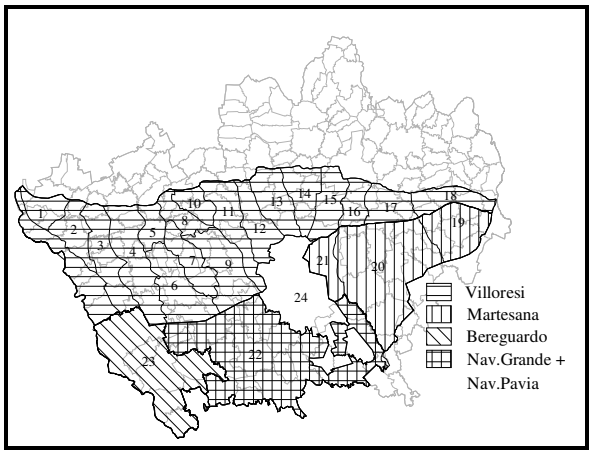

Figure 5.14 – Location of each consortium within the Province of Milan.

Consortium	Canal	Code	Area (m^2)	Avg. monthly discharge (m^3/s)
Villoresi		1-18	803219.985	282.624
	Castano I and Castano II	1	20169.473	5.085
	Cuggiono	2	27031.155	17.795
	Magenta	3	434081.848	21.268
	Corbetta	4	60964.658	25.210
	Parabiago	5, 6, 7, 8, 9	18207.000	68.959
	Rho	10	16877.000	1.229
	Passirana and Arese	11	55237.734	9.205
	Garbagnate	12	31482.300	2.867
	Val Seveso	13	35234.100	2.319
	Nova and Cinisello	14	31011.100	0.654
	Brugherio	16	18921.500	1.605
	Carugate and Cernusco	17	27653.617	7.914
	Gorgonzola and Pessano	18	26348.500	3.472
Martesana		19, 20, 21	224696.396	148.010
Nav. Grande and Nav. Pavia		22	778822.422	218.776
Nav. Bereguardo		23	324400.000	59.957

Table 5.2 – Main characteristics of each canal within the irrigation net in the Province of Milan.

The rainfall map for Milan (Fig. 5.15) was generated by interpolating the mean annual rainfall values registered by seven stations located within the study area with records longer than twenty years (courtesy of the Hydrographic Service of Po River).

Isohyets show a decreasing trend in rainfall from NW to SE according to altitude changes in the same direction.

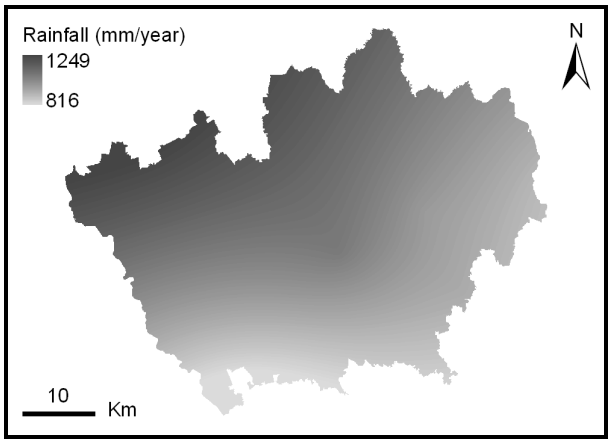

Figure 5.15 – Rainfall distribution in the Province of Milan.

For Milan the land-use map was obtained modifying the map, at scale 1:10000, prepared by the Regional Agency for Agriculture and Forestry Services as part of the DUSAF project (ERSAF, 2003). In particular, different land uses where reclassified as urban, urban green, cultivated, and natural areas. Most of the southern and western sector of study area is occupied by agricultural areas whereas urban areas are mainly located in the central and northern sector (Fig. 5.16).

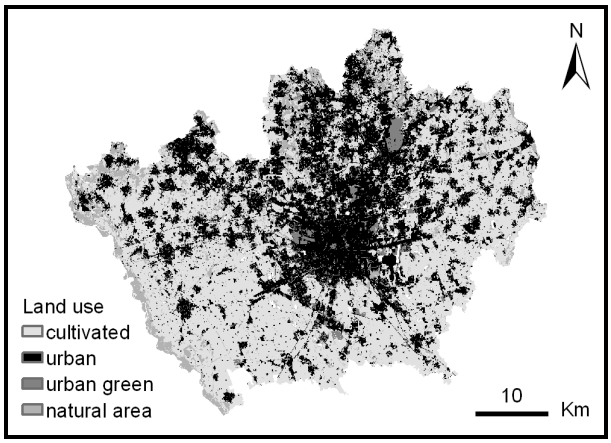

Figure 5.16 – Land use in the Province of Milan.

Piacenza: the effective infiltration (*EI*) map was generated by combining rainfall (*R*), and land use through a simple function being:

$$EI = R * Ci \qquad (5.2)$$

where *Ci* represents an infiltration coefficient being a function of the land use (USSCS 1964; Schwab et al. 1993).

Effective infiltration results highly influenced by the land use being the lowest effective infiltration values located in correspondence of the urban areas (Fig. 5.17).

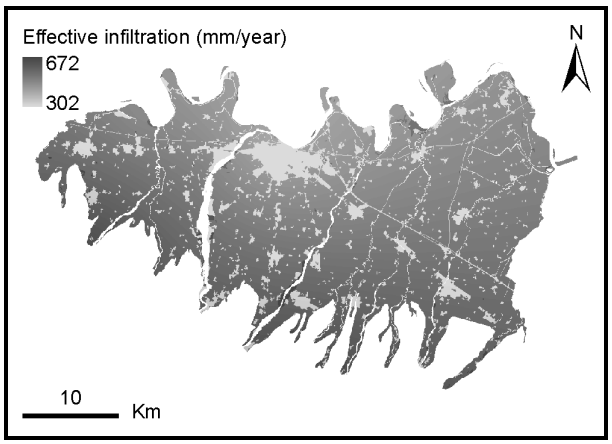

Figure 5.17 – Effective infiltration in the study area within the Province of Piacenza.

The rainfall map for Piacenza was generated interpolating the 2008 mean annual rainfall values registered in 8 stations located within and outside the study area (Regione Emilia Romagna, 2008).

Isohyets show a decreasing trend in rainfall from SW to NW according with altitude changes in moving away from the Appenine toward the Po plain (Fig. 5.18).

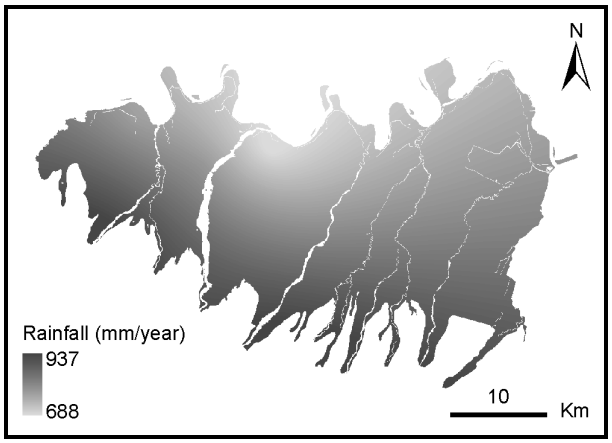

Figure 5.18 – Rainfall distribution in the study area within the Province of Piacenza.

For Piacenza the land-use map, was obtained modifying the map, at scale 1:25000, prepared by the Region of Emilia-Romagna (2006). In particular, different land uses where reclassified as urban, cultivated, natural areas and wetlands. Almost the whole study area is occupied by

agricultural and subordinated urban areas, the biggest one located in correspondence of the municipality of Piacenza (Fig. 5.19).

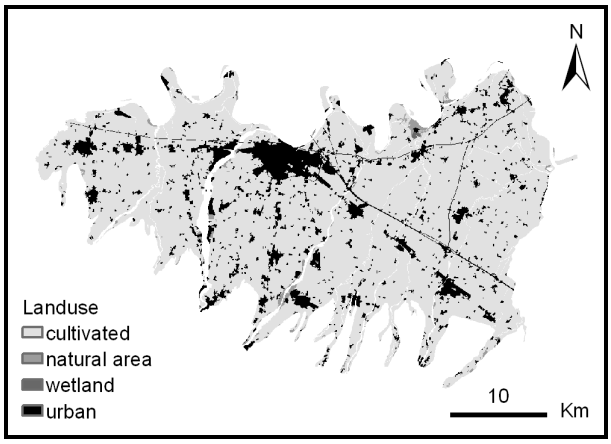

Figure 5.19 – Land use in the study area within the Province of Piacenza.

5.2.8 Aquifer confinement

Confinement represents a protection against contaminants leaching from the surface.

This explanatory variable was considered only for **Piacenza:** the aquifer confinement map for Piacenza was generated considering the upper portion of the aquifer, identified as the Aquifer Complexes A1 and A2, in terms of being confined or unconfined (courtesy of Direzione Tecnica ARPA Emilia-Romagna).

The aquifer results unconfined in the central part of the study area and confined in the western and eastern part of it (Fig. 5.20).

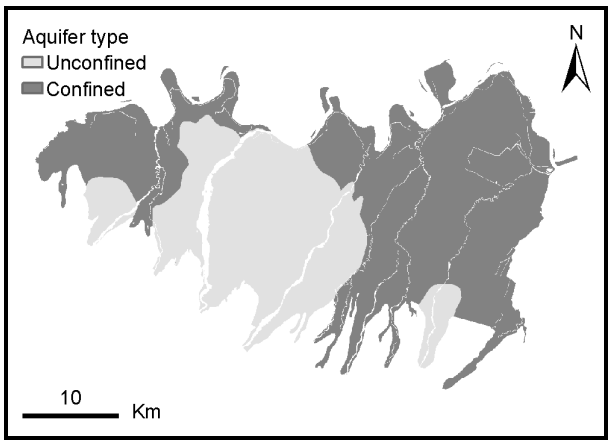

Figure 5.20 – Upper portion of the aquifer within the Province of Piacenza classified in terms of being confined or unconfined.

Chapter 6
Using positive and negative evidences of contamination

Since the early 1990s, following the rapid development of computer and Geographic Information System (GIS) technology, there has been a growing interest in applying GIS-based statistical techniques to model spatially-related issues (Raines and Bonham-Carter, 2007) in geosciences (Bonham-Carter, 1994) as in many other fields (e.g., Kulldorff et al., 1997; Duke and Steele, 2010). Applications in geosciences have mainly focused on mineral exploration and resource appraisal (e.g., Agterberg et al., 1993; Raines and Mihalasky, 2002; Harris et al., 2003; Cheng, 2004; Corsini et al., 2009), landslide susceptibility assessment (e.g., Carrara et al., 1991; Lee et al., 2003a; Lee et al. 2007, Dahal et al., 2008), and groundwater quality/vulnerability assessment (e.g., Rupert, 1998; Lee et al., 2003b; La Motte and Greene, 2007; Masetti et al., 2008).

All statistical techniques used for predicting undiscovered resources and future landslides, and most of the techniques used to assess groundwater vulnerability use binary-response variables (representing either occurrences or non-occurrences of an event) as a function of one or more explanatory variables to depict the probability of being in a response category (usually expressed as the probability of the occurrence of an event). Thus, in terms of groundwater vulnerability assessment, the modeled response gives the probability of contamination and not the actual concentration of the contaminant being considered (Helsel and Hirsch, 1992). For this reason, statistical techniques that model binary-response variables are extremely well-suited for assessing groundwater vulnerability (Tesoriero et al., 1998), even when water-quality data sets contain several concentrations reported as being below the detection limit (e.g., Nolan et al., 2002). In predicting undiscovered resources and especially future landslides it is relatively easy to distinguish between occurrences and non-occurrences. However, such distinction becomes less clear-cut when considering groundwater contamination, mostly because the concentration of a contaminant is a continuous variable that can potentially range from zero to an unknown value. Thus, there is a need to select an arbitrary threshold allowing distinguishing between positive and negative evidences of contamination indicating, respectively, where groundwater has to be considered impacted and non-impacted by a given contaminant. When using statistical methods

estimating the conditional probability of occurrence of an event, such as the Weights of Evidence (e.g., Arthur et al., 2007; Masetti et al., 2007) or the Likelihood Ratio Function (Masetti et al., 2009), regardless of the selected threshold, only the water-quality data subset constituted by the positive evidences of contamination (henceforth just positive evidences) is considered for being used in the modeling process. Indeed, such methods model binary-response variables using only known occurrences. Negative evidences are then sometimes used solely in the validation process to test the capability of the model output to correctly predict known non-occurrences (model output specificity; i.e., Nolan 2002). One potential limit of this approach is that the entire data subset constituted by the negative evidences of contamination (henceforth just negative evidences) is completely neglected.

In this Chapter, both subsets of evidences were used as TPs in the WofE model to assess groundwater vulnerability to nitrate contamination in the porous, unconfined, shallow aquifer located in the Province of Milan (which hydrogeological characteristics and nitrate distribution are described in Chapter 4, Paragraph 4.1 and Chapter 5, Paragraph 5.1, respectively). Positive and negative evidences were alternatively identified as occurrences and thus used as TPs in two different models in order to generate two different probability outputs (with both models and outputs hereafter referred to as positive and negative depending on the type of evidences identified as occurrences) expected to be quasi-complementary in terms of the probability of occurrences and similar in terms of groundwater vulnerability. This was done to better understand the individual and the combined role of the considered explanatory variables in protecting/exposing shallow groundwater from/to nitrate contamination in the study area and to further test the robustness of the WofE modeling technique. The idea behind this approach is that, for a given aquifer, each explanatory variable must have a univocal effect on the physical process of groundwater contamination. Indeed, according to Goldscheider (2005), “the terms vulnerability to contamination and natural protection against contamination can be used alternatively, where high vulnerability means low natural protection”. Thus, if a continuous explanatory variable shows a direct relationship with the presence of positive evidences, the same variable is expected to show an inverse relationship with the presence of negative evidences. Additionally, if a class of a categorical explanatory variable shows a positive correlation with the presence of positive evidences, the same class is expected to show a negative correlation with the presence of negative evidences.

6.1 Training points and evidential themes

The water-quality data set collected in 2001 (described in Chapter 5, Paragraph 5.1) is the one used in the study presented in this Chapter. Because the frequency histogram of nitrate concentrations showed a non-normal (slightly right-skewed) distribution (Table 6.1), the median of 19.5 mg/l was identified as the most appropriate value to be used as threshold.

Survey	Year	No. of wells	Nitrate concentration					Skewness
			Min	Max	Mean	Median	Std. Dev.	
2	2001	323	0.8	63.0	22.5	19.5	15.1	0.43

Table 6.1 – Basic descriptive statistics of water-quality dataset collected in 2001.

Thus, wells from which samples showed a nitrate concentration higher than or equal to the threshold value were identified as impacted wells (positive evidences) and used as TPs (162 positive TPs) in the positive model, whereas wells from which samples showed a nitrate concentration lower than the threshold value were identified as non-impacted wells (negative evidences) and used as TPs (161 negative TPs) in the negative model (Fig. 6.1).

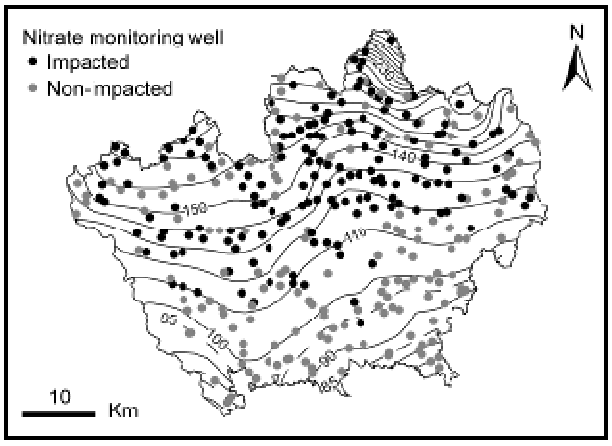

Figure 6.1 – Locations of the wells in the 2001 monitoring network: nitrate concentration in samples from impacted and non-impacted wells is, respectively, greater than or equal to and lower than 19.5 mg/l.

From the hydrogeological conceptual model, seven explanatory variables (described in Chapter 5, Paragraph 5.2), already proved to control nitrate contamination of shallow groundwater in the

study area (Masetti et al., 2007), were considered for being used as evidential themes in the analysis (Table 6.2).

Explanatory variable	Type	Minimum	Maximum
Population density [persons/km^2][a]	Continuous	43	8027
Nitrogen load [kg/ha per year][a]	Continuous	0	289
Soil protective capacity	Categorical	-	-
Groundwater depth [m]	Continuous	0	70
Unsaturated hydraulic conductivity [m/s]	Continuous	3.21E-10	8.40E-02
Groundwater velocity [m/s]	Continuous	8.79E-09	2.10E-05
Effective infiltration [mm/year]	Continuous	178	1866

[a] computed at municipality level

Table 6.2 – Explanatory variables considered for being used in the analysis.

6.1.1 Generalization of the evidential themes

To facilitate unbiased comparisons between positive and negative model outputs, an objective (semi-guided) procedure for multiclass generalization was developed as part of the study presented in this Chapter. Because the contrast represents the measure of the class usefulness in predicting the location of the TPs (Raines, 1999; Chapter 3, Paragraph 3.2), for each continuous explanatory variable statistically significant high contrasts were used to identify breaking points (i.e., explanatory variable values) delineating classes having a strong spatial association with the TPs.

The steps in identifying breaking points and generalizing all ordered evidential themes, alternatively using positive or negative evidence as TPs, were as follows:

1 using either the cumulative ascending or descending method (Raines, 1999), contrasts and confidence values were calculated for all cumulative classes (Table 6.3);
2 statistically significant contrasts representing relative peaks in the "Contrast-Cumulative class" graph (e.g., black dots in Fig. 6.2) were identified, and the corresponding values (breaking points) were used to generalize the evidential theme being considered (e.g., unsaturated hydraulic conductivity values of 1136 and 1143 [-100×ln(m/s)] in Table 6.3);
3 using the categorical method (Raines, 1999), contrasts and confidence values were calculated for all classes identified in step 2 (Table 6.4);

4 to reduce the initial amount of statistically non-significant classes, contiguous classes with confidence values below the chosen statistical level of significance were merged together (e.g., from class 3 to class 22, from 24 to 28, and from 31 to 40 in Table 6.4);

5 using the categorical method again, contrasts, and confidence values were calculated for all classes that were obtained in step 4 (Table 6.5);

6 classes with confidence values that still below the chosen statistical level of significance were merged either:

6.1 with the contiguous significant class that had the same contrast sign, if only one significant contiguous class had the same contrast sign as the class being merged (e.g., class 3 with class 2, and 8 with 9 in Table 6.5);

6.2 or with the contiguous significant class that kept the lower contrast as high as possible in terms of absolute value (in an effort to delineate spatial associations between classes and TPs as strongly as possible), if the contrasts of both of the contiguous significant classes had the opposite or the same sign as the class being merged (e.g., class 5 with class 4 in Table 6.5);

7 steps 5 and 6 were repeated until all obtained classes became statistically significant.

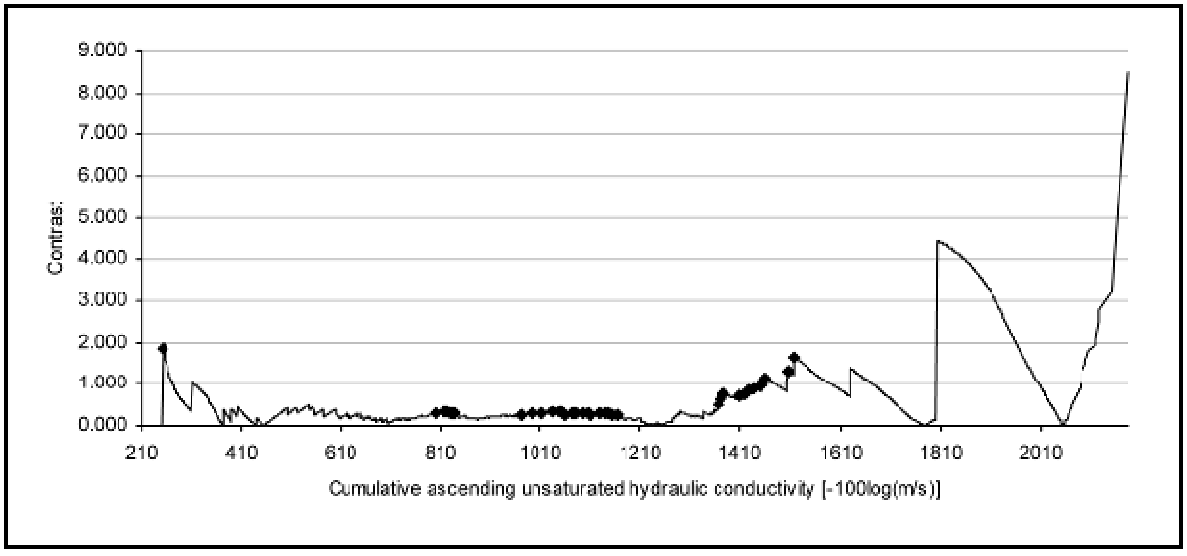

Figure 6.2 – Cumulative ascending unsaturated hydraulic conductivity values plotted against contrasts calculated using positive training points: black dots represent the breaking values used to generalize the unsaturated hydraulic conductivity evidential theme.

Cumulative class	Contrast	Confidence	First step generalized class
210	0	0	1
…	…	…	…
1128	-0.279	-1.764	25
1129	-0.283	-1.788	
1130	-0.287	-1.813	
1131	-0.291	-1.837	
…	…	…	
1134	-0.303	-1.913	
1135	-0.307	-1.935	
1136	-0.311	-1.961	
1137	-0.289	-1.824	26
1138	-0.268	-1.687	
…	…	…	
1142	-0.284	-1.788	
1143	-0.288	-1.814	
...	...	...	...
2186	-8.486	-0.6	41

Table 6.3 – Selected "cumulative classes" of the unsaturated hydraulic conductivity evidential theme (1st column), their corresponding contrasts and confidence values calculated using positive training points (2nd and 3rd column, respectively), and selected "first step generalized classes" delineated by the breaking points identified in Figure 6.3 (4th column).

First step generalized class	Contrast	Confidence	Second step generalized class
1	1.878	1.871	1
2	-0.323	-1.801	2
3	-1.162	-1.159	3
...	...	...	
22	-0.454	-0.452	
23	1.273	1.788	4
24	-0.892	-0.889	5
25	-0.278	-0.277	
26	0.655	0.920	
27	0.490	0.689	
28	0.141	0.198	
29	0.614	3.607	6
30	2.120	2.976	7
31	1.462	1.457	8
...	...	...	
40	0.087	0.087	
41	-1.648	-2.316	9

Table 6.4 – Selected "first step generalized classes" defined in Table 6.3 (1st column), their corresponding contrasts and confidence values calculated using positive training points (2nd and 3rd column,

respectively), and all "second step generalized classes" obtained by merging together the contiguous non-statistically significant "first step generalized classes" (4th column).

Second step generalized class	Contrast	Confidence	Third step generalized class
1	1.878	1.871	1
2	-0.323	-1.801	2
3	-0.056	-0.315	
4	1.273	1.788	3
5	0.033	0.091	
6	0.614	3.607	4
7	2.120	2.976	5
8	-0.203	-0.650	6
9	-1.648	-2.316	

Table 6.5 – All "second step generalized classes" defined in Table 6.4 (1st column), their corresponding contrasts and confidence values calculated using positive training points (2nd and 3rd column, respectively), and all "third step generalized classes" obtained by merging each non-statistically significant "second step generalized class" with a contiguous, statistically significant one (4th column).

A confidence value of |1.654|, corresponding approximately to a 95% level of significance, was chosen as the minimum acceptable value to consider a class as statistically significant.

The above described procedure was designed to obtain (through an objective method) the maximum number of statistically significant classes for each ordered evidential theme, both when using positive and negative TPs in the analysis. Here, it is important to note that the above procedure lead to obtain different multiclass generalizations of the same evidential theme, regarding both/either the number of identified classes and/or their range of values, when alternatively using positive or negative TPs in the analysis. However, using either the equal-interval or natural-breaks classification method to generalize the evidential themes would have not guaranteed that all identified classes were statistically significant (due to the diverse spatial distribution of the positive and negative evidences). On the other hand, a knowledge-driven generalization would introduce a degree of subjectivity that could ultimately affect the comparison between positive and negative model outputs.

6.2 Results and discussion

6.2.1 Contrasts

The individual role of each explanatory variable in influencing groundwater contamination in the study area was examined by considering, for each evidential theme, the contrasts of each statistically significant class identified alternatively using positive or negative TPs.

All classes of the evidential theme representing the soil protective capacity were found to be statistically non-significant, when correlated with the presence of both positive and negative evidences.

The statistically significant classes of the evidential themes representing the population density and the groundwater depth showed a general direct relationship with the presence of positive evidences (histogram A in Fig. 6.3) and a general inverse relationship with the presence of negative evidences (histogram B in Fig. 6.3). This result indicates that the probability of nitrate contamination generally increases with increasing of population density and groundwater depth values.

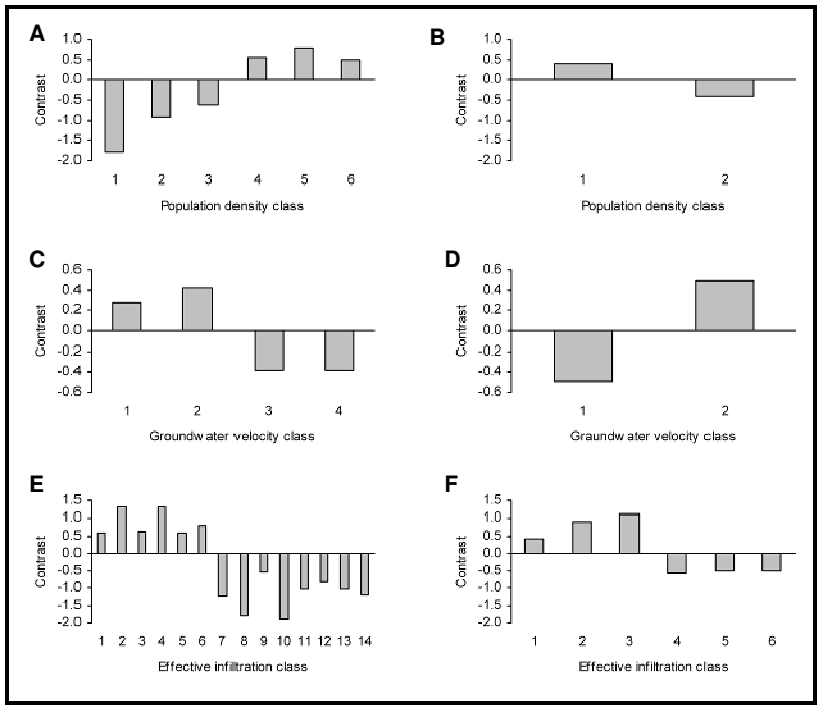

Figure 6.3 – Contrasts of each statistically significant class of the generalized evidential themes representing population density, groundwater velocity and effective infiltration: histograms A, C, and E (on

the left) represent contrasts calculated using positive TPs; histograms B, D and F (on the right) represent contrasts calculated using negative TPs.

On the contrary, the statistically significant classes of the evidential themes representing the unsaturated hydraulic conductivity, groundwater velocity, and the nitrate loading showed a general direct relationship with the presence of negative evidence (histogram C in Fig. 6.3) and a general inverse relationship with the presence of positive evidences (histogram D in Fig. 6.3). This result indicates that the probability of nitrate contamination generally increases with increasing of unsaturated hydraulic conductivity and groundwater velocity, and decreasing of nitrogen loading values (indeed, to avoid dealing with very large decimal values, the evidential themes representing the unsaturated hydraulic conductivity and the groundwater velocity are expressed as the natural logarithm of the actual values of the variables to be represented multiplied by minus 100).

The statistically significant classes of the evidential themes representing the effective infiltration showed a general direct relationship with the presence of both positive and negative evidences (histograms E and F, respectively, in Fig. 6.3). This result indicates, incongruously, that the probability of nitrate contamination seems to increase with both increasing and decreasing of effective infiltration values.

The unexpected behavior of the explanatory variable representing the effective infiltration could be due to the presence of a bias affecting the results both when using the positive and the negative TPs in the analysis. In this case, the bias with respect to the effective infiltration evidential theme could be related to a single variable used to generate it (namely irrigation, rainfall, and land use) or it could have been introduced when combining them.

Due to its non-univocal relationship with the presence of positive and negative evidences, the effective infiltration evidential theme (hereafter referred as a “puzzling” evidential theme) was first included and then excluded from both the positive and the negative model to test how its presence/absence would have affected the model outputs in terms of vulnerability assessment.

6.2.2 Response themes and reclassified groundwater vulnerability maps

All generalized evidential themes with all of their classes that were found to be statistically significant were combined to evaluate their simultaneous influence on nitrate contamination of shallow groundwater in the study area.

Thus, four response themes, in terms of predictive probability outputs, were generated (a negative and a positive response theme including the effective infiltration evidential theme in the analysis, and a negative and a positive response theme not including the effective infiltration evidential theme in the analysis).

Typically, groundwater vulnerability maps represent a limited number of classes; subjective rating methods, such as GOD (Foster, 1987) and EPIK (Doerfliger and Zwahlen, 1995), individuate from four to five classes. Vulnerability scores, ranging from 23 to 226, obtained through the widely known DRASTIC method (Aller et al., 1987), are generally reclassified into fewer classes (Rupert, 2001; Hamza et al., 2007). Indeed, scientifically defensible aquifer vulnerability response themes, expressed as probability maps, require additional interpretation before being usable for most of the end-user purposes (Focazio et al., 2002). This need for additional interpretation is mainly due to the excessive number of classes, which is inappropriate for land-use regulations and/or prescriptive purposes. In fact, final maps obtained from statistical methods tend to be represented by a limited number of classes, rarely more than six (Tesoriero and Voss, 1997; Nolan et al., 2002).

Furthermore, a vulnerability map depicting few classes of vulnerability is also a useful way to smooth uncertainty. Indeed, often the necessity to cover the whole study area with the evidential themes requires a pre-interpolation process to define the spatial distribution of the variables. Therefore, it does not appear reasonable to represent a map with as many classes as the number of probability values, given that the statistical significance of a single value can be very low.

Thus, the response themes were reclassified to obtain four vulnerability maps consisting of five classes, each one reflecting a different degree of vulnerability increasing from class 1 to class 5 (Fig. 6.4).

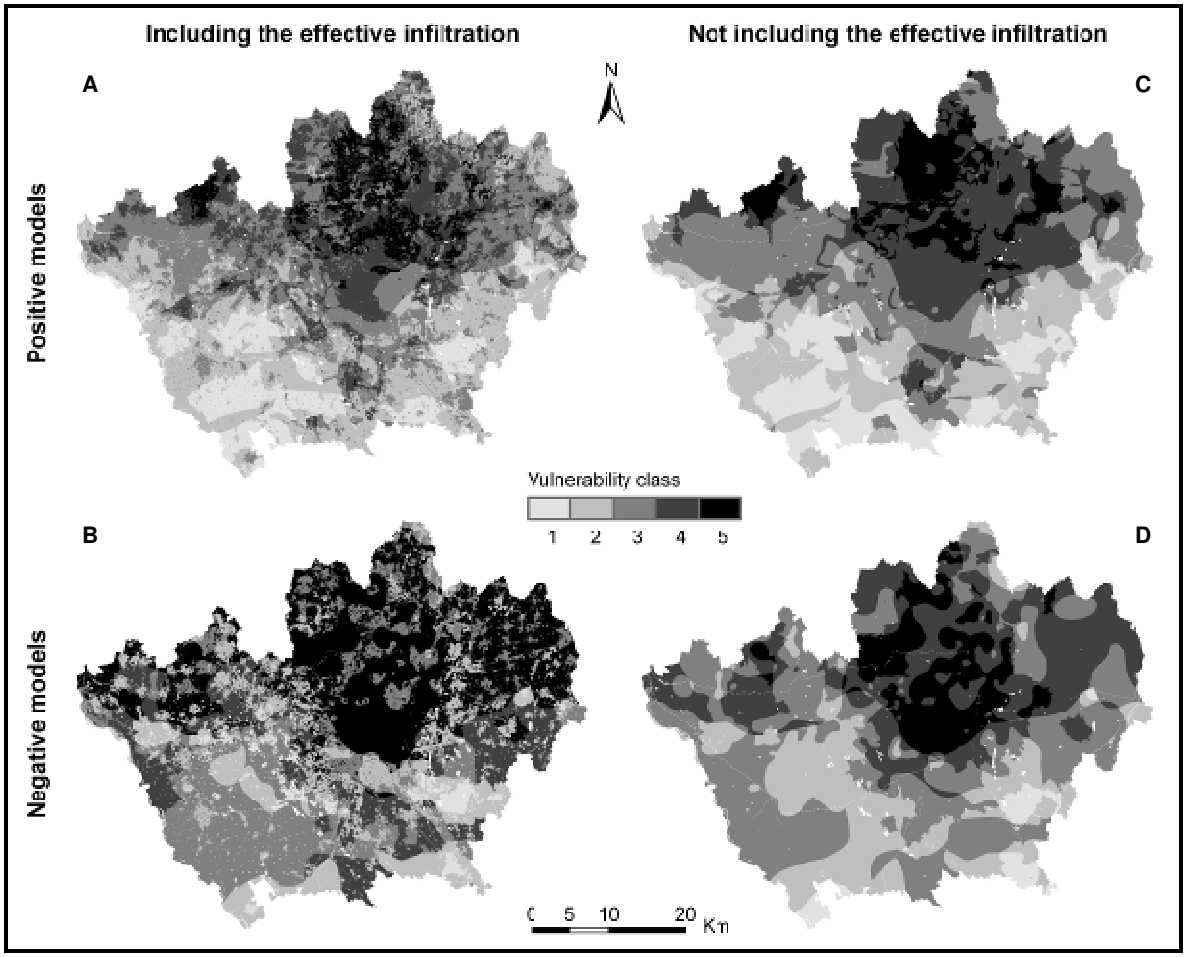

Figure 6.4 – Positive and negative model outputs as vulnerability maps in which the degree of vulnerability increases from class 1 to 5: maps A and B (on the left) were obtained by including the effective infiltration evidential theme in the positive and negative model, respectively; maps C and D (on the right) were obtained by not including the effective infiltration in the positive and negative model, respectively.

All response themes were reclassified using the Geometrical Interval Classification method (ESRI, 2007) which ensures that each class contains approximately the same number of different post probability values. This reclassification method was preferred to the equal area method, proposed by other authors, considering a practical aspect to be faced when dealing with vulnerability or hazard in general. In a five-class reclassification procedure, for example, the identification of the most vulnerable area does not imply that it must cover 20% of the area. Zones with high probability values could easily be concentrated on a smaller amount of surface. Consequently there is no need to artificially extend the surface to occupy the 20% of the total

area, considering the practical consequences it would have in terms of environmental planning and management. The same would be true if the most vulnerable area is actually larger than the 20%. The geometrical interval allows the identification of classes as a function of the actual values and ranges of probability obtained in the response theme and can be considered equivalent to the equal interval method if the probability values are transformed using the dense ranking method (Fig. 6.5).

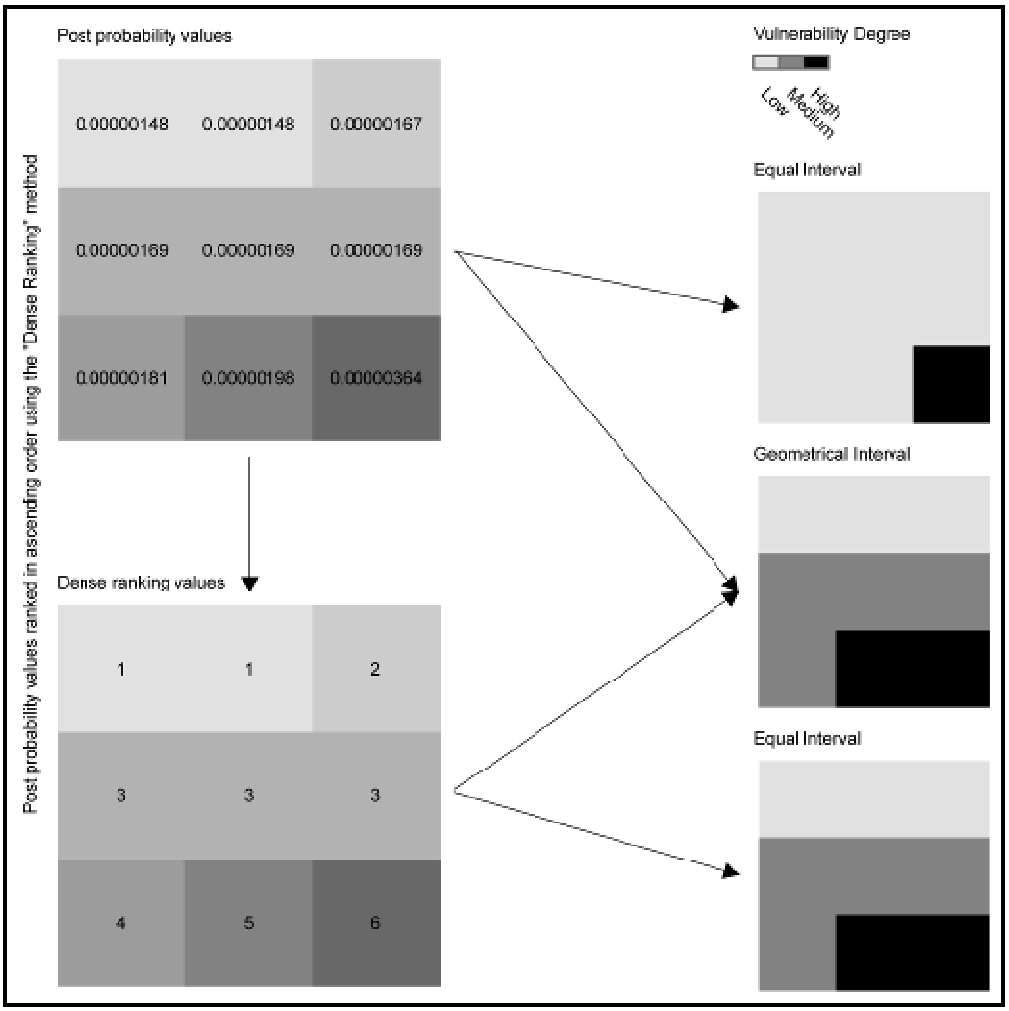

Figure 6.5 – Comparison between outputs obtained using different Reclassification method on the same input.

To this regard, it is important to note that the probability values represent the probability of contamination and the probability of non-contamination in the positive and the negative response themes, respectively. Thus, even if the degree of vulnerability increases from class 1 to 5 in all

vulnerability maps, the probability values increase from class 1 to 5 in the positive maps while they increase from class 5 to 1 in the negative ones.

The effect of including the effective infiltration evidential theme in the analysis was evaluated by considering the spatial agreement between the positive and negative reclassified vulnerability maps, both of which were alternatively obtained by including or not including the effective infiltration in the analysis and by validating separately each reclassified vulnerability map.

6.2.3 Spatial agreement

At first, the spatial agreement between positive and negative maps was evaluated through a simple pixel-by-pixel comparison. The results, expressed as the percentage of pixels being in the same vulnerability class in both compared maps, showed that there was a lower agreement between the maps obtained including the effective infiltration evidential theme in the analysis (A and B in Fig. 6.4) than between the maps obtained not including it (C and D in Fig. 6.4). Indeed, in the first case, the percentage of pixels being in the same vulnerability class in both maps is approximately 14% while, in the second case, this percentage increased to approximately 36% (Table 6.6).

Vulnerability increasing/decreasing factor (n)	Including the effective infiltration		Not including the effective infiltration	
	No. of pixels	% of pixels	No. of pixels	% of pixels
3	47031	6.05	-	-
2	224847	28.92	49945	6.42
1	208855	26.86	287188	36.94
0	105433	13.56	280260	36.05
-1	80864	10.4	140926	18.13
-2	96807	12.45	18585	2.39
-3	13391	1.72	551	0.07
-4	227	0.03	-	-

Table 6.6 – Number and percentage of pixels in the negative vulnerability maps B (2nd and 3rd column, respectively) and D (4th and 5th column, respectively) in Figure 6.4, that are in the same vulnerability class (n=0), in an n-degrees higher (n>0) and in an n-degrees lower (n<0) vulnerability class when compared, respectively, with positive maps A and C in Figure 6.4.

Furthermore, in terms of a more general comparison, it is important to note that, when the effective infiltration evidential theme was included in the analysis, the percentage of pixels that

were in the same or in a 1-degree higher or lower vulnerability class in both maps was approximately 50%. This percentage increased to approximately 91% when the effective infiltration evidential theme was not included in the analysis (Table 6.6).

The degree of inter-class agreement was subsequently evaluated through the Cohen's Kappa coefficient, κ, which represents a more robust measurement of spatial agreement, than the simple percent calculation previously illustrated, due to the fact that it takes into account the agreement occurring by chance (Cohen, 1960).

The Cohen's Kappa coefficient can be calculated as:

$$\kappa = \frac{P(a) - P(e)}{1 - P(e)} \tag{6.1}$$

where *P(a)* is the relative observed agreement between two raters (i.e., reclassified vulnerability maps) and *P(e)* is the probability that the agreement is due to pure chance.

Kappa statistics expresses the degree of agreement between different classified maps and not the agreement between a map and the measured or observed data. Indeed, Cohen's Kappa measures the agreement between two raters, each one classifying *N* items into *v* mutually exclusive classes. The procedure for calculating the Kappa statistic is based on the creation of a confusion matrix of the class frequencies of two maps.

Thus, if two maps are in complete agreement then $\kappa = 1$ while if there is no agreement (other than that that would be expected by chance) then $\kappa \leq 0$.

Because the calculation of κ is not symmetric, as *P(a)* in Equation (6.1) may change due to differences in the relative area of each class in the two compared maps, κ values ware calculated using the ratio of agreement of the positive over the negative maps and vice versa, both for the positive and negative maps obtained including the effective infiltration evidential theme in the analysis and for the positive and negative maps obtained without including it (Fig. 6.6).

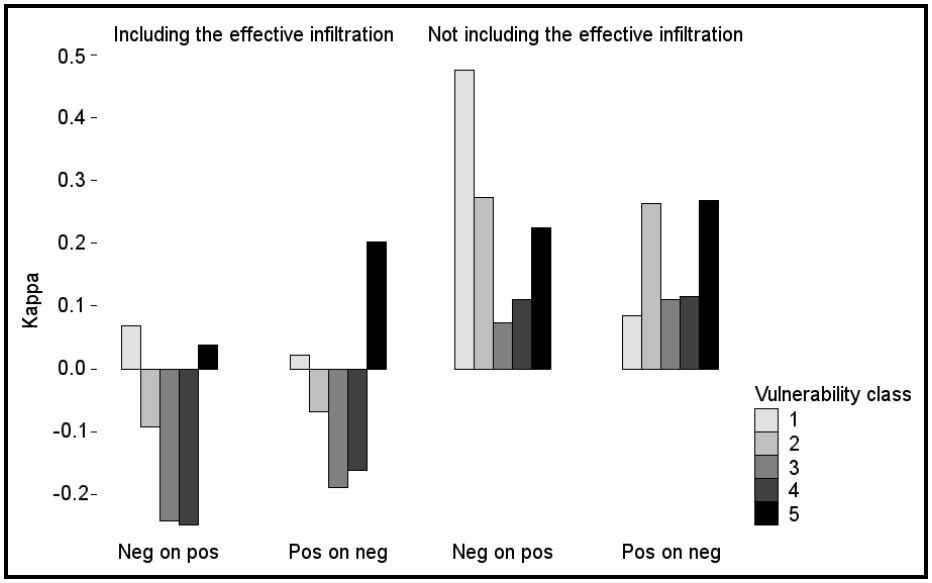

Figure 6.6 – Degree of inter-class agreement between vulnerability maps A and B in Figure 6.4, both obtained including the effective infiltration evidential theme in the analysis (leftmost and second histogram), and between vulnerability maps C and D in Figure 6.4, both obtained not including the effective infiltration evidential theme in the analysis (third and rightmost histogram): in both cases, the Cohen's kappa coefficient was computed both by considering the negative vulnerability map with respect to the positive one (leftmost and third histogram) and vice versa (second and rightmost histogram).

Again, the results showed that there is a lower agreement between the maps obtained including the effective infiltration evidential theme in the analysis (maps A and B in Fig. 6.4) than between the maps obtained not including it (maps C and D in Fig. 6.4). Indeed, in the first case, κ values were generally very low for all classes and even negative for classes 2, 3, and 4 (histograms on the left in Fig. 6.6), which indicates spatial disagreement between these classes. In contrast, in the second case, κ values were always positive and relatively high, especially for vulnerability classes 1, 2, and 5 (histograms on the right in Fig. 6.6).

6.2.4 Validation

The predictive power of each vulnerability map was evaluated by computing the density of known non-occurrences in each vulnerability class, meaning that negative evidences were used with the positive maps while positive evidences were used with the negative maps.

Because the study area was divided into pixels having all the same size (50 meters of resolution), the density of known non-occurrences, *D*, can be expressed as:

$$D = N\{E_v\} / N\{T_v\} \tag{6.2}$$

where $N\{E_v\}$ is the number of pixels containing known non-occurrences within the vulnerability class v and $N\{T_v\}$ is the total number of pixels within the same vulnerability class v.

The density of positive and negative evidences is expected to monotonically increase and monotonically decrease from vulnerability class 1 to 5, respectively. Furthermore, the density value of both positive and negative evidences in the medium-vulnerability class (class 3 in Fig. 6.4) is expected to be as close as possible to the prior probability value.

Both maps obtained including the effective infiltration evidential theme in the analysis (maps A and B in Fig. 6.4) performed very poorly (histograms A and B in Fig. 6.7), whereas both maps obtained not including it (maps C and D in Fig. 6.4) performed fairly well in terms of predicting the location of known non-occurrences (histograms C and D in Fig. 6.7).

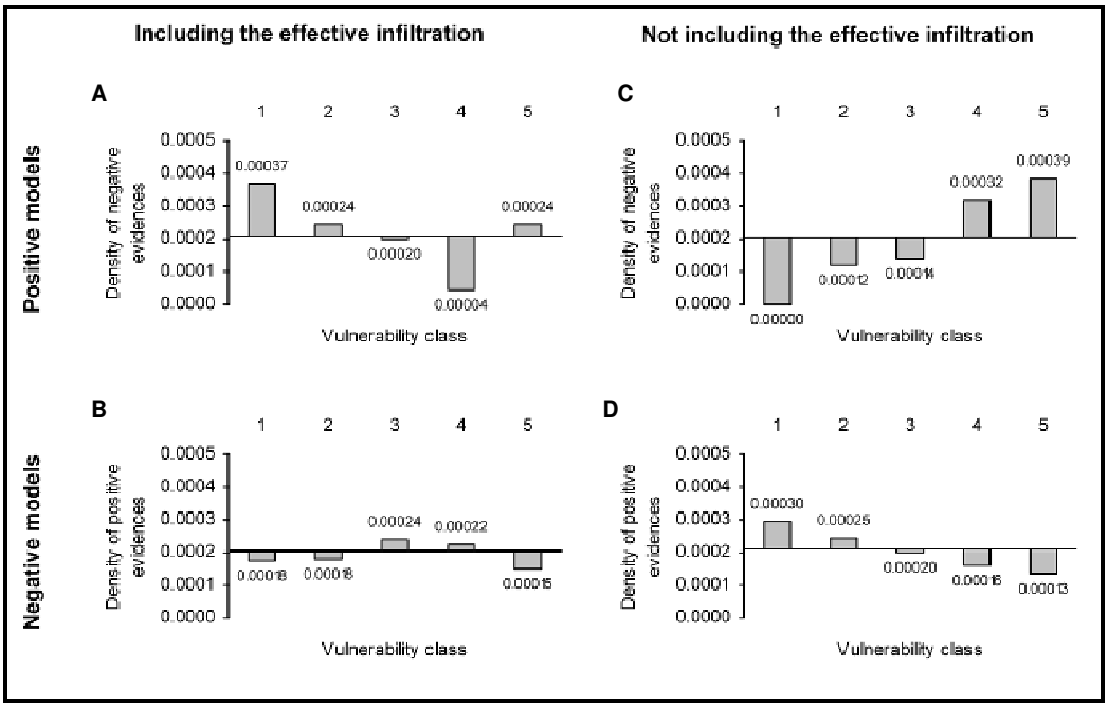

Figure 6.7 – Density of known non-occurrences within each vulnerability class (the degree of vulnerability increases from class 1 to 5); histograms A, B, C and D refer, respectively, to maps A, B, C and D in Figure 6.4.

The performance of each map was also evaluated considering the average nitrate concentration of all samples collected in the wells located within each vulnerability class (Chowdury, 2003). The average nitrate concentration, C_{avg}, referring to each vulnerability class can be expressed as:

$$C_{avg} = \sum_{i=1}^{N\{S_v\}} C_{iv} / N\{S_v\} \tag{6.3}$$

where C_{iv} is the nitrate concentration of a sample i collected within the vulnerability class v and $N\{S_v\}$ is the total number of samples collected within the same vulnerability class v.

The average nitrate concentrations were calculated using all collected samples (with nitrate concentration either above or below the selected threshold).

However, these data can be used without falling into an internal validation. In fact, the statistical procedure applied to produce the positive and negative vulnerability maps only used information concerning the location of the impacted or non impacted wells respectively, that is, where wells had concentrations higher, or lower, than the threshold value. No additional information on the actual value of concentration was used to produce the final maps, although this is the variable on which this validation procedure is based.

The advantage of using all data is that a quasi equal number of non-impacted and impacted wells does not unbalance the mean concentration value toward low values.

The average nitrate concentration is expected to monotonically increase from vulnerability class 1 to 5. Furthermore, because all of the samples were used to calculate the average concentration, in the medium-vulnerability class (class 3 in Fig. 6.4), it is expected to be as close as possible to the selected threshold value of 19.5 mg/l.

The positive map obtained including the effective infiltration evidential theme in the analysis (map A in Fig. 6.4) and both maps obtained not including it (maps C and D in Fig. 6.4) performed fairly well (histograms A, C, and D in Fig. 6.8). In this case, only the negative map obtained including the effective infiltration evidential theme in the analysis (map B in Fig. 6.4) performed poorly, showing neither a general monotonic trend nor an average concentration in the medium-vulnerability class fairly close to the selected threshold value (histogram B in Fig. 6.8).

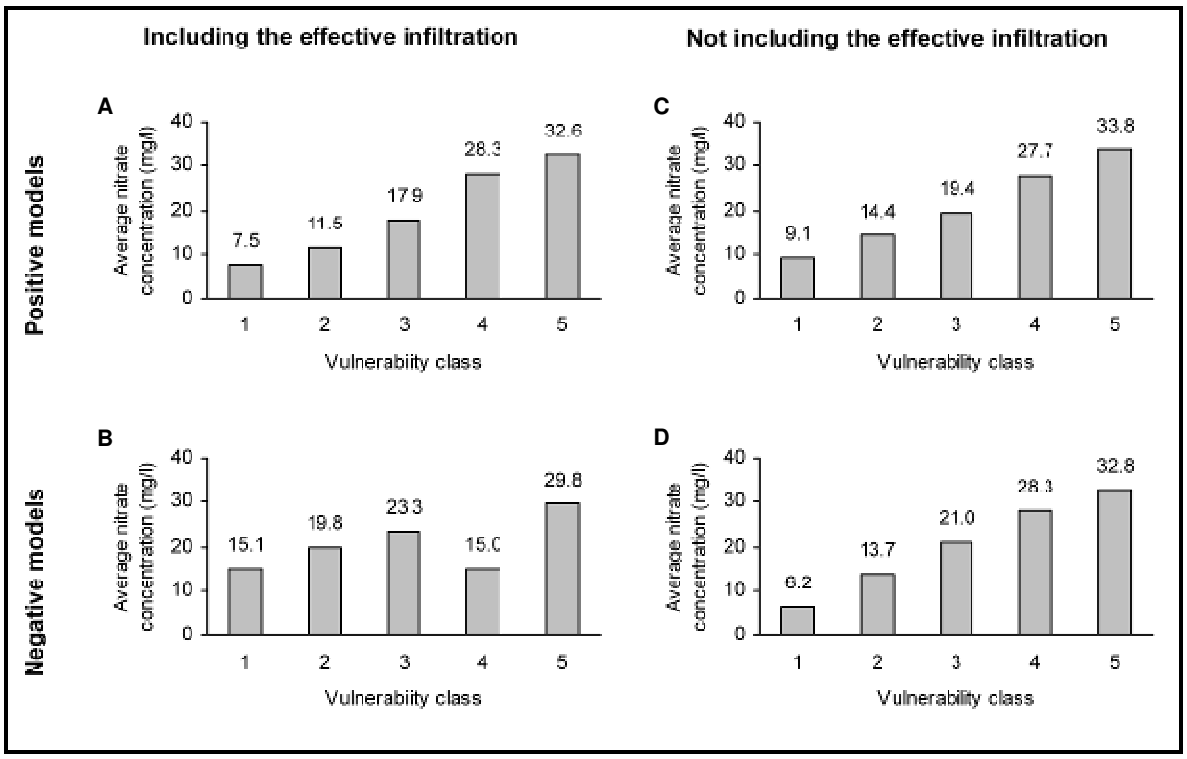

Figure 6.9 – Average nitrate concentration of samples collected in the wells located within each vulnerability class (the degree of vulnerability increases from class 1 to 5); histograms A, B, C and D refer, respectively, to maps A, B, C and D in Figure 6.4.

6.3 Conclusions

In the study presented in this Chapter, both positive and negative evidences were alternatively identified as TPs. All ordered evidential themes considered for being included in the analysis showed opposite relationships with the presence of positive and negative evidences, with the exception of the effective infiltration evidential theme. Hence, even if an evidential theme appears to be a good and statistically significant predictor of occurrences, it can yield a non-univocal relationship with the presence of positive and negative evidences. Thus, in the study presented in this Chapter, the effective infiltration evidential theme can be defined as a "puzzling" evidential theme characterized by a contradictious relationship with the presence of positive and negative TPs. This result may be caused by the presence of a bias, between the location of the TPs and the evidential theme, that could be subtle and thus difficult to identify

(Coolbaugh et al., 2007), particularly when an evidential theme is generated combining diverse explanatory variables (i.e., effective infiltration evidential theme in this Chapter). Regardless of the reason for the non-univocal relationship, its present should suggest to not include the "puzzling" evidential theme in the analysis. Using both positive and negative evidences as TPs allowed to determine the presence of a "puzzling" evidential theme and to make comparisons between maps that had to be similar in terms of vulnerability, highlighting whether they presented a significant disagreement in terms of their vulnerability pattern.

The drawbacks caused by including "puzzling" evidential themes in the analysis are shown by results of the pixel-by-pixel analysis and by the global Kappa value. Indeed, the global Kappa value was approximately 0.16 when considering the maps obtained not including the effective infiltration evidential theme in the analysis and approximately -0.09 when considering the maps obtained including it.

Furthermore, the validation of all maps considering the density of known non-occurrences showed that both positive and negative maps performed well in terms of prediction only when the "puzzling" evidential theme was not included in the analysis.

Thus, when the evidential themes to be used are appropriately selected through a deep analysis of their impact on the results, WofE proved to be a reliable modeling technique for assessing groundwater vulnerability. The results obtained and the validation tests indicated excellent performance of the WofE in identifying different vulnerability classes, when the final map was produced either using positive or negative evidences as TPs. Furthermore, following the principle upon which each explanatory variable must have a univocal effect on the physical process of groundwater contamination, the robustness of the WofE was confirmed by the good spatial agreement between the two final maps obtained not including the "puzzling" evidential theme in the analysis. Indeed, the two final vulnerability maps obtained not including the "puzzling" evidential theme in the analysis are nearly identical, being more than 90% of the study area classified within the same degree or within a difference of one degree of vulnerability in both maps.

The approach presented in this Chapter was demonstrated to be extremely powerful for appropriately selecting the explanatory variables to be used in the analysis and for testing the robustness of the modeling technique employed. It can be easily applied to other statistical techniques, such as the likelihood ratio function, that model binary-response variables using only one type of evidences (occurrences or non-occurrences).

Chapter 7
Reliability of vulnerability maps obtained using statistical methods

Hazard maps determined through statistical methods are extremely useful tools to support decisions necessary for environmental planning and management. The final results of these studies are represented by maps of the study area identifying zones with different degree of susceptibility to hazardous events. Various methods, such as logistic regression (Tesoriero and Voss, 1997, Nolan et al., 2002, Gardner and Vogel, 2005), discriminant analysis (Carrara, 1983), likelihood ratio functions (Chung, 2006) and Weights of Evidence (van Westen et al,. 2003, Neuhäuser and Terhorst, 2007, Poli and Sterlacchini, 2007, Masetti et al., 2008) have been used either as a single approach to a specific study area or for comparison (Harris et al., 2003; Antonakos and Lambrakis, 2007). One of the key features in all these studies is the validation of the model outputs (Brenning, 2005). Validation is usually performed through the application of several techniques to analyze the quality and reliability of the final results and to evaluate the model that has the best performance. These techniques are crucial to evaluating the quality of the results and as reported by Fabbri and Chung (2008), the current emphasis in the field should be on the development and application of reliable and robust procedures rather than in new methods.

Although many validation techniques can be used (Fabbri and Chung, 2008), little attention has been paid to the comparison of results obtained using the same technique, especially in terms of the spatial agreement of predicted hazard patterns (Sterlacchini et al., 2011). Final maps from different combinations of predictors can lead to maps with very different spatial distributions vulnerability but having a quality that is apparently similar (Fabbri et al., 2003). This concept is extremely important because it may happen that two or more maps with similar predictive power show poor agreement in terms of the predicted spatial patterns. This discrepancy generates numerous problems when disseminating the final results to the users including how to use maps to develop efficient land use policies.

Groundwater vulnerability assessment requires a particular approach to evaluating the quality of the final results. In landslide hazard assessment, validation procedures can be rightfully

concentrated on the ability of the method to correctly identify classes with the highest hazard values, with less interest on the classes with low values. However the situation is different in groundwater vulnerability assessment, which is not a property that can be directly measured or surveyed in the field (Gogu and Dassargues, 2000). Every aquifer can be considered vulnerable, even if some areas are more vulnerable to groundwater contamination than others (Vrba and Zaporozec, 1994). Therefore, the reliability of a model that allows vulnerability assessment should be evaluated for the entire study area and not only on its ability to correctly identify the most vulnerable zones.

The study presented in this Chapter focus on two main aspects such the application of a series of validation techniques to evaluate the best groundwater vulnerability map in terms of representing the nitrate distribution in the study area and the spatial agreement among maps showing similar performances but different spatial predicted patterns. This was done in order to demonstrate that a rigorous validation procedure is fundamental to identify the map best representing the actual distribution of the nitrate contamination in the study area and thus the most suitable one to be used for environmental planning and management.

Because statistical modeling techniques are widely recognized as providing scientifically defensible outputs (Focazio et al., 2002), with WofE among them (Arthur et al., 2007), their meaningfulness and reliability have been the key aspects considered in the process of final product selection.

7.1 Training points and evidential themes

In this Chapter, the WofE model was used to assess groundwater vulnerability to nitrate contamination in the porous, unconfined, shallow aquifer located in the Province of Milan (which hydrogeological characteristics and nitrate distribution are described in Chapter 4, Paragraph 4.1 and Chapter 5, Paragraph 5.1, respectively).

The water-quality data set from the 2001 survey (described in Chapter 5, Paragraph 5.1) is the data set that was used in the study presented in this Chapter.

Because the frequency histograms of nitrate concentration in the study area revealed a light right-skewed (non-normal) distribution (Fig. 7.1), the median of 19.5 mg/l was identified as the best measure of its central tendency and thus selected to be used as the threshold.

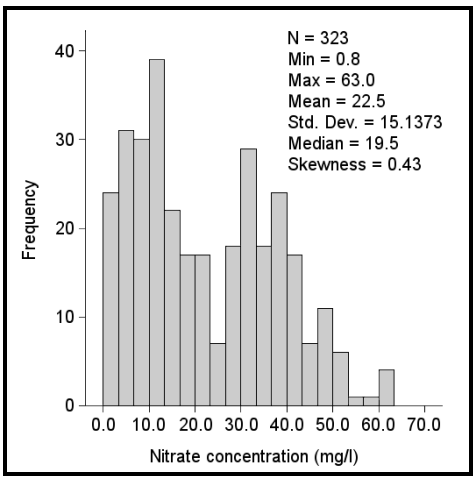

Figure 7.1 – Frequency histograms of nitrate concentration of water-quality dataset collected in 2001.

Wells showing concentrations higher than the median value were considered as impacted wells (162) and those below as non-impacted wells (161) (Fig. 7.2).

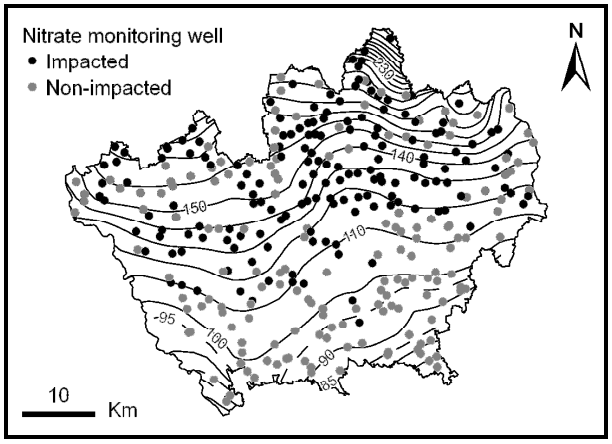

Figure 7.2 – Locations of the wells in the 2001 monitoring network: nitrate concentration in samples from impacted and non-impacted wells is, respectively, greater than or equal to and lower than 19.5 mg/l.

Impacted wells were divided into two mutually exclusive subsets (each one containing 81 wells) through a spatially random selection performed by the Hawth's Analysis Tools for ArcGIS (Beyer, 2004). One subset (training subset) was used to calibrate the response themes obtained through the WofE modelling technique, the other one (predictive subset) to evaluate the predictive power of the response themes (Chung and Fabbri, 1999).

From the hydrogeological conceptual model, five explanatory variables (described in Chapter 5, Paragraph 5.2), already proved to control nitrate contamination of shallow groundwater in the study area (see Chapter 6), were included in the analysis and thus used as evidential themes (Table 7.1).

Explanatory variable	Type	Minimum	Maximum	Alias
Population density [persons/km^2][a]	Continuous	43	8027	pop
Nitrogen fertilizer loading [kg/ha per year][a]	Continuous	0	289	nfl
Groundwater depth [m]	Continuous	0	70	gwd
Unsaturated hydraulic conductivity [m/s]	Continuous	3.21E-10	8.40E-02	uhc
Groundwater velocity [m/s]	Continuous	8.79E-09	2.10E-05	gwv

[a] computed at municipality level

Table 7.1 – Explanatory variables used as evidential themes.

7.2 Response themes

Six groundwater vulnerability response themes, showing different spatial vulnerability patterns in terms of post probability, were generated using six different combinations of evidential themes (Table 7.2).

Combination of explanatory variables	Model output name
gwd, gwv, nfl, pop, uhc	A
gwd, gwv, pop, uhc	B
gwd, gwv, nfl, uch	C
gwv, nfl, pop, uhc	D
gwd, nfl, pop, uhc	E
gwd, gwv, nfl, pop	F

Table 7.2 – Combination of explanatory variables used to generate response themes (variable alias are in Table 7.1).

The general quality of each response theme, expressed as post probability output, was evaluated by the predictive rate curve (PRC) method (Chung and Fabbri, 1999). For each combination, PRC was performed by plotting on the X-axis the cumulative percentage of vulnerable areas (from the highest probability values to the lowest) and, on the Y-axis, the cumulative percentage of occurrences being in the predictive subset. The percent of events falling into each cumulative

post probability class gives the prediction rate, which is useful for supporting the result of each model and assessing their robustness. According, steeper is the curve, better is the capability of the model to adequately describe the groundwater vulnerability of the study area.
PRCs are represented in Figure 7.3, which shows that all of the curves had a similar performance except for response theme D, which performed relatively worse in correspondence of the middle-low post-probability values.

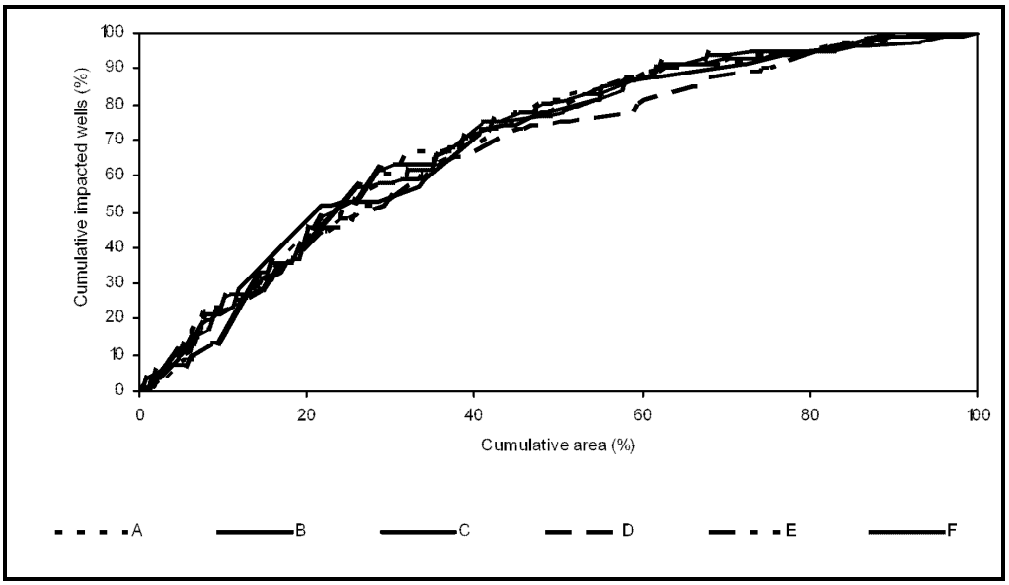

Figure 7.3 – Predictive rate curves of the response themes in Table 7.2.

The curves have a high degree of overlap crossing each other at many points, so that it becomes difficult to establish which has the best performance. It must be considered that the technique for determining the best model based on the percentage of cumulative occurrences in a specified percentage of cumulative area (Fabbri et al., 2003; van Westen et al., 2003) should not be used for groundwater vulnerability. Indeed, as already mentioned, the reliability of a model for vulnerability assessment should be evaluated over the entire study area and not only its ability to correctly identify the most vulnerable zones. Furthermore, this method could lead to an arbitrary selection of the best response theme, being the selection based on the specific percent of area considered for evaluating the predictive power. In other words, the model having the higher percentage of cumulative occurrences in a given percent of area could be a different one if a diverse percent of area is considered. While these curves are extremely useful in discriminating models of greatly varying quality, they are not always able to sort models that are not greatly

different; this is especially the case when a good performance is preferred for every range of post probability values. These limitations have important consequences on how to select the response theme, and so the groundwater vulnerability map to be proposed as the best one to be used for environmental planning and management.

7.3 Results and discussion

7.3.1 Spatial agreement

The spatial variability among different groundwater vulnerability maps, obtained reclassifying the best performing response themes in (Fig. 7.3), was assessed to evaluate whether different model outputs, showing apparently similar quality, can be considered equivalent in terms of the spatial distribution of vulnerability classes.

As already described in Chapter 6, Paragraph 6.2, response themes were reclassified using the Geometrical Interval Classification method (ESRI, 2007).

Cohen's Kappa coefficient (Cohen, 1960) was then used in this case to compare maps with the same thematic classification which results are in Figure 7.4 the heatmap indicating the spatial agreement among the six reclassified maps.

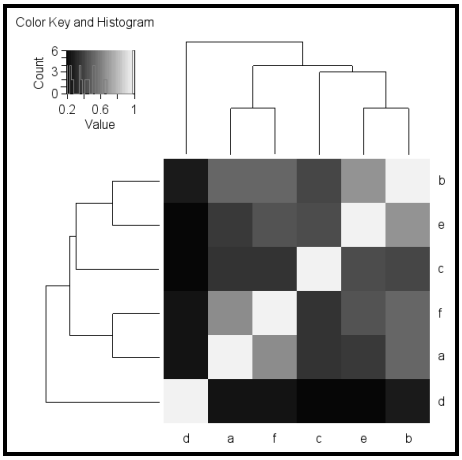

Figure 7.4 – Heatmap of reclassified vulnerability maps indicating their spatial agreement in terms of spatial distribution of their vulnerability classes: the colors from white to black indicate respectively the degrees of coincidence going from high to low.

The graph indicates that two pairs of maps, B with E and F with A, are in a very good mutual agreement although map B also shows a good agreement with the other pair of maps. Map D, already identified as the worst one by the PRCs (Fig. 7.3), shows a poor agreement with all other maps. Map C indicates a spatial agreement that is extremely variable, from good with E to poor with A and F, and very poor with D.

7.3.2 Validation of the reclassified groundwater vulnerability maps

Not considering map D, the analysis of spatial agreement indicates the need to provide a deeper insight into the validation procedure to give more quantitative evidence to adequately support the selection of the best performing map, or at least to help in reducing the indecision in choosing the best one.

Thus, the reliability of each reclassified vulnerability map was evaluated by considering its global performance in classifying the occurrences (i.e., not only its performance considering a percentage of the most vulnerable area). Three statistical validation procedures were used to select, among the different models, the vulnerability map that better represents the actual nitrate distribution in the study area.

The first procedure used to evaluate the global prediction performance of the reclassified maps, was the evaluation of the density of impacted wells in each vulnerability class, already described in Chapter 6, Paragraph 6.2.

Histograms were derived using the group of impacted wells from the predictive subset. The density of impacted wells is expected to monotonically decrease according to the degree of vulnerability, being as close as possible to the prior probability value for the central vulnerability class. The performance of each map was evaluated by considering the density value for each class (density trend), the angular coefficient of the regression line, the regression coefficient and the density agreement with the prior probability value (Fig. 7.5).

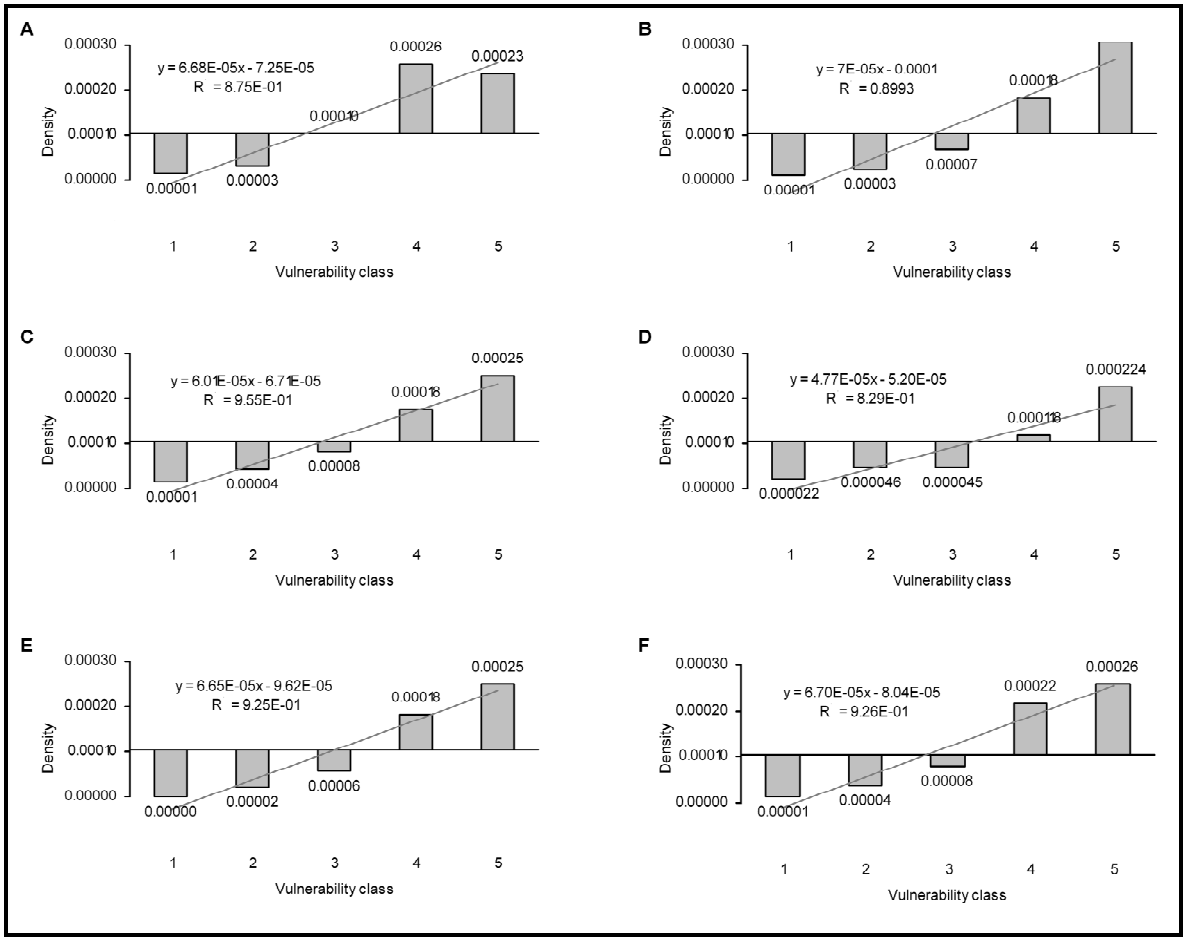

Figure 7.5 – Histograms of the density of impacted wells in the vulnerability classes for each map (the degree of vulnerability increases from class 1 to class 5).

The second validation technique adopted was the evaluation of the frequency of impacted wells, F_{iw}, expressed by the ratio:

$$F_{iw} = N\{W_{cv}\} / N\{W_v\} \tag{7.3}$$

where $N\{W_{cv}\}$ is the number of impacted wells in a vulnerability class v and $N\{W_v\}$ is the total number of wells in the same vulnerability class v. This technique adds some important information to the validation process because it includes the use of all the wells having concentrations lower than the threshold value, which were not used to perform the simulations. The histograms were derived using all non-impacted wells and the group of impacted wells in

the predictive subset. Frequency is expected to increase monotonically as the degree of vulnerability increases (Fig. 7.6).

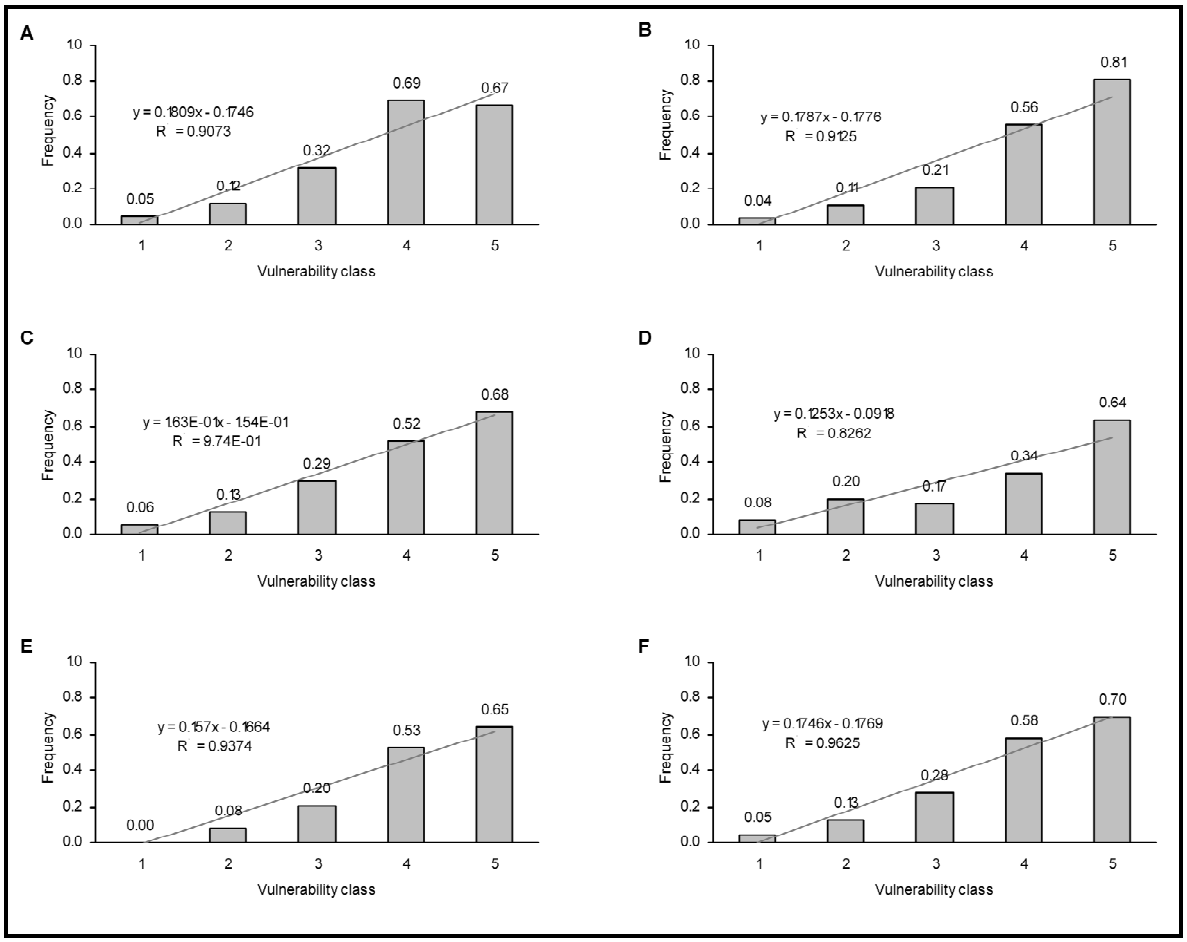

Figure 7.6 – Histograms of the frequency of impacted wells in the vulnerability classes for each map (the degree of vulnerability increases from class 1 to class 5).

The third and last technique was based on the evaluation of the average nitrate concentration of all wells, C_a, within each vulnerability class (Fig. 7.7), already describe in Chapter 6, Paragraph 6.2. Due to the poor performances of maps A and D considering the results obtained applying the first two techniques, C_a was evaluated only for maps B, C, E, and F.

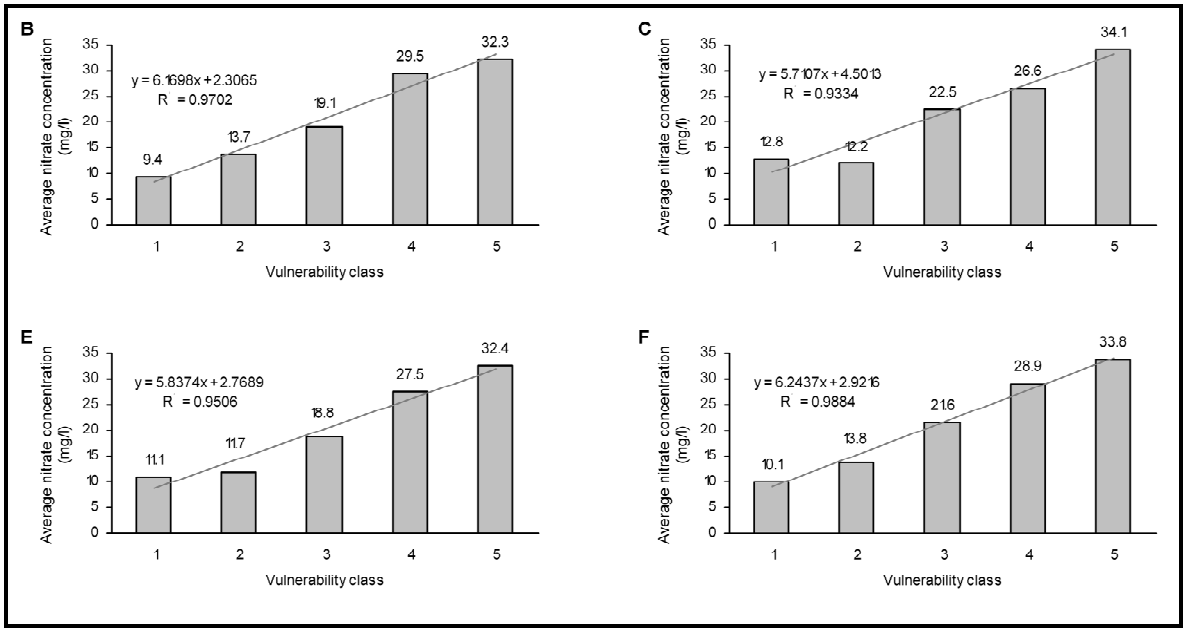

Figure 7.7 – Histograms of the average nitrate concentration in the vulnerability classes for maps B, C, E, and F (the degree of vulnerability increases from class 1 to class 5).

As in Chapter 6 this analysis was performed using all wells stored in the database.

Again, considering the results obtained applying the three techniques described above, the quality of each vulnerability map was evaluated considering the angular coefficient of the regression line and the regression coefficient. In all histograms, the degree of vulnerability increased from class 1 to class 5. A map should be considered reliable if it passes all three of the above mentioned procedures.

7.3.3 Discussion

The analysis of the density of the impacted wells (Fig. 7.5) confirms the relatively poor global performance of map D in identifying areas reflecting different vulnerability degrees; the density does not monotonically increase according to the degree of vulnerability. Map A expresses the same result, but its main drawbacks are in the identification of the highest vulnerability classes instead of the lowest. It should also be noted that the density value of class 4 is closer to the prior probability value than the density value of class 3. The global performances of the reclassified vulnerability maps B, C, E and F are excellent and are quite similar to each other. For all these

maps, the density values of the central class is the closest to the prior probability value, which suggests that the method used to reclassify the maps is quite good because it has accurately identified the average vulnerability class and has accurately distinguished higher from lower classes.

According to the criteria adopted to evaluate density histograms, map B can be considered the one that performs best, closely followed by map F. Both maps show the best angular coefficient of the regression line and regression coefficient values.

The histograms representing the frequency of impacted wells (Fig. 7.6), confirm the similar global performances of all maps. Once again, maps D and A do not show a monotonic increase with the increase of the degree of vulnerability, while the other four maps have nearly the same result. The evaluation of angular and regression coefficients still seems to highlight map B and F as the best.

The histograms representing the average nitrate concentration (Fig. 7.7) clearly show that maps B and F represent the actual spatial distribution of nitrate contamination better than maps E and C. The average concentration for classes 1 and 2 in map E is quite the same, whereas it is the higher one for class 1 in map C. Map F gives the best angular and regression coefficients. It is worth mentioning that the average concentration of the central vulnerability class of the best maps is very close to the median concentration used as the threshold, 19.5 mg/l. This result confirms that the used reclassification technique is suitable for identifying different classes each one characterized by a different degree of vulnerability (i.e., very low, low, medium, high and very high).

Among the best performing maps showed in Figure 7.8, the spatial variability assessment was quantitatively evaluated by performing a pixel-by-pixel analysis showing the difference, expressed as a percentage, in the unit cell classification for the selected maps.

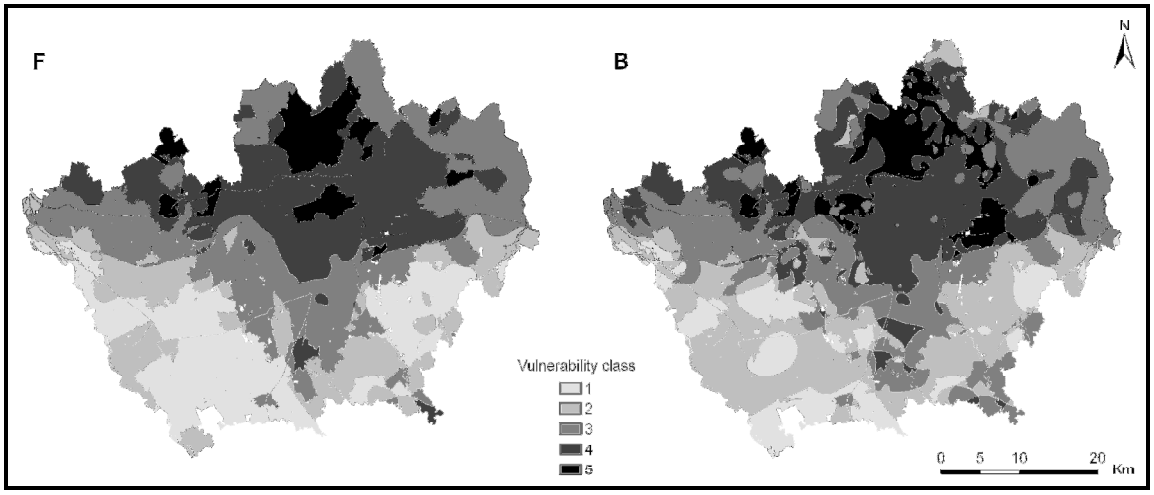

Figure 7.8 – Vulnerability maps of simulation B and F (the degree of vulnerability increases from class 1 to class 5).

A comparison between maps B and F (Fig. 7.9) shows that, in terms of vulnerability degree, 63% of the area is classified with the same degree of vulnerability in both maps whereas 36.6% of it difference for one degree of vulnerability. Only 0.4% of the total area shows differences in the classification of two degrees of vulnerability. These results show that, even if B and F are not the most similar maps resulting from the Kappa analysis, their global spatial agreement is excellent and the areas of high uncertainty are highly limited.

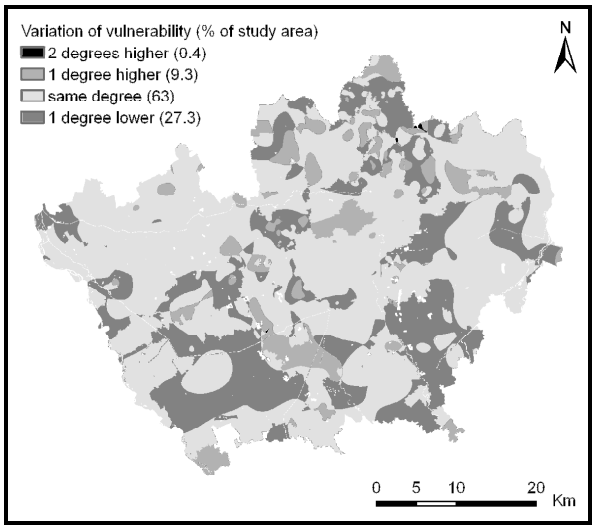

Figure 7.9 – Variation of vulnerability between map F and B, expressed as the study area vulnerability depicted in map F with respect to the one depicted in map B.

Because Kappa calculation is not symmetric (see Chapter 6, Paragraph 6.2), Figure 7.10 shows the Kappa values for both combinations of maps B and F. “B on F” and “F on B” means that the value of per class Kappa was calculated using the ratio of agreement of B over F and of F over B respectively.

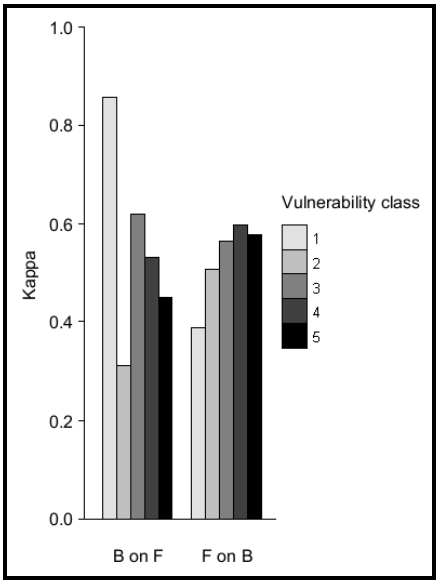

Figure 7.10 – Degree of agreement (Kappa) between vulnerability classes of maps B and F calculated considering map B with respect to map F (left) and vice versa (right).

As shown in Figure 7.10, all classes seem to be in mutual agreement, but vulnerability class 1 seems to have a high degree of concordance in map B over map F. This result could be due to the partial inclusion of class 2 into class 1, a hypothesis that is confirmed by the lower Kappa value for class 2 and the relatively low value of the Kappa of class 1 in the “F on B” comparison (the relative values of Kappa tend to have opposite trends in the two comparisons).

It should also be noted that the two best performing models were obtained using only four of the five considered evidential themes. The three explanatory variables present in both the simulations are population density, groundwater depth and groundwater velocity. The hydraulic conductivity of the vadose zone and nitrogen fertilizer loading are present in simulations B and F respectively. Population density, groundwater depth and groundwater velocity therefore, seem to be the most important factors influencing groundwater quality in the area, and they represent respectively a source of nitrate, a feature of the vadose zone, and one of the saturated zone, ideally following the path of contamination from the topographical surface to its spreading in

groundwater. Moreover, the nitrate sources from urban areas are more prevalent to those that are due to breeding and agricultural activities.

7.4 Conclusions

Characterizing the vulnerability of shallow aquifers to nitrate contamination should help decision makers evaluate current land use practices and make recommendations for regulation changes and/or the introduction of new prescriptions to better prevent or decrease groundwater contamination. Using statistical techniques can greatly support this activity through the production of vulnerability maps obtained by statistical methods. Obtained groundwater vulnerability maps should then be used to facilitate land-use planners and other potential end-users, such as environmental professionals and local governments, to minimize impacts on groundwater quality.

However, to be effective tools, groundwater vulnerability maps must be scientifically defensible, meaningful and reliable. Little attention is generally paid to the evaluation of the spatial variability of different maps that have similar performances in identifying areas reflecting different degrees of vulnerability (spatial predictive patterns).

In the study presented in this Chapter, different vulnerability maps were generated using the WofE modelling technique, with each map using different combinations of predictor factors. A spatial variability assessment between a pair of well performing maps showed that variability in vulnerability patterns is always present to some degree. It is important to determine which map (and, thus, which combination of explanatory variables) gives the most reliable results. Because a vulnerability map is meaningful and useful only if it represents the study area in a limited number of classes with different degrees of vulnerability, the spatial agreement of different reclassified maps was determined, and a series of validation procedures were applied to evaluate the reliability of the results.

The comparison shows that map performance is not directly related to the number of input predictor factors used and that it is possible to identify, among apparently similar maps, the one(s) that best represent groundwater vulnerability in a specific area.

The proposed validation procedures also indicate that the adopted reclassification method seems to correctly reflect the spatial distribution of the vulnerability as depicted in the pre-reclassified probability maps.

In conclusion, vulnerability maps represent essential tools to minimize impacts on groundwater quality only if they are reliable. Thus, vulnerability maps generated using statistical modeling techniques must be carefully handled before they are disseminated.

Indeed, the results may appear to be excellent and the final maps perform well while the spatial distribution of vulnerability might be very different from the actual distribution. For this reason, it is necessary to carefully evaluate the obtained results using multiple statistical techniques capable of giving quantitative insight in the analysis of the results. This should be done to at least to reduce the number of potential choices.

Chapter 8
Influence of thresholds in assessing groundwater vulnerability

The use of statistical methods to assess groundwater vulnerability, especially due to non-point sources of contamination, has increased considerably during the last few years. As already mentioned in Chapter 6, the most used statistical techniques to assess groundwater vulnerability model binary-response variables, as a function of one or more explanatory variables, to depict the probability of being in a response category. Hence, the necessity to select a threshold, allowing distinguishing between occurrences and non-occurrences of an event (i.e., impacted and non-impacted wells, respectively), represents a key issue in their application. Even if the threshold can be ideally selected form the complete range of the measured contaminant concentration values, it should be considered that using different thresholds very different results, depending on the adopted value were obtained for the same area (Muller and Helsel, 1997; Frans, 2000; Greene et al., 2004).

The European Groundwater Directive 2006/118/CE established that threshold values, defining groundwater quality, will be important instruments to assess the status of groundwater bodies. Furthermore, the definition of threshold values indirectly point out where groundwater has to be considered contaminated and thus where remediation measures have to be implemented to improve its status. In this context, it is extremely important to analyze the impact of different threshold values on the level of environmental protection (Hinsby et al., 2008).

In this Chapter, using three different threshold values, two different statistical methods were used to assess groundwater vulnerability to nitrate contamination in the unconfined, porous shallow aquifer located in the Province of Milan (which hydrogeological characteristics and groundwater nitrate distribution are described in Chapter 4, Paragraph 4.1, and Chapter 5, Paragraph 5.1, respectively) in order to compare the obtained reclassified maps, check their reliability and evaluate how the importance of each explanatory variable changes when using a different threshold.

In fact, while many research papers focused mainly on evaluate the technique which give more reliable estimation of background and threshold values (see Panno et al., 2006; Reimann and

Garrett, 2005; Reimann et al., 2005; for an extended bibliography), less attention has been given to the effect, on environmental planning and management, that could derive from the use of different threshold values.

8.1 Threshold analysis

Presently, several studies reported the difficulty of determining the natural background value of a contaminant in a specific environmental matrix due to the strong human influence on the whole planet. Background nitrate concentration in groundwater is among the most difficult to determine because of its multiple natural and anthropogenic, especially non-point, sources. Therefore, many techniques, ranging from evaluation of large data sets, analysis of historical data, sampling in pristine areas or in areas relatively uninfluenced by human activities (see Panno et al., 2006 for an extended bibliography), to statistical techniques (see Reimann and Garrett, 2005; Reinmann et al., 2005 for an extended bibliography), have been developed for determining significant background and threshold values. Although, all these techniques require making assumptions and present limitations, statistical techniques seem to be the most used in the scientific community due to the fact that allow performing rigorous analysis minimizing the subjective interpretation of the results.

A statistical technique borrowed from geochemistry exploration (Sinclair, 1974; 1991) was used to determine threshold values on the base of the actual distribution of nitrate contamination in the study area. The use of cumulative probability plots allows identifying two or more populations within the dataset of nitrate concentration in groundwater (Panno et al., 2006). The populations identified in the plot represent the background value and one or more anomalies, and inflection points identified the threshold values. This is based on the fact that the values of a single normally or log-normally distributed population will form a straight line on the plot while two or more mixed populations will result in a curved line showing inflection points. Thus, the inflection points can be considered as the threshold values distinguishing different populations. The main limitations of this technique are that at least 100 values are needed and that as any other statistical procedure it is subject to random and systematic error (Sinclair, 1991). However it is important to highlight that the aim of this work is to evaluate the effects on the vulnerability assessment due to the use of different threshold values for distinguishing between occurrence and non-occurrences and not to analyze which technique would give more reliable results in

terms of identifying background and threshold values. In the study area, four populations can be distinguished in the cumulative probability graph (Fig. 8.1).

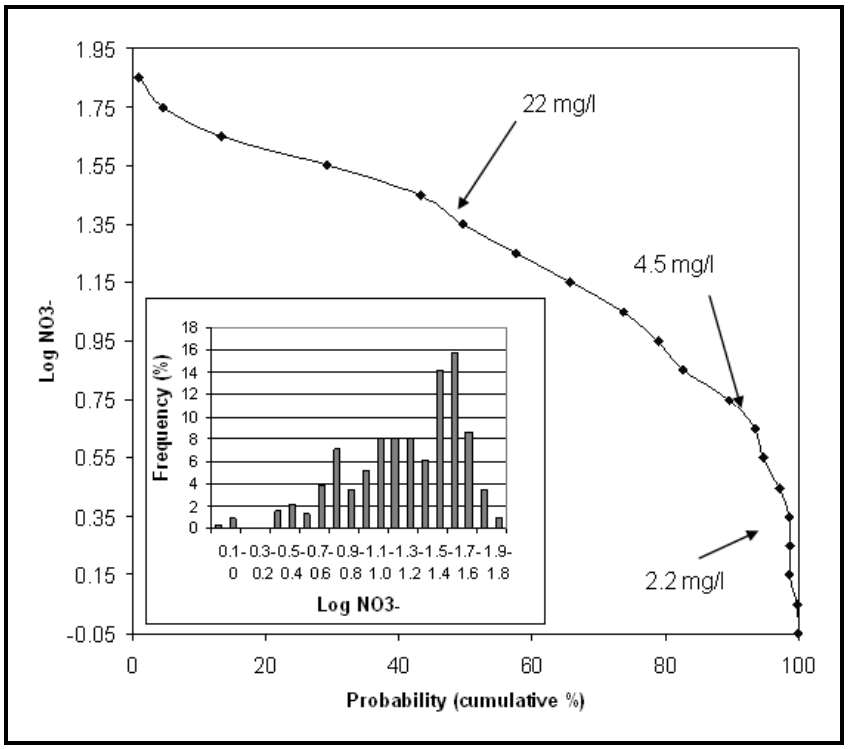

Figure 8.1 – Probability graph and threshold values representing the background value and two anomalies in the study area.

The identified threshold values were 2.2, 4.5 and 22.0 mg/l. According to Panno et al. (2006) these values can be roughly identified as “natural background”, “present day background” and “anthropogenic impact”.

8.2 Statistical analysis and evidential themes

Two different statistical methods were used in order to evaluate the effect on groundwater vulnerability assessment to nitrate contamination of using the three different threshold values identified in Figure 8.1.

- The Likelihood Ratio Function method (briefly described in the next section) was preliminary used to evaluate the effect on obtaining different vulnerability patterns in the reclassified maps.
- The WofE method (described in Chapter 3, Paragraph 3.2) was then used to evaluate the effect on the importance of the explanatory variables in controlling the vulnerability.

A different combination of explanatory variables, already proved to control nitrate contamination of shallow groundwater in the study area (Masetti et al., 2007), were used in the analysis with the LRF and the WofE method (Table 8.1). In particularly land use, rainfall and irrigation were not considered as inputs in the WofE method.

Explanatory variable	Type	Min	Max	Alias
Population density [persons/km^2] [a,b]	Continuous	43	8027	pop
Nitrogen load [kg/ha per year] [a,b]	Continuous	0	289	nfl
Soil protective capacity [b]	Categorical	-	-	spc
Groundwater depth [m] [b]	Continuous	0	70	gwd
Unsaturated hydraulic conductivity [m/s] [b]	Continuous	3.21E-10	8.40E-02	uhc
Groundwater velocity [m/s] [b]	Continuous	8.79E-09	2.10E-05	gwv
Land use [c]	Categorical	-	-	
Rainfall [mm/year] [c]	Continuous	816	1249	
Irrigation [mm/year] [c]	Continuous	0	1532	

[a] computed at municipality level; [b] used in both methods; [c] used only in the LRF method

Table 8.1 – Explanatory variables considered for being used in the analysis.

8.2.1 Likelihood Ratio Function

Vulnerable areas can be identified by the LRF of the multivariate frequency distribution calculated for each considered explanatory variables. Each pixel with k pixel values (a_1,..., a_k), one for each explanatory variables in the study area, where the subarea T is represented by those pixels where nitrate concentration in a well is higher than the a given threshold, while the remaining non vulnerable area $\overline{T}$ is represented by those pixels where no events are surveyed (i.e., measures of nitrate concentration are not available or below the selected threshold). LRF (Kshirsagar, 1972; Press, 1972; Cacoullos, 1973) is defined as:

$$\lambda(a:a_1,...,a_h)=\frac{f\{a_1,...,a_h \mid T\}}{f\{a_1,...,a_h \mid \overline{T}\}} \tag{8.1}$$

where $f\{a_1,...,a_h \mid T\}$ and $f\{a_1,...,a_h \mid \overline{T}\}$ represent the frequency distribution functions of the considered explanatory variables. Factors used were both categorical and continuous. Because the LRF is based on two multivariate distribution functions, there is the need neither to simplify the data nor to unify two data types into one data type. The multivariate generalization of the LRF is:

$$\lambda(a:a_1,...,a_h)=\frac{f\{a_1,...,a_h,b_1,...,b_m \mid T\}}{f\{a_1,...,a_h,b_1,...,b_m \mid \overline{T}\}} \tag{8.2}$$

where the first h and the last m values represent categorical and continuous variables, respectively. Based on the assumption of the conditional independence among factors, the $(h + m) = k$ dimensional multivariate frequency distribution function, the final LRF is simply a multiple of two LRF:

$$\lambda(a_1,...,a_h,b_1,...,b_m)=\lambda(a_1,...,a_h)*\lambda(b_1,...,b_m) \tag{8.3}$$

Thus, the LRF estimation is a multiplication of two estimated LRF, the first for categorical and the second for continuous variables, respectively.

The two functions can be estimated by each single categorical and continuous variable in conjunction with the distribution of the occurrences (Chung, 2006).

It is important to note that also in this case, as when using the WofE method, the vulnerability index calculated using the LRF has to be interpreted as a relative index and not as an absolute one, and thus it represents a sort of propensity of each pixel to be vulnerable.

8.3 Results and discussion

The threshold values identified in Figure 8.1 (2.2, 4.5 and 22 mg/l) were used to define three different subsets of occurrences (i.e., impacted wells) within the water-quality data set from 2000

and 2001 surveys (see Chapter 5, Paragraph 5.1) for being used as occurrences in the LRF and WofE method, respectively. However, being the number of occurrences in the subset identified using the value of 2.2 mg/l (315 for both years) very close to the one identified using the value of 4.5 mg/l (294 and 286 for 2000 and 2001, respectively), the former subset was not used in the analysis. Rather, a new subset was defined considering a threshold value of 50 mg/l (16 and 12 for 2000 and 2001, respectively), representing the quality standard of groundwater nitrate concentration as stated in the 2000/60/EC Directive (EU, 2000). Using the value of 22 mg/l 158 and 147 occurrences were identified for 2000 and 2001, respectively.

Each subset was then used as an independent dataset to assess the groundwater vulnerability of the study area and thus to obtain three different reclassified maps. Subsets obtained from the 2000 water quality data were used as TPs in the LRF method while the ones obtained from the 2001 water quality dataset were used as TPs in the WofE method. Each obtained map underlies the influence of the considered threshold, both regarding the spatial distribution of the vulnerability and the importance of each explanatory variable in controlling it.

8.3.1 Influence of using different thresholds on predicted vulnerability patterns

To better compare each other the vulnerability pattern predicted in each map, and thus the effect of the different threshold, the three probability outputs generated using the LRF method were reclassified to obtain groundwater vulnerability maps of ten vulnerability classes. Because the LRF allow using simultaneously categorical and continuous explanatory variables, the relative probability of contamination is calculated on a continuous scale at every pixel. In this case, in which each pixel should have a different value of post probability, the use of the Equal Area Classification method correspond to the use of the Geometrical Intervals Classification method, both allowing to obtain classes containing almost the same number of different post probability values.

Thus, the total area was divided into a number of classes each one having a similar number of pixels so that each class represented a similar amount of area (corresponding to using the Geometrical Interval Classification method when the probability outputs are generated using the WofE). Indeed, in this way, the first class consists of the pixels with the highest values and the next subsequent class is made up of the same number of pixels with the next highest values

(Chung and Fabbri, 1999). Ten equal classes were created, each one representing about the 10% of the study area. Class 10 containing pixels with the highest propensity to be vulnerable; whereas, class 1 held the lowest propensity, thus with the degree of vulnerability increasing from class 1 to 10.

Reclassified maps showing the relative vulnerability to nitrate contamination of the study area, named A-4.5, B-22 and C-50 according to the threshold used in the analysis, are presented in Figure 8.2.

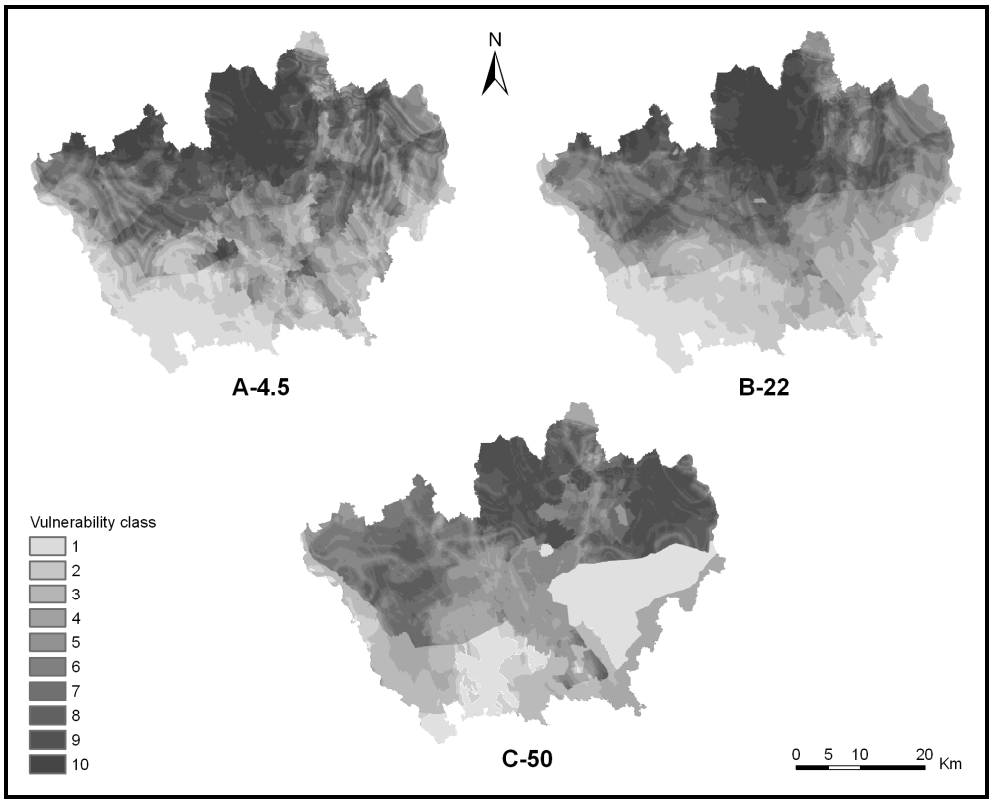

Figure 8.2 – Vulnerability maps, obtained using the LRF method, in which the degree of vulnerability increases from light grey to black: maps A-4.5, B-22 and C-50 were obtained using a threshold value of 4.5, 22 and 50 mg/l, respectively.

Even if some differences among the reclassified maps can be easily noticed, in all of them a general decrease in vulnerability from north to south can be highlighted, with the central area in the north as the most vulnerable to nitrate contamination in all maps.

Results show that changing the number of TPs, according to the different thresholds, leads to a different spatial distribution of the vulnerability classes. Using a large number of TPs, identified

by the 4.5 mg/l threshold, in most cases the total area representing each single vulnerability class results in smaller and more articulate separated areas, if compared with the one representing the same vulnerability class obtained using fewer TPs. Indeed, using the number of TPs, identified by the 50 mg/l threshold, the final map tends to delineate contiguous macro areas for each vulnerability class. Moreover, the shape of these macro areas seems to be more sensitive to the spatial distribution of a single explanatory variable. For example, the shape of the less vulnerable area in the south-eastern sector results highly influenced by the spatial distribution of the mean annual irrigation. Indeed, its boundary follows the limit between an irrigated area and a non-irrigated one.

To perform a more detailed and quantitative comparative analysis among the three different reclassified maps the Cohen's kappa coefficient, κ, (Cohen, 1960) was used. Comparing map C-50 and B-22 it is possible to note that most of the classes of a map are spatially coincident with another class of another map, although often not with the corresponding class (i.e. class 1 of map B-22 is more coincident with class 3 than with the class 1 of map C-50).

Moreover, as shown in Figure 8.3, the behavior of map agreement tends to be split between higher vulnerability classes and lower ones. By comparing A-4.5 and B-22, it is possible to distinguish two major spatial patterns: one common to classes ranking from 1 to 4 and another common to classes ranking from 5 to 10. Classes ranking from 1 to 4 are substantially interchangeable between the two maps, i.e. class 2 of B-22 is likely to spatially intersect class 1, 2, 3 and 4 of A-4.5 with almost the same probability.

In other words, in both maps the classes from 1 to 4 and the classes from 5 to 10 are correlated as they tend to occupy the same area in both maps. This means that the predicted vulnerability pattern of each map is different if ten vulnerability classes are considered but should become similar if only two vulnerability classes are considered and the probability value dividing class 4 from class 5 is used to separate the two classes.

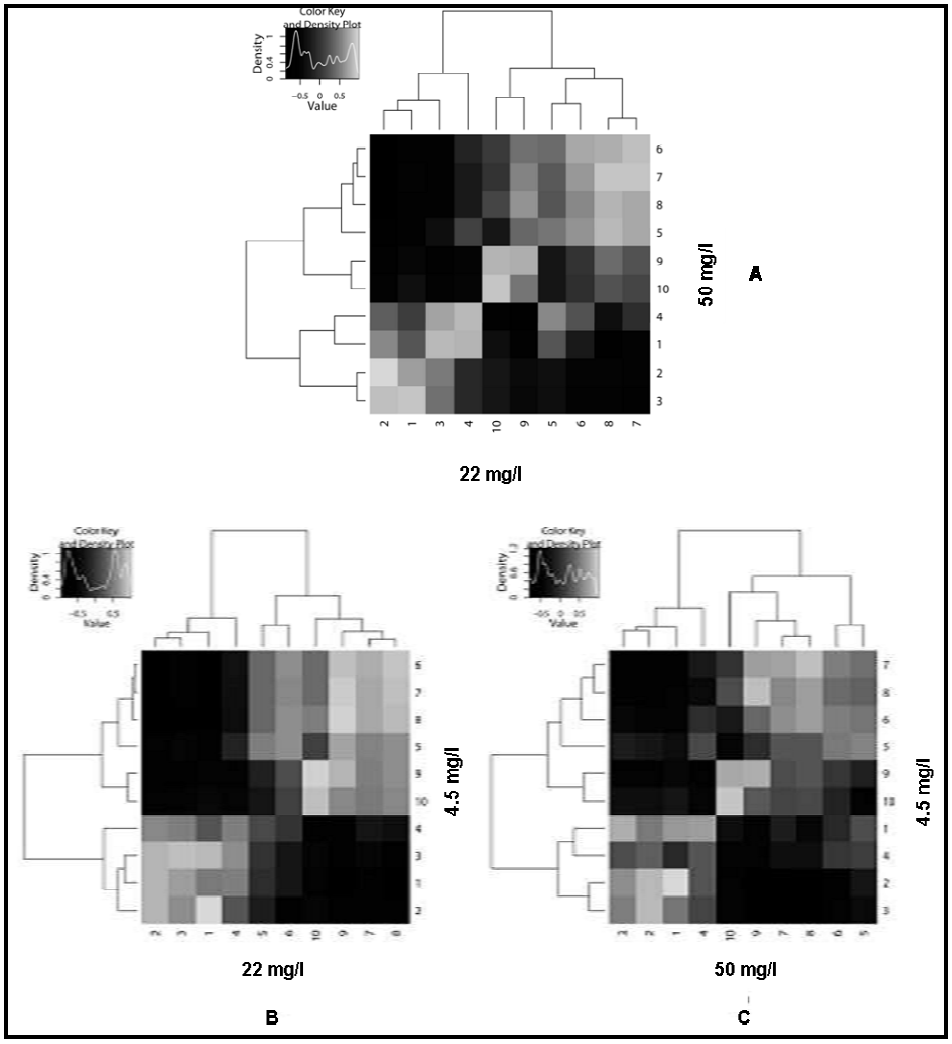

Figure 8.3 – Heatmaps of interclass reliability; heatmaps A B and C represent, respectively, the interclass reliability between maps B-22 and C-50, A-4.5 and B-22, and A-4.5 and C-50- in Figure 8.2.

As already mentioned in Chapter 7, in prediction modeling, a very important and essential component is the validation of the prediction results. Thus, the next step was to validate each final map by a procedure taking into account the predictive power of the results.

Being all water quality data sets collected between the 2000 and 2002 the expression of the same, almost unchanged nitrate-contamination pattern characterizing the shallow aquifer in the study area in that period (Table 8.2), in order to obtain a new data set to be used in the validation procedure the surveys 2 (2001), 3 (early 2002) and 4 (late 2002) were combined into one. This was done selecting only the wells not investigated in the survey 1 (2000).

Survey	Year	No. of wells	Nitrate concentration					Skewness
			Min	Max	Mean	Median	Std. Dev.	
1	2000	324	0.9	71.0	22.6	21.0	15.0	0.56
2	2001	323	0.8	63.0	22.5	19.5	15.1	0.43
3	Early 2002	307	1.0	70.0	22.4	20.0	15.3	0.36
4	Late 2002	249	1.0	52.0	21.5	20.0	14.1	0.42

Table 8.2 – Basic descriptive statistics of water-quality dataset collected in 2000, 2001, early 2002 and late 2002.

The obtained dataset resulted in a total of 110 wells, having nitrate concentration values both above and below the considered thresholds.

The average nitrate concentration of all samples collected in the wells located within each vulnerability class was calculated (as described in Chapter 6, Paragraph 6.2) to test the reliability of the three final vulnerability maps obtained using the LRF method. In this case another advantage of this procedure is that the same dataset is used in the validation of each map, regardless of the specific threshold value used to select the occurrences, avoiding comparing results that can be biased by the use of a different number of points in the validation.

A quantitative comparison among all models was done considering the angular coefficient of the regression line and the regression coefficient, leading to a rank of the goodness of the results.

Even if some differences can be easily pointed out, histograms show that all maps identify a general positive trend relating the average nitrate concentration in the wells and vulnerability classes they belong to. Validation procedure for the map A-4.5 (Fig. 8.2) gives the poorest performance as testified by both the lowest R^2 and angular coefficient: this result is mainly due to the poor ability to correctly classify wells in vulnerability classes ranging from 4 to 8, while extreme classes (from 1 to 3 and 9 to 10) seems to be well interpreted (histogram A in Fig. 8.5).

The performance of the other two maps is definitely better: map B-22 gives the highest angular coefficient (histogram B in Fig. 8.5) while map C-50 gives the highest R^2 (histogram C in Fig. 8.5). However, both models present some defects in wells classification; the former in the middle range classes while the latter in the extreme ones.

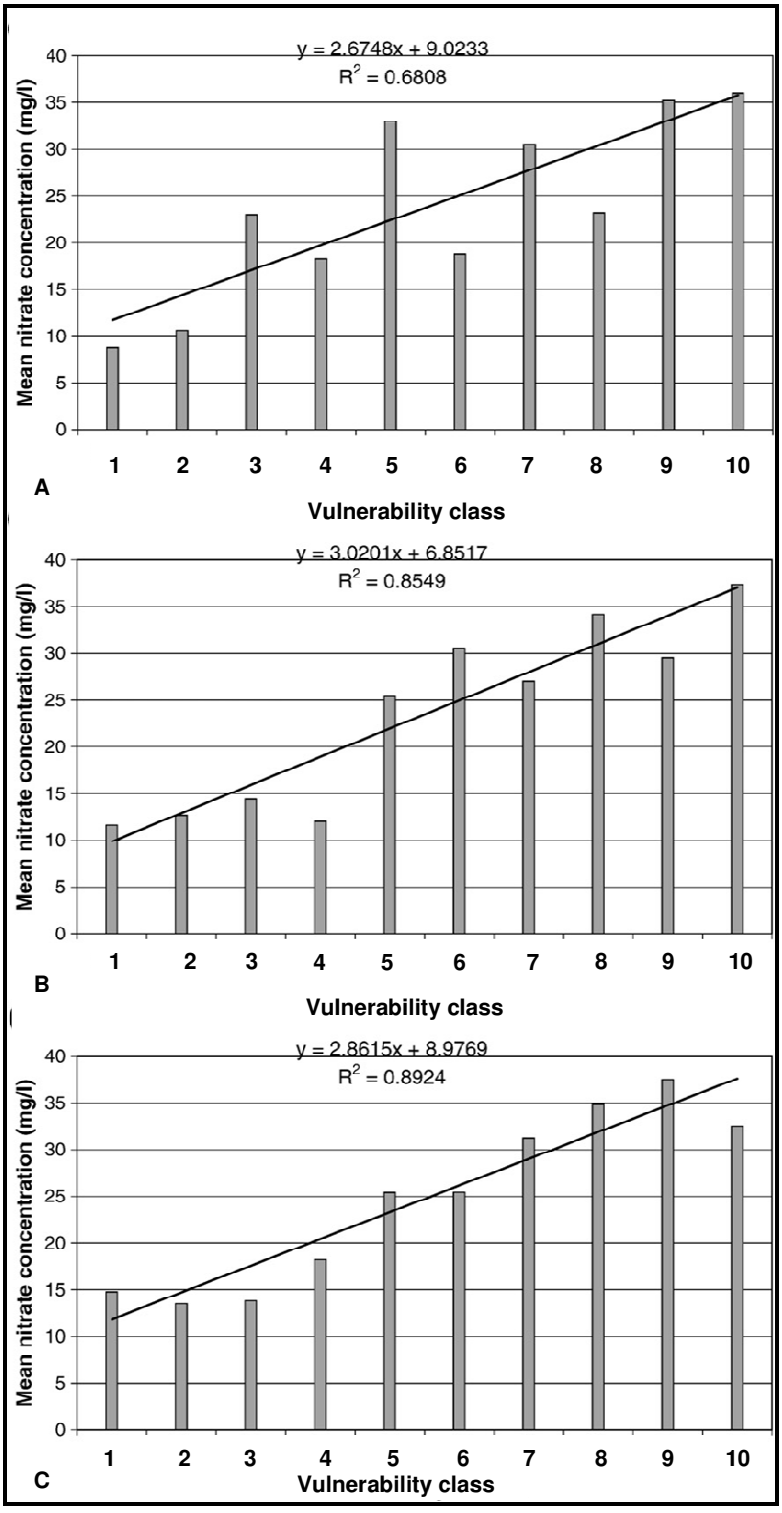

Figure 8.5 – Average nitrate concentration of samples collected in the wells located within each vulnerability class (the degree of vulnerability increases from class 1 to 10); histograms A, B and C refer, respectively, to maps A-4.5, B-22 and C-50 in Figure 8.2.

8.3.2 Influence of using different thresholds on the importance of each variable

Probability outputs generated using the WofE method, with the three threshold values identified in Paragraph 8.1, were reclassified using the Geometrical Interval method to obtain maps consisting of five classes, each one reflecting a different degree of vulnerability increasing from class 1 to 5 (Fig. 8.6).

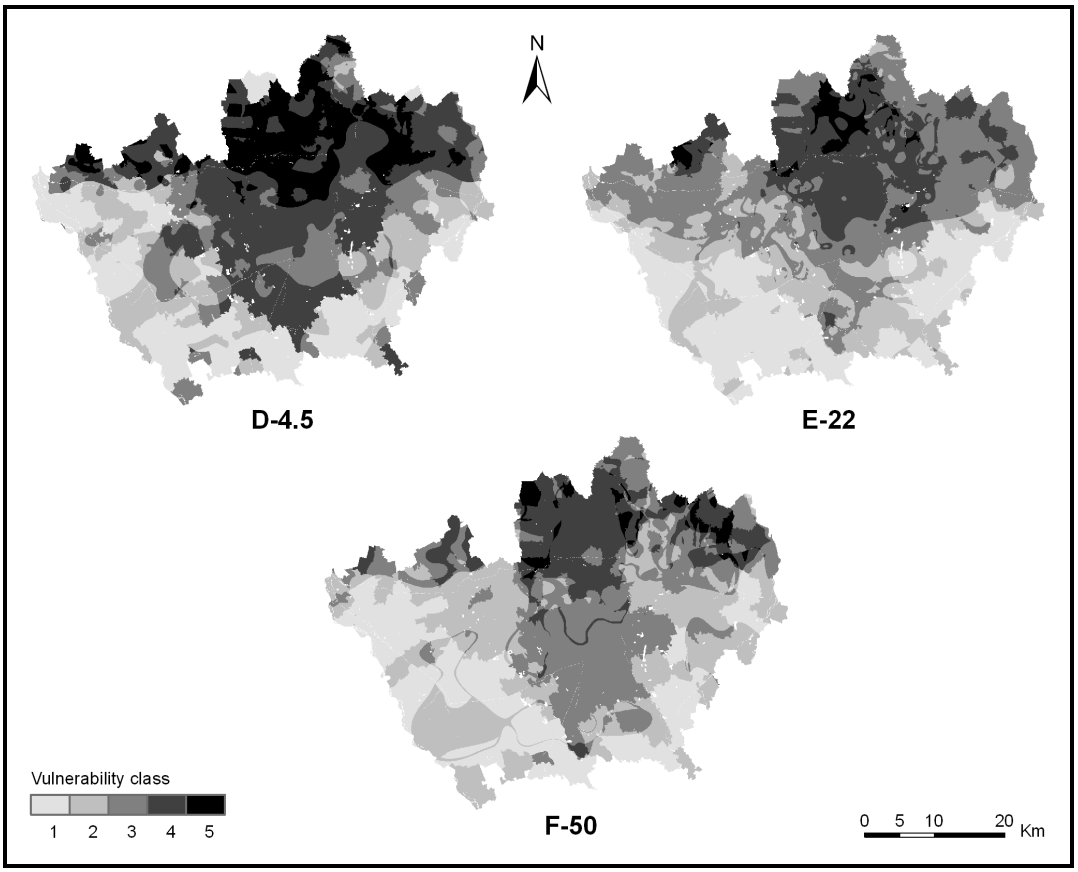

Figure 8.6 – Reclassified vulnerability maps D-4.5, E-22 and F-50 obtained using the WofE method and considering a threshold value of 4.5, 22 and 50 mg/l, respectively (the degree of vulnerability increases from class 1 to 5).

To investigate the effect of using different threshold values on the importance of each parameter in influencing groundwater vulnerability in the study area, both the contrast of each variable

class and their spatial distribution within the most and less vulnerable areas (respectively class 5 and 1 in all maps in Fig 8.6) were considered with respect to the threshold used in the analysis. From the analysis of the class contrasts of each explanatory variable for each considered threshold (Fig. 8.7), it is possible to evaluate how the importance of each single variable and thus of its ranges of values in influencing, both positively (positive contrast) and negatively (negative contrast), groundwater vulnerability to nitrate contamination change according with the considered threshold.

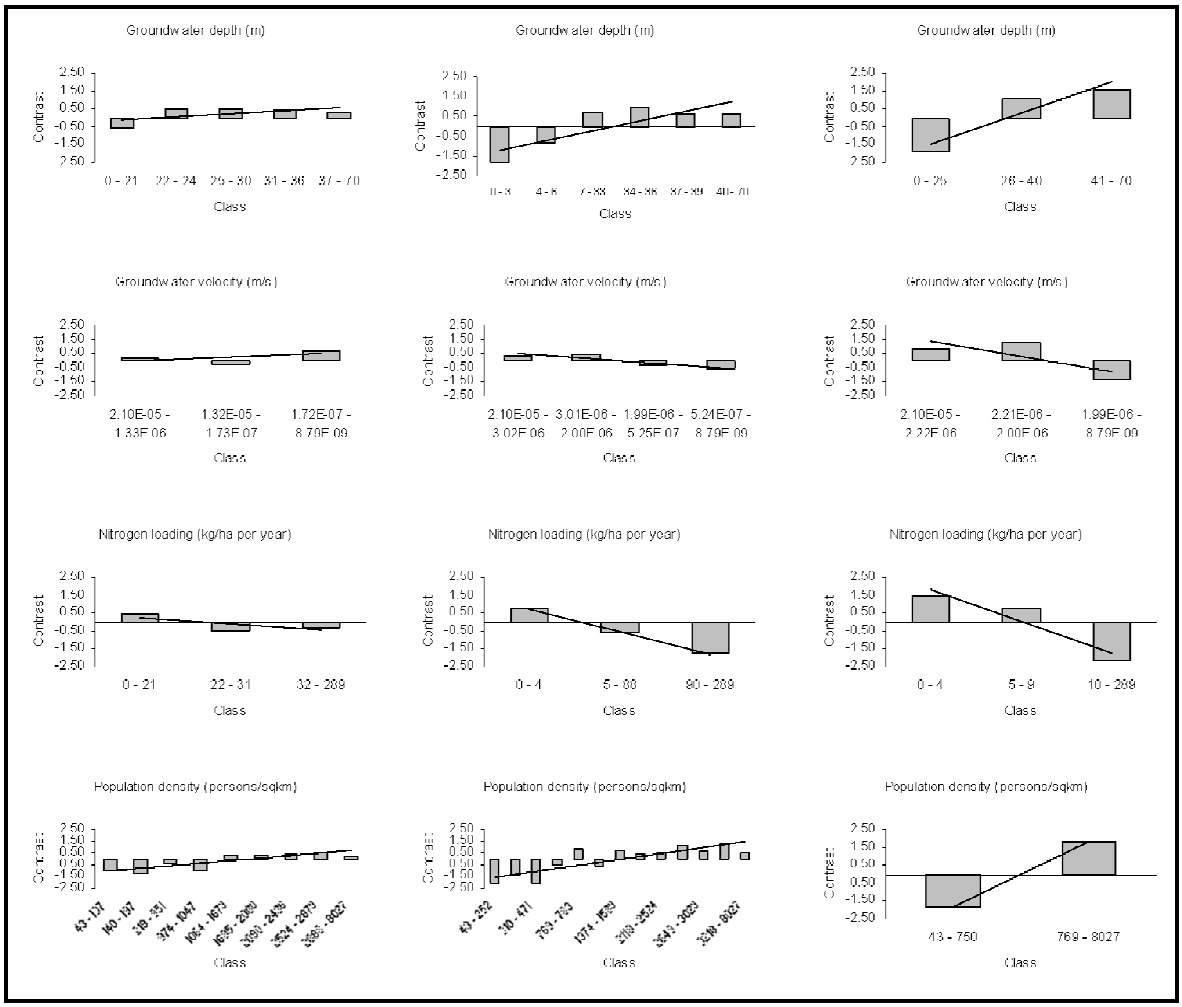

Figure 8.7 – Figure continues on next page.

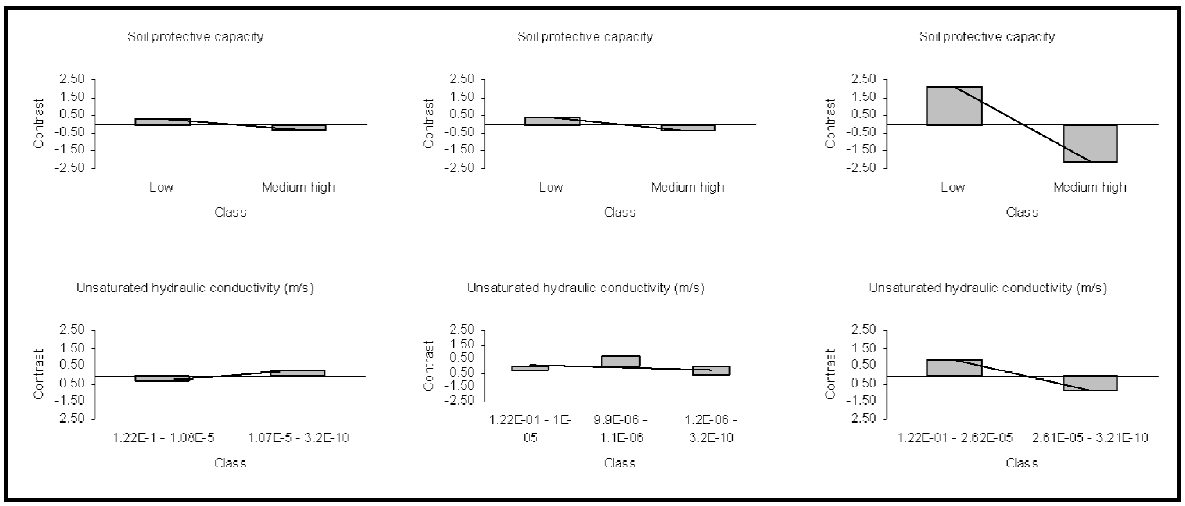

Figure 8.7 – Contrasts for each explanatory variable class identified by using a different threshold value in the analysis; histograms in the first, second and third column refer, respectively, to the model obtained considering a threshold value of 4.5, 22 and 50 mg/l.

From the histograms in Figure 8.7 a clear positive correlation between the increase of groundwater depth and population density and occurrences and a negative correlation between the increase of nitrogen load and occurrences can be identified in the study area regardless the threshold used in the analysis. Similarly, independently of the used threshold, high soil protection capacity class results always to be positively correlated with the presence of occurrences. Instead, the increase of both groundwater velocity and unsaturated hydraulic conductivity shows a positive correlation with occurrences when concentrations of 22 and 50 mg/l are used as thresholds in the analysis and conversely a negative correlation when the value of 4.5 mg/l is used.

It is interesting to note that:

- the explanatory variables showing the same trend regardless the threshold used in the analysis are also the ones having classes with higher contrasts and thus the stronger spatial relationship with the presence or absence of occurrences;
- the higher contrasts (and thus the higher spatial relationship between variable classes and presence of occurrences) are obtained when the threshold of 50 mg/l is used.

Thus, the explanatory variables showing the same relationship with the occurrences regardless of the threshold used in the analysis seem to be the most important ones in influencing nitrate

contamination in the study area. Conversely groundwater velocity and saturated hydraulic conductivity seem become influential only when the threshold used was higher than 22 and equal to 50 mg/l, respectively. Indeed, for groundwater velocity no clear spatial correlation is shown (contrast vary irregularly with increasing of the variable value) when the threshold of 4.5 is used in the analysis. Similarly for unsaturated hydraulic conductivity either there is no clear spatial correlation with the occurrences (22 mg/l) or contrasts are close to zero indicating a small influence on nitrate contamination above the considered threshold.

The higher contrasts obtained when using a threshold value of 50 mg/l could be due to the fact that few TPs allowed identifying only few statistically significant classes having a very strong correlation with them but representing a wider ranges of values for each variables.

The distribution of variable classes in the most and less vulnerable areas for each threshold was evaluated in order to define the combinations of the most important range of values of each variable associated with the lowest and highest probability to find nitrate concentration greater and lower of each specific threshold (Table 8.3 and 8.4, respectively).

Groundwater vulnerability map	D-4.5	E-22	F-50
Variables			
pop (persons/km^2)	> 1500	> 2500	> 750
gwd (m)	> 25	> 34	> 26
gwv (m/s)	> 1.3e-6	> 2e-6	> 2e-6
uhc (m/s)			> 2e-5

Table 8.3 – Combinations of explanatory variable classes most influencing the presence of high nitrate concentration.

Groundwater vulnerability map	D-4.5	E-22	F-50
Variables			
pop (persons/km^2)	< 200	<400	< 750
gwd (m)	< 21	< 3	< 25
gwv (m/s)	< 1.3e-6	< 2e-6	< 2e-6
uhc (m/s)			< 2e-5

Table 8.4 – Combinations of explanatory variable classes most influencing the presence of low nitrate concentration.

Regarding the spatial pattern of vulnerability, also in this case, using a different number of TPs (according to the different thresholds) leads to a different spatial distribution of the vulnerability classes but once again, as for the maps obtained using the LRF method, it is qualitatively

observable that, even if some differences among the reclassified maps can be easily noticed, a general decrease in vulnerability from north to south can be highlighted, with the central area in the northern sector always being as the most vulnerable to nitrate contamination (Fig. 8.6).

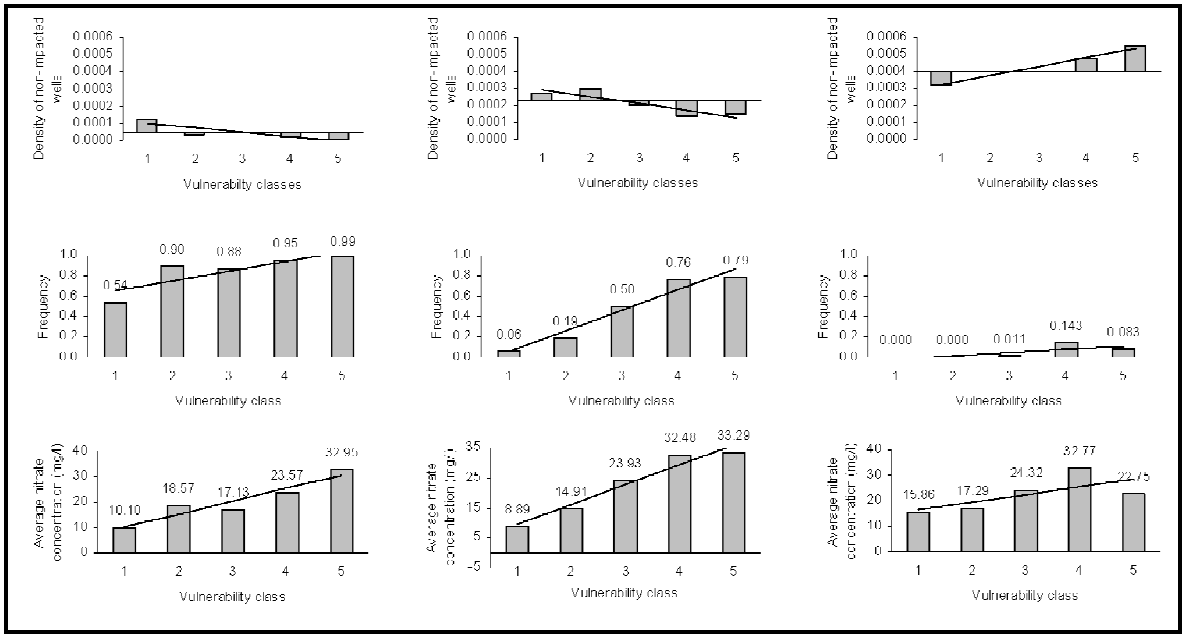

Figure 8.8 – Density of non-impacted wells within each vulnerability class (first row), frequency of impacted wells (impacted wells out of total wells) within each vulnerability classes (second row) and average nitrate concentration of samples collected in all wells located within each vulnerability class (third row); histograms in the first, second and third column refer, respectively, to reclassified vulnerability maps D-4.5, E-22 and F-50 in Figure 8.6 (in all histograms the degree of vulnerability increases from class 1 to 5).

Similarly, as for the reclassified maps obtained using the LRF method, the validation considering the density of non impacted wells (see Chapter 6, Paragraph 6.2), the average nitrate concentration (see Chapter 6, Paragraph 6.2), and the frequency of impacted wells (see Chapter 7, Paragraph 7.3) within each class, showed that the map obtained using the threshold of 22 mg/l is the more reliable (Fig. 8.8).

This finding could seem in contrast with the results form success rate curves that indicate the map F-50 as the best one (Fig. 8.9).

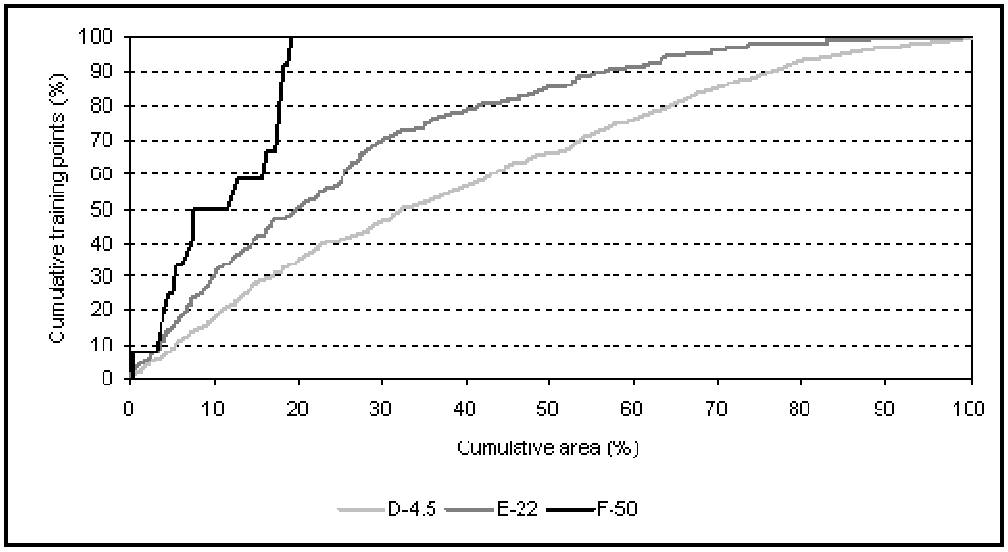

Figure 8.9 – Success rate curves of the three probability outputs (models) obtained using the WofE method and the three different threshold values identified in Paragraph 8.1.

Indeed, it must be considered that the forms of these curves are strongly influenced by the number of TPs and that it is relatively easy to obtain a very steep curve with a limited number of TPs while, in general, these curves tend to be less steep as the number of training points increase. So, due to the different number of training points used, these curves can not be considered as the only way to judge and compare the reliability of the three different models.

8.4 Conclusions

In this study, three different threshold values were used to analyze the consequences on the definition of groundwater vulnerability assessment in a shallow porous unconfined aquifer and to evaluate the importance of each explanatory variable in controlling groundwater vulnerability. Threshold values were selected both on a statistical basis and considering the regulatory limit established by the European Union concerning nitrate contamination (EU, 2000).

In both cases (LRF and WofE), concerning the predicted spatial pattern of vulnerability, the use of different thresholds did not seem to determine different vulnerability assessment if results are analyzed on a broad scale. Indeed, as confirmed by both the histograms (for all maps obtained using both methods) and the heatmaps (for the maps obtained using the LRF method), all

vulnerability maps showed the same general spatial pattern (with vulnerability decreasing southward) and trend (with vulnerability generally increasing from the lower to the higher class in both cases) regardless of the selected threshold value, even if the vulnerability maps obtained using the lower threshold value gave always the poorest performance in terms of map reliability.

Nevertheless, a more detailed analysis of the results shows that many differences can be pointed out. Looking in detail at the two clusters in the heat maps, it is easy to see that each class does not overlap with the same class in another map. Thus, the spatial distribution of a detailed vulnerability assessment is strongly influenced by the selected threshold used to identify the occurrences, suggesting that there is a strong relationship among the number of identified occurrences, the scale of the maps representing the explanatory variables and the model efficiency in discriminating different vulnerable areas.

The selection of low threshold led to have a higher number of training points, being an over-representative population due to the fact that the scale of maps representing explanatory variables is too low and not adequate to the number of TPs. In this case, the model does not adequately represent the vulnerability within the study area, probably because of the many combinations of classes of explanatory variables (critical unique conditions) found where TPs are located. The identification of many critical unique conditions makes the model inefficient in effectively discriminating which variables are actually responsible of groundwater contamination and determining groundwater vulnerability.

On the contrary, when the threshold is high, the low number of TPs seems to be sufficient to individuate the combination of classes of explanatory variables which mostly influence vulnerability allowing achieving more reliable results. However, in this case, analysis can be greatly influenced by a single or few classes of explanatory variables so that the final map tends to follow the spatial distribution of these predictor factors losing part of the potentiality of the model to work in a multivariate framework.

Chapter 9
Limits, drawbacks and future plans

To further test the robustness of the WofE modeling technique and its applicability in different hydrogeological conditions, this modeling technique was also used for assessing groundwater vulnerability to nitrate contamination of the shallow porous mixed (confined-unconfined) aquifer located within the Province of Piacenza. Such aquifer, with respect to the shallow aquifer located in the Province of Milan, is characterized by a substantial different hydrogeological setting (see Chapter 4, Paragraph 4.2) and is a constantly monitored by a lower number of wells being in this case less than 40 (see Chapter 5, paragraph 5.1). Regarding this latter aspect, it is important to note that the number of wells is significantly lower even considering the smaller extension of the aquifer located within the Province of Piacenza. It has also to be pointed out that a monitoring network constituted by relatively few wells represents probably a more common situation than the one observed in the province of Milan, where the shallow aquifer was monitored by more than 300 wells between 2000 and 2002.

Moreover the Region of Emilia Romagna started to monitor the quality of its aquifers in 1987 and thus the availability of appropriate time series allowed identifying long term trends of nitrate contamination. Thus, a semi-quantitative attempt was made to try to integrate groundwater vulnerability assessment and trend analysis in order to determine groundwater quality deterioration. Indeed, as summarized below, such integration is required by both European and Italian laws regulating groundwater quality related matter, in particular:

- Article 10 of Nitrate Directive (Directive 91/676/EEC; EU, 1991) requires that Member States identifies areas where groundwater is or will be potentially affected by nitrate contamination;
- Article 4 of the Water Framework Directive (Directive 2000/60/EC; EU, 2000 – acknowledged by the Italian Law D.Lgs. 152/2006) requires the achievement of the "good status" and the identification and reversal of significant and sustained upward trends in the concentration of contaminants, including nitrate, within a given groundwater body;
- Groundwater Directive (Directive 2006/118/EC; EU, 2006 – acknowledged by the Italian Law D.Lgs. 30/2009) has the objective of preventing and reducing nitrate contamination, implying the obligation to avoid further deterioration of groundwater quality.

Thus, it is clear that there is the necessity not only to identify vulnerable areas where nitrate concentrations are susceptible to exceed a pre-established threshold, which could be also identified with the limit of 50 mg/l representing the quality standard of groundwater nitrate concentration fixed by the 2000/60/EC Directive (EU, 2000) (see chapter 8 for an exhaustive discussion about threshold values), but also areas where nitrate contamination show upward trends.

In this Chapter this aspect was preliminary evaluated by overlapping nitrate contamination trends, identified for each well surveyed in 2008, on top of two similar groundwater vulnerability maps to nitrate contamination, referring to the same year, both obtained reclassifying the same predictive probability output obtained using the WofE modeling technique.

9.1 Training points and evidential themes

The water-quality data set collected in 2008 (described in Chapter 5, Paragraph 5.1) is the one used in this study (Table 9.1) and the median value of 20.1 mg/l was selected as threshold.

Year of survey	No. of wells	Nitrate concentration (mg/l)					Skewness
		Min	Max	Mean	Median	Std. Dev.	
2008	37	1	72.3	24.1	20.1	19.9	0.61

Table 9.1 – Basic descriptive statistics of water-quality dataset collected in 2008.

Thus, wells from which samples showed a nitrate concentration higher than or equal to the threshold value were identified as impacted wells (19) and used as TPs in the model, whereas wells from which samples showed a nitrate concentration lower than the threshold value were identified as non-impacted wells (18) and used to validate the obtained reclassified groundwater vulnerability maps (Fig. 9.1).

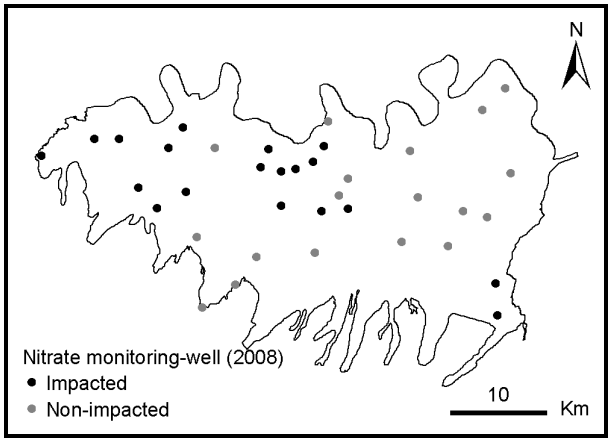

Figure 9.1 – Locations of the monitoring wells sampled in 2008: nitrate concentration in samples from impacted and non-impacted wells is, respectively, greater than or equal to and lower than 20.1 mg/l.

Considering the hydrogeological conceptual model of the study area (described in Chapter 4, Paragraph 4.2), five explanatory variables (described in Chapter 5, Paragraph 5.2), thought to control nitrate contamination of shallow groundwater, were used as evidential themes in the analysis (Table 9.2).

Explanatory variable	Type	Minimum	Maximum
Population density [persons/km^2][a]	Continuous	25	861
Nitrogen load [kg/ha per year][a]	Continuous	0	241
Confinement	Categorical	-	-
Groundwater depth [m]	Continuous	0	95
Effective infiltration [mm/year]	Continuous	302	672

[a] computed at municipality level

Table 9.2 – Explanatory variables used as evidential themes the analysis.

9.2 Trend analysis

In order to identify a trend inversion in nitrate contamination and assuming that a time series can be represented by two linear trends with a change of the slope within the considered time interval, a “two-sections” test was applied to detect the nitrate contamination trend in each wells surveyed in 2008.

In this study, the GW-Stat software (Grath et al., 2001) was used to divide the time interval under consideration (i.e., 1987-2008) into "two time sections" and estimate the corresponding regression lines in order to identify a trend inversion or a changing of the trend slope. Such method, developed by Grath et al. (2001), automatically optimize the choice of the final "two time sections" with regard to the fit of the resulting model and perform statistical test to check whether the two-sections model is significantly better than a simple linear regression.
Three examples of trend analysis graphs, obtained using the above cited software, are showed below in Figure 9.2.

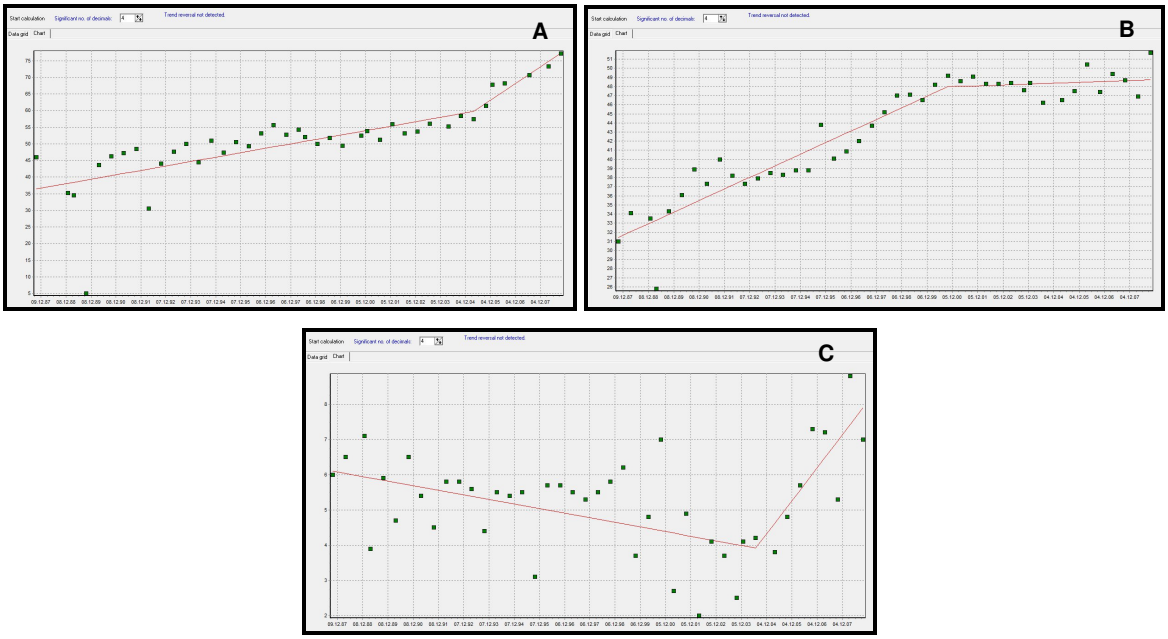

Figure 9.2 – Three examples of trend analysis graph: in the first two examples (A and B) the nitrate concentration in the monitored well is always increasing during the whole monitoring time (upward trend), but a marked changing of the slope between "two time sections" can be clearly identified in both cases (slop increasing upward and decreasing upward, respectively); in the last example (C) the nitrate concentration was initially decreasing and then increasing (downward and then upward trend), again with a different slope.

Nitrate contamination trends ware analyzed and classified as in Table 9.3 where Class 1 indicates the most dangerous situation, represented by an upward trend showing an increasing slope in the second "time section" (i.e., the nitrate concentration is increasing faster during the second span of time considered), whereas Class 10 indicates the less dangerous situation, represented by a continuous downward trend. When an inversion was detected (i.e., an upward trend turning

downward or vice versa), such as in the plot C in Figure 9.2, it was highlighted if the inversion happened more or less than five years ago, in order to distinguish between two situations indicating a different degree of hazard.

Class	Trend	Inversion
1	Slope increasing upward	
2	Upward	
3	Slope decreasing upward	
4	Downward and then upward	More than 5 years ago
5	Downward and then upward	Less than 5 years ago
6	Downward and then constant	
7	Upward and then constant	
8	Upward and then downward	Less than 5 years ago
9	Upward and then downward	More than 5 years ago
10	Downward	

Table 9.3 – Classification of the identified trend observed in the wells monitored in 2008, the most dangerous situation is the one in Class 1 while the less dangerous is the one in Class 10.

9.3 Results and discussion

The response theme, in terms of predictive probability outputs, generated using all 19 impacted wells as TPs, was reclassified to obtain two maps consisting of five and three classes of vulnerability (maps A and B in Fig. 9.3, respectively), with each class reflecting a different degree of vulnerability. Both maps were reclassified using a classification method ensuring that each class contains approximately the same number of different post probability values.

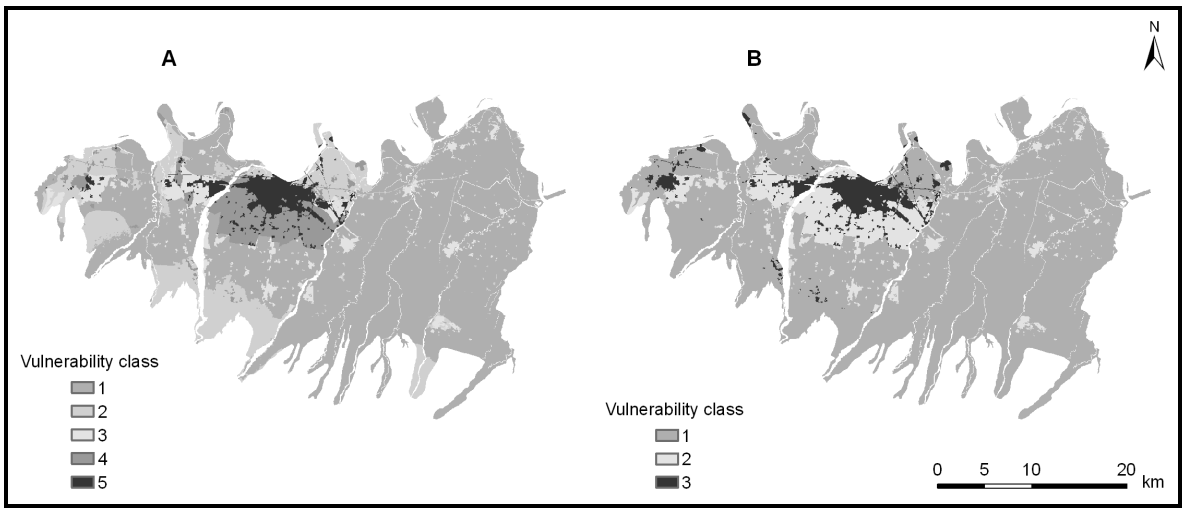

Figure 9.3 – Reclassified groundwater vulnerability maps consisting of five and three classes (A and B, respectively) obtained reclassifying the same predictive probability output (the degree of vulnerability increases from class 1 to 5 and from class 1 to 3).

9.3.1 Groundwater vulnerability maps

Although the success curve of the WofE predictive probability output (Chung and Fabbri, 1999) performed very well (Fig. 9.4), as demonstrated by the fact that more than 70% of the impacted wells fall within less than 15% of the most vulnerable area, the validation of both groundwater vulnerability maps A and B in Figure 9.3 showed poor results (Fig. 9.5) especially in terms of density of non-impacted wells (histograms A-5 and A-3 in Fig. 9.5).

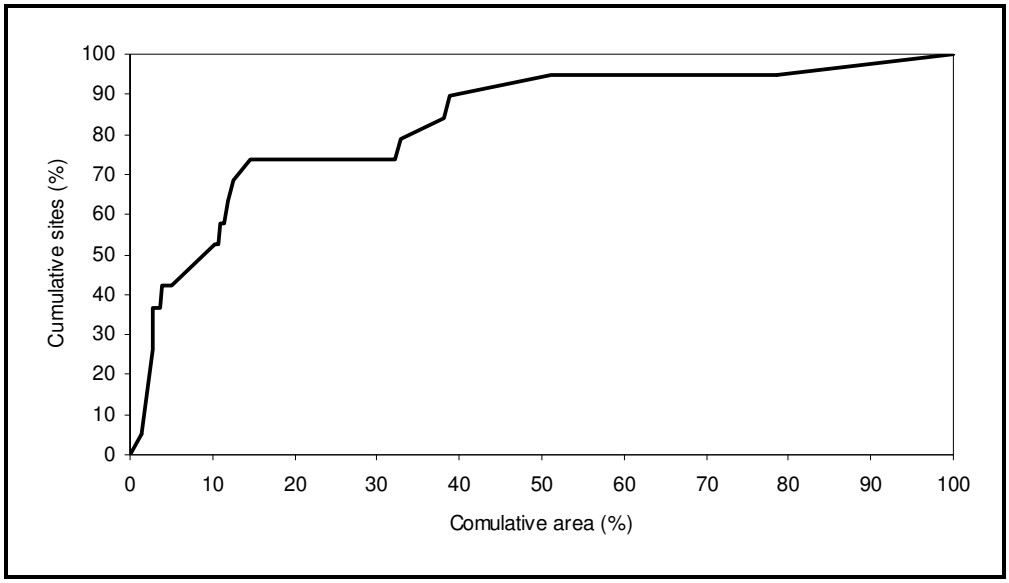

Figure 9.4 – Success curve of the WofE predictive probability output from which were obtained both reclassified groundwater vulnerability maps A and B in Figure 9.3.

Observing the validation histograms in Figure 9.5, it has to be considered that poor results could be due to the relatively low number of wells being in the monitoring network. This is partially confirmed by the fact that at least two of them results moderately improved for the map consisting of only three vulnerability classes. Indeed, histograms showing the average nitrate concentration (histograms B-5 and B-3 in Fig. 9.5) and the frequency of impacted wells in each class (histogram C-5 and C-3 in Fig. 9.5) both perform better for the vulnerability map consisting of three classes. A reduction of classes represents an increasing of the number of monitoring wells within each class. However, it has to be noted that histograms representing the density of non-impacted wells (histograms A-5 and A-3 in Fig. 9.5) performed very poorly in both cases.

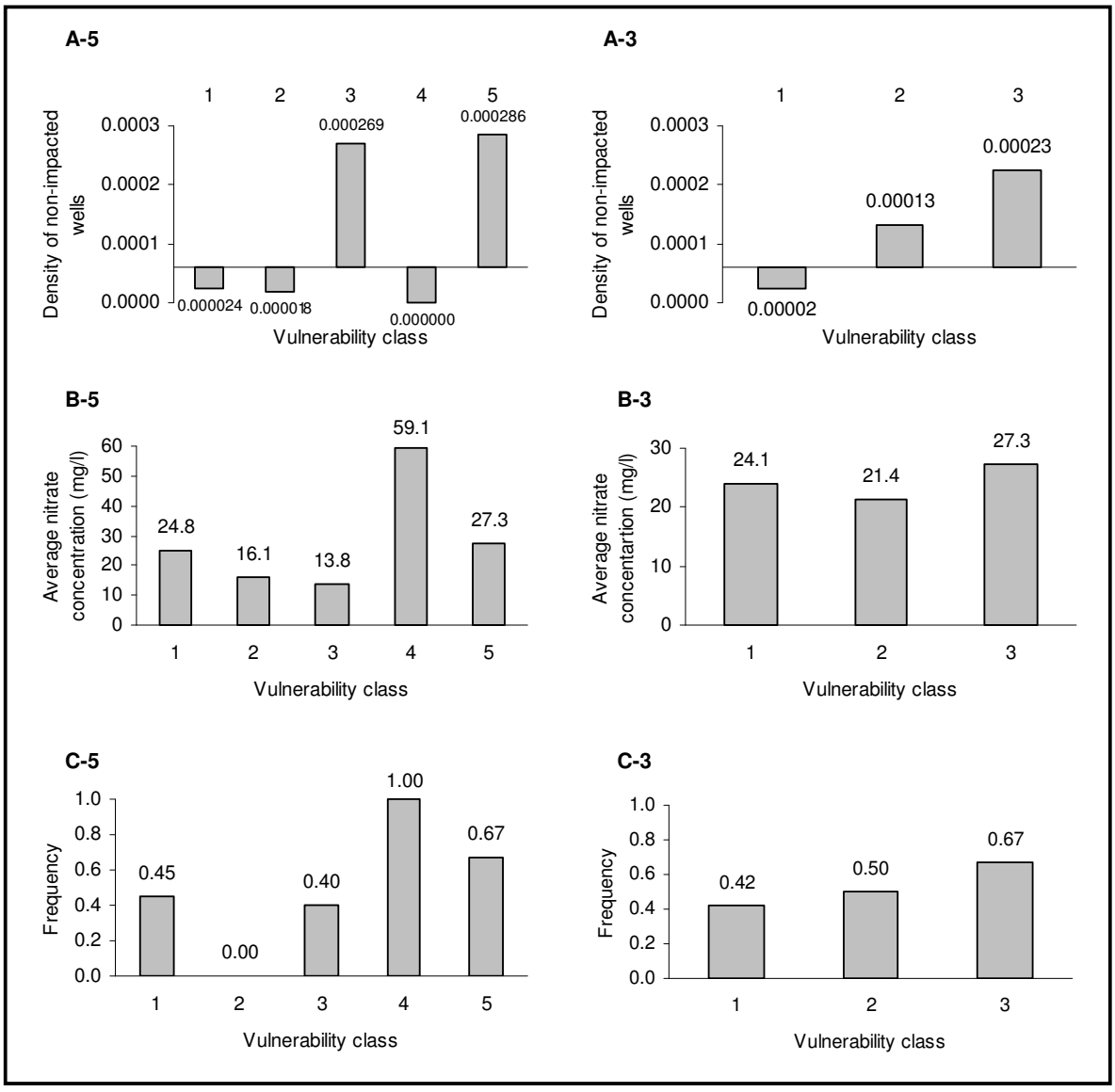

Figure 9.5 – Validation histograms for the groundwater vulnerability maps A and B in Figure 9.3 in the left and right column, respectively.

9.3.2 Groundwater vulnerability maps and trend analysis

Overlapping the nitrate contamination trend identified for each wells surveyed in 2008 to both maps A and B showed in Figure 9.3, it is possible to note that there is a discrepancy between the areas identified as less vulnerable and the location of the wells presenting the most dangerous situation in terms of nitrate contamination trend. Such situation is well observable in the south-

eastern part of the study area where four wells showing upward trends are located in an area classified as the less vulnerable. The opposite situation instead is observable in the outskirt of the city of Piacenza (north-central part of the study area) where three wells showing an upward-downward trend are located in an area classified as the most vulnerable.

Thus, it seems to be the possibility that, in general, and even when specific vulnerability maps represent well enough the present status of groundwater contamination, they could not be able to identify areas characterized by upward trend and therefore could not be a useful tool for preventing further deterioration of groundwater particularly where there is the presence of an upward trend associated with a concentration lower than the threshold chosen to select the wells to be used as TPs in the model.

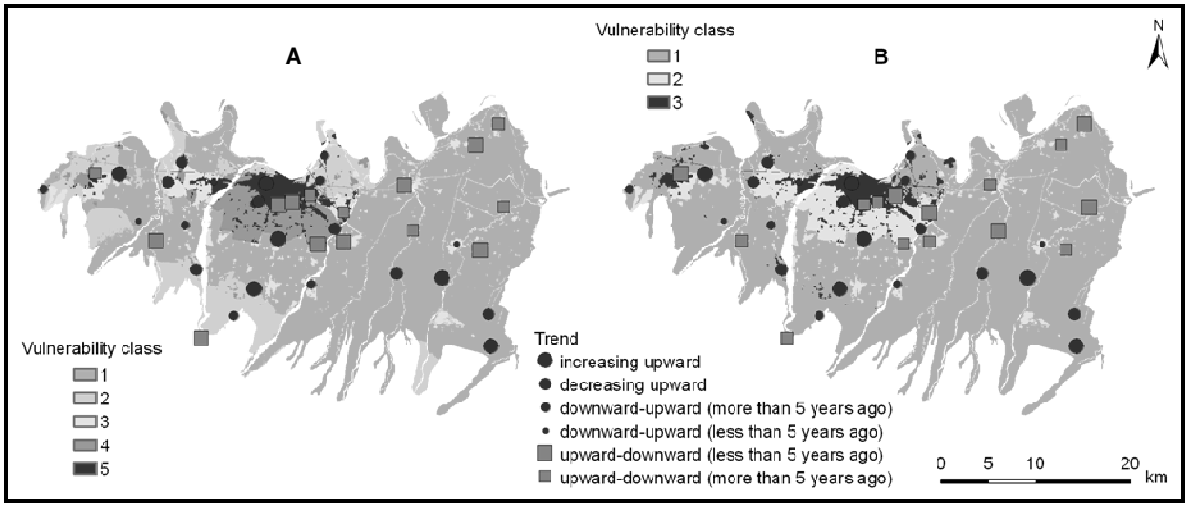

Figure 9.6 – Nitrate trends identified in the monitoring wells, and classified as in Table 9.3, overlapped to the groundwater vulnerability maps A and B in Figure 9.3 (A and B, respectively).

9.4 Conclusions and future plans

Monitoring networks constituted by few wells with respect to the extension of the study area are very common situations. In all these cases, although it would be possible to obtain a good model in terms of success and maybe of prediction rate using statistical methods, it could not be possible to further validate the reclassified groundwater vulnerability maps, especially in terms of their reliability in depicting the actual spatial distribution of the contamination. Indeed,

because of the limited number of wells falling within each obtained vulnerability class, it is not possible to consider the average of any considered parameter as a representative value of the vulnerability class they fall within (indeed, if only very few wells are within a vulnerability area, the effects on contamination due to local phenomena would be difficult to be averaged).

Another important point is that, in terms of groundwater vulnerability assessment, the identification of areas where groundwater is characterized by upward concentration trend of contaminants is nowadays required by EU and Italian laws.

To this regard, it has to be considered that even when groundwater vulnerability maps correctly represent the actual status of present groundwater contamination, most probably, they could not be able to identify areas characterized by upward contamination trend. Therefore they could not be a useful tool for preventing further deterioration of groundwater quality, especially where the contaminant concentrations are below the threshold value used in the analysis.

A possible approach has to be tested yet and that hopefully could help at least to minimize such drawback is described below.

It consists in identifying the TPs to be used in the analysis not only considering the contaminant concentration measured in the wells but also considering their detected contamination trend.

To this end, each well being part of the monitoring network, other than being classified as in Table 9.3 considering contamination trend, is also classified considering its contaminant concentration as in Table 9.4 below.

Concentration class	C (Nitrate concentration in mg/l)
1	C>50
2	45<C<50
3	40<C<45
4	35<C<40
5	30<C<35
6	25<C<30
7	20<C<25
8	15<C<20
9	10<C<15
10	10<C<5
11	C<5

Table 9.4 – Classification of the wells in the monitoring network based on their nitrate concentration measured in 2008.

Then, in order to rank each well with respect to both its concentration class (Table 9.4) and trend class (Table 9.3) the formula written below could be used (e.g., Stillwell et al., 1981):

$$W = (n - r_j + 1) / \sum_{j=1}^{n} (n - r_j + 1) \quad (9.1)$$

where n is the number of classes and r_j is the rank of the class j.

Once each well is ranked both with respect to its trend and concentration, the average rank (5th column in Table 9.5) on which identifying the TPs to be used in the analysis can be computed as the simple average of the trend rank value (2nd column in Table 9.5) plus the concentration rank value (4th column in Table 9.5).

Trend class	Trend rank	Concentration class	Concentration rank	Average rank
1	0.1818	1	0.1667	0.1742
5	0.1091	10	0.0303	0.0697
9	0.0364	9	0.0455	0.0409
3	0.1455	1	0.1667	0.1561
…	…	…	…	…

Table 9.5 – Classification of the wells in the monitoring network based on both their nitrate contamination trend up to 2008 and their nitrate concentration measured in 2008.

Of course, a different formula than the Equation 9.1 could be used to obtain a different rank, for example in the case it would be more opportune to let the trend rank of a well being more important than its concentration rank, or vice versa, depending on the final scope of the study.

In conclusion, it is important to note that the simple and semi-quantitative results and the approach presented in this Chapter are intended to highlight the urgency to integrate the “time variable” in groundwater vulnerability assessment in order to further and better support land-use planners and managements to take decisions.

Chapter 10
Conclusions

Nowadays, groundwater vulnerability maps are largely considered as an essential component for sustainable land use planning and management both in developed and especially in developing and underdeveloped countries. Groundwater vulnerability maps represent the final result of implementing a spatial model to depict the relative susceptibility of groundwater to contaminant loads applied on the land surface. Thus, characterizing the vulnerability of shallow aquifers to contamination should help decision makers to evaluate current land use practices, make recommendations, implement regulation changes and/or introduce new prescriptions, all in order to better prevent or minimize groundwater contamination and hence preserve its quality.

Since the first attempt by Margat in 1970, many different approaches and methods to produce groundwater vulnerability maps were developed. Although, it is not possible to identify a method being the best one for all situations, being the its choice a function of numerous parameters including the scale and the objective of the vulnerability assessment, the final product of the chosen method should always be scientifically defensible, meaningful and reliable, in order to be effective tools for land use planning and management (Focazio et al., 2002). Statistical methods can greatly support this activity through the production of scientifically defensible groundwater vulnerability maps which meaningfulness and reliability has however to be carefully checked before being used (Fabbri and Chung, 2008).

The Weigth of Evidence method (WofE) was used in this study for assessing groundwater vulnerability to nitrate contamination of two different shallow aquifers characterized by different hydrogeological settings and monitored by a different number of wells. The study focused on testing its robustness as exploratory and predictive tool and on addressing more general issues related to the use of statistical methods to produce groundwater vulnerability maps. The main aspects were the spatial variability of different groundwater vulnerability maps showing similar performances in term of predictive power, the influence of using different threshold in the analysis, the limits and drawbacks of using statistical methods and the possibility of new research challenges in this field.

Results showed that using positive and negative evidences of contamination as Training Points (TPs), the WofE modeling technique can be used to appropriately select the evidential themes to

be used in the analysis allowing excluding the ones characterized by a contradictious relationship with the presence of positive and negative TPs. Once evidential themes to be used were properly selected the WofE proved to be a reliable modeling technique for assessing groundwater vulnerability. Validation tests indicated excellent performance of the WofE in identifying different vulnerability classes when the final map was produced either using positive or negative evidences as TPs and also by their good spatial agreement in terms of spatial distribution of vulnerability.

Regarding the spatial variability of different groundwater vulnerability maps showing similar performances it was verified that different maps, generated using different combinations of explanatory variables, always present some degree of spatial variability in terms of spatial distribution of vulnerability. However, it was also demonstrated that using multiple statistical techniques capable of giving quantitative insight in the analysis of the results, it is possible to identify, among apparently similar maps, the one(s) that best represent the spatial distribution of the vulnerability in a given area.

Concerning the effect of using different threshold values in the analysis, results showed that the use of different thresholds produced the same general spatial pattern and trend (with respect to the identified vulnerability classes). Thus they did not seem to determine a different spatial distribution of the vulnerability if the outcomes are analyzed on a broad scale while many differences can be pointed out through a more detailed analysis. In other words, the spatial distribution of a detailed vulnerability assessment is strongly influenced by the selected threshold used to identify the TPs, suggesting that there is a strong relationship, to be further investigated, among the number of identified TPs, the scale of the maps representing the explanatory variables and the model efficiency in discriminating different vulnerable areas.

It is important to note that the use of statistical methods to produce groundwater vulnerability maps presents also limitations, especially when only very few monitoring wells are available with respect to the extension of the study area. Indeed, in these situations although it is possible to obtain good models in terms of success and maybe of prediction rate, it became difficult to further validate the reclassified groundwater vulnerability maps, especially in terms of their reliability in depicting the actual spatial distribution of the contamination.

Furthermore, considering that the identification of areas where groundwater is characterized by upward trends of contamination is required by EU and Italian laws, it has to be showed that, groundwater vulnerability maps could not be able to identify areas characterized by upward contamination trend. Therefore they could not be a useful tool for preventing further

deterioration of groundwater quality as requested by the law, especially where the contaminant concentrations are below the threshold value used in the analysis.

To this end, a new research challenges could be identified in using the available spatial statistical approaches and integrate them with the “time variable” in order to create valuable tools allowing understanding the cause-effect relationship among contaminant concentrations, contamination trends and the variations of explanatory variables controlling the contamination.

Bibliography

Acutis M., and Provolo M., 2003. Stime dei carichi diffusi di Azoto, Fosforo e Fitofarmaci da agricoltura nelle acque di superficie della Lombardia. Piano di Tutela delle Acque della Regione Lombardia, Istitutto Regionale di Ricerca della Lombardia (IreR), Allegato 7, pp. 53.

Afifi A.A., and V. Clark, 1984. Logistic Regression. In: Computer-Aided Multivariate Analysis. Lifetime Learning Publ., Belmont, CA, pp. 287-308.

Agterberg F.P., Bonham-Carter G.F., Cheng Q., and Wright D.F., 1993. Weights of evidence modeling and weighted logistic regression for mineral potential. In: Davis J.C., Herzfeld U.C. (Editors), Computers in Geology-25 Years of Progress, Oxford University Press, New York, NY, pp. 13-32.

Alberti L., De Amicis M., Masetti M., Sterlacchini S., 2001. Bayes' rule and GIS for evaluating sensitivity of groundwater to contamination. In: Proceedings of the International IAMG Conference - Cancun, Mexico.

Alberti L., Francani V., Masetti M., and Parri A., 2000. Valutazione del livello massimo raggiungibile dalla falda nel Comune di Milano. Quaderni di Geologia Applicata, vol. 7, no. 4, Pitagora Editrice, Bologna.

Albinet M., and Margat, J., 1970. Cartographie de la vulnérabilité à la pollution des nappes d'eau souterraine (Mapping of groundwater pollution vulnerability). Bull. BRGM 2ème Série, vol. 3, no. 4, pp. 13-22.

Aller L., Bennet T., Lehr J.H., and Petty R.J., 1987. DRASTIC: a standardised system for evaluating groundwater pollution potential using hydrologic settings. US EPA Report, 600/2–87/035, "Robert S. Kerr" Environmental Research Laboratory, Ada, OK.

Antonakos A.K., and Lambrakis N.J., 2007. Development and testing of three hybrid methods for the assessment of aquifer vulnerability to nitrates, based on the drastic model, an example

from NE Korinthia, Greece. Journal of Hydrology, vol. 333, pp. 288-304. doi: 10.1016/j.jhydrol.2006.08.014

Appelo C.A.J., and Postma D., 1996. Geochemistry, Groundwater and Pollution, Balkema, Rotterdam, pp. 536.

Arthur J.D., Baker A.E., Cichon J.R., Wood A.R., and Rudin A., 2005. Florida Aquifer Vulnerability Assessment (FAVA): Contamination potential of Florida's principal aquifer systems. Division of Resource Assessment and Management, Florida Geological survey, pp. 156 Available at: http://publicfiles.dep.state.fl.us/FGS/WEB/fava/fava_final_dep_report/FAVA_REPORT_MASTER_DOC_3-21-05.pdf (accessed Aug 01, 2010)

Arthur J.D., Wood H.A.R., Baker A.E., Cichon J.R., and Raines G.L., 2007. Development and Implementation of a Bayesian-based Aquifer Vulnerability Assessment in Florida. Natural Resources Research, vol. 16, no. 2, pp. 93-107. doi: 10.1007/s11053-007-9038-5

Aspinall P., and Hill A.R., 1983. Clinical inferences and decisions–I. Diagnosis and Bayes' Theorem. Ophthalmic and Physiological Optics, vol. 3, pp. 295-304. doi: 10.1111/j.1475-1313.1983.tb00616.x

Aspinall R.J., 1992. An inductive modelling procedure based on Bayes' Theorem for analysis of pattern in spatial data. International Journal of Geographic Information Systems, vol. 6, no. 2, pp. 105-121.

Avanzini M., Beretta G.P., Francani V., and Nespoli M., 1995. Indagine preliminare dell'uso sostnibile delle falde profonde nella Provincia di Milano. CAP Milano Consorzio per l'acqua potabile, pp.85.

Bayes T., 1763. An Essay towards solving a Problem in the Doctrine of Chances. By the late Rev. Mr. Bayes, communicated by Mr. Price, in a letter to John Canton, M.A and F.R.S. Philosophical Transactions of the Royal Society of London, vol. 53, pp. 340-418.

Beyer H. L., 2004. Hawth's Analysis Tools for ArcGIS. Available at: http://www.spatialecology.com/htools (accessed October 21, 2010).

Bidlack W.R., Wang W., and Clemens R., 2004. Water: The World's Most Precious Resource. Journal of Food Science, vol. 69, no. 2, pp. 55-60.

Bojorquez-Tapia L.A., Cruz-Bello G.M., Luna-Gonzalez L., Juarez L., and Ortiz-Perez M.A., 2009. V-DRASTIC: Using visualization to engage policymakers in groundwater vulnerability assessment. Journal of Hydrology, vol. 373, pp. 242-255. doi: 10.1016/j.jhydrol.2009.05.005

Bonham-Carter G.F., 1994. Tools for Map Analysis: Map Pairs. In: Merriam, D.F. (Editor), Geographic Information Systems for Geoscientists: Modelling with GIS. Pergamon Press Ltd./Elsevier Science Ltd., Kidlington, Oxfordshire, pp. 221-265.

Bonham-Carter G.F., Agterberg F.P., and Wright D.F., 1989. Weights of Evidence modeling: a new approach to mapping mineral potential. In: Agterberg F.P., Bonham-Carter G.F. (Editors), Statistical Applications in the Earth Sciences, Geological Survey of Canada, pp. 171-183.

Brenning A., 2005. Spatial prediction models for landslide hazards: review, comparison and evaluation. Natural Hazards and Earth System Sciences, vol. 5, pp. 853-862.

Brooks N., 2003. Vulnerability, risk and adaptation: a conceptual framework. Working Paper 38, Tyndall Centre for Climate Change Research, Norwich, UK.

Cacoullos T., 1973. Discriminant analysis and applications. Academic Press, New York, pp. 434.

Calabrese E.J., and Kostecki P.T., 1988. Soils contaminated by petroleum:Environmental and public health effects. John Wiley & Sons, New York, pp. 458.

Carrara A., 1983. Multivariate models for landslide hazard evaluation. Mathematical Geology, vol. 15, no. 3, pp. 403-427.

Carrara A.M., Cardinali M., Detti R., Guzzetti F., Pasqui V., and Reichenbach P., 1991. GIS techniques and statistical models in evaluating landslide hazard. Earth Surf Process Landforms vol. 16, pp. 427-445.

Carter A.D., Palmer R.C., and Monkhouse R.A., 1987. Mapping the vulnerability of groundwater to pollution from agricultural practice, particularly with respect to nitrate. In: Duijvenbooden W van, Waegeningh HG van (eds) TNO Committee on Hydrological Research, The Hague. Vulnerability of soil and groundwater to pollutants, Proceedings and Information, vol. 38, pp. 333-342.

Cheng Q., 2004. Application of Weights of Evidence Method for Assessment of Flowing Wells in the Greater Toronto Area, Canada. Natural Resources Research, vol.13, pp. 77-86.

Chowdury S., Kehew A., and Passero R., 2003, Correlation between nitrate contamination and ground water pollution potential. Ground Water, vol. 41, pp. 735-745.

Chung C.F., and Fabbri, A. G., 1999, Probabilistic prediction models for landslide hazard mapping, Photogrammetric Engineering & Remote Sensing, vol. 65, no. 12, pp. 1389-1399.

Chung C.F., 2006. Using likelihood ratio functions for modeling the conditional probability of occurrence of future landslides for risk assessment. Computer & Geosciences, vol. 32, pp. 1052-1068.

Civita M., 1987. La previsione e la prevenzione del rischio d'inquinamento delle acque sotterranee a livello regionale mediante le Carte di Vulnerabilità. In: Atti del Convegno "Inquinamento delle Acque Sotterranee: Previsione e Prevenzione", Mantova, pp.9-18.

Civita M., 1994. Le carte della vulnerabilità all'inquinamento. Teoria e pratica. Pitagora Editrice, Bologna, pp. 325.

Civita M., and De Maio M., 2004. Assessing and Mapping groundwater vulnerability to contamination: The Italian "combined" approach. Geofisica Internacional, vol. 43, n. 4, pp. 513-532.

Cohen J., 1960. A coefficient of agreement for nominal scales. Educational and Psychological Measurement, vol. 20, pp. 37-46.

Coolbaugh M.F., Raines G.L., and Zehner R.E., 2007. Assessment of Exploration Bias in Data-Driven Predictive Models and the Estimation of Undiscovered Resources. Natural Resources Research, vol. 16, pp. 199-207.

Coplen T. B., Herczeg A. L., and Barnes C., 1999. Isotope Engineering – Using stable isotopes of the water molecule to solve practical problems. In: Cook P.G., and Herczeg A.L. (Editors), Environmental tracers in subsurface hydrology, Kluwer Academic Publishers, Boston, MA, pp. 79-110.

Corsini A., Cervi F., and Ronchetti F., 2009. Weight of evidence and artificial neural networks for potential groundwater spring mapping: an application to the Mt. Modino area (Northern Apennines, Italy). Geomorphology vol. 111, pp. 79-87.

Dahal R.K., Hasegawa S., Nonomura A., Yamanaka M., Masuda T., and Nishino K., 2008. GIS-based weights-of-evidence modelling of rainfall-induced landslides in small catchments for landslide susceptibility mapping. Environment Geology, vol. 54, pp. 311-324.

Daly D., Dassargues A., Drew D., Dunne S., Goldsheider N. Neale., Popescu I.C., and Zwahlen F., 2002. Main concepts of the “Europen Approach“ to karst-groundwater-vulnerability assessment and mapping. Hydrogeology Journal, vol. 10, pp. 340-345. doi: 10.1007/s10040-001-0185-1.

Doerfliger N., and Zwahlen F., 1995. EPIK: a new method for outlining of protection areas in karst environment. In: Günay G, Johnson I (Editors), Proceedings 5th International symposium and field seminar on karst waters and environmental impacts. Antalya, Balkema, Rotterdam, pp. 117-123.

Duke C., and Steele J., 2010. Geology and lithic procurement in Upper Palaeolithic Europe: a weights-of-evidence based GIS model of lithic resource potential. Journal of Archaeological Science, vol. 37, pp. 813-824.

Eckardt D.A., and Stackelberg P.E., 1995. Relation of groundwater quality to land use on Long Island, New York. Ground Water, vol. 33: pp. 1019-1033.

Ente di Ricerca per lo Sviluppo Agricolo e Forestale (ERSAF), 2004. Strumenti ed indirizzi per la gestione multifunzionale dei suoli agricoli (SIGMA). Piano di Tutela delle Acque della Regione Lombardia, Istitutto Regionale di Ricerca della Lombardia (IreR), Allegato 10, pp.102.

Ente di Ricerca per lo Sviluppo Agricolo e Forestale (ERSAF), 2003. Carta di Uso del Suolo Agricolo e Forestale della Regione Lombardia. Destinazione d'Uso dei Suoli Agricoli e Forestali (DUSAF). http://www.cartografia.regione.lombardia.it/geoportale/ptk

Environmental Systems Research Institute (ESRI), 2007. Geometrical Interval, ArcGIS 9.2 Desktop Help. Available at: http://webhelp.esri.com/arcgisdesktop/9.2/index.cfm?topicname=geometrical_interval (accessed May 01, 2010)

European Commission (EC), Directorate-General XII Science, Research and Development, 2003. Vulnerability and Risk Mapping for the Protection of Carbonate (Karst) Aquifers, Final Report (COST Action 620). Zwahlen, F. (Editor), Brussels, Luxemburg, pp. 297.

European Union (EU), 1991. European Directive 91/676/EEC.

European Union (EU), 2000. European Directive 2000/60/EC.

European Union (EU), 2006. European Directive 2006/118/EC.

Fabbri A.G., Chung C F., Cendrero A., and Remondo J., 2003. Is Prediction of Future Landslides Possible with a GIS? Natural Hazards, vol. 30, pp. 487-499.

Fabbri G.A., and Chung C.F., 2008. On Blind Test and Spatial Prediction Models. Natural Resources Research, vol. 17, no. 2, pp. 107-118.

Ferrara V., 1990. Carta della vulnerabilità all'inquinamento dell'acquifero vulcanico dell'Etna alla scala 1:50000. S.E.L.C.A., Firenze.

Focazio M.J., Reilly T.E., Rupert M.G., and Helsel D.R., 2002. Assessing Ground-Water Vulnerability to Contamination: Providing Scientifically Defensible Information for Decision Makers. U.S. Geological Survey Circular 1224. ISBN: 0-607-89025-8

Foster S.S.D., 1987. Fundamental concepts in aquifer vulnerability, pollution risk and protection strategy. In: Duijvenbooden W. van, and Waegeningh H.G. van (Editors), Vulnerability of soil and groundwater to pollutants, Proceedings and Information, TNO Committee on Hydrological Research, The Hague, vol. 38, pp. 69-86.

Francani V. and Pozzi R., 1981.Condizioni di alimentazione delle reserve idriche del territorio Milanese. La Rivista della Strada, L 303, Milano.

Frans L.M., 2000. Estimating the probability of elevated nitrate (NO2+NO3-N) concentrations in ground water in the Columbia Basin ground water management area. USGS Water-Resources Investigations Report 4110, Washington.

Frind E.O., Molson J.W., and Rudolph D.L., 2006. Ground Water, vol. 44, no. 5, pp. 732-742. doi: 10.1111/j.1745-6584.2006.00230.x

Frind, E.O., and Martin P., 2004. 3D colour schemes for complex glacial aquifer/aquitard systems. In: Third Workshop on Three-Dimensional Geological Mapping for Groundwater Applications GAC/MAC Conference, Brock University, St. Catharines, Ontario.

Füssel H.-M., 2007. Vulnerability: A generally applicable conceptual framework for climate change research. Global Environmental Change, vol. 17, pp. 155-176.

Gardner K.K., and Vogel R.M., 2005. Predicting ground water nitrate concentration from land use. Ground Water, vol. 43 no.3, pp.1-10.

Global Water Partnership (GWP), 2000. Integrated water resources management. TEC Background Papers No. 4, Stockholm, Sweden. Available at: www.gwpforum.org/gwp/library/TACNO4.PDF (accessed August 01, 2010).

Gogu R.C., and Dassargues A., 2000. Current trends and future challenges in groundwater vulnerability assessment using overlay and index methods. Environmental Geology, vol. 39, no. 6, pp. 549-459.

Gogu R.C., Hallet V., and Dassargues A., 2003. Comparison of aquifer vulnerability assessment techniques. Application to the Ne´blon river basin (Belgium). Environmental Geology, vol. 44, no. 6, pp. 881-892. doi: 10.1007/s00254-003-0842-x

Goldscheider N., 2005. Karst groundwater vulnerability mapping: application of a new method in the Swabian Alb, Germany. Hydrogeology Journal, vol. 13, pp. 555-564. doi: 10.1007/s10040-003-0291-3

Goossens M., and Van Damme M., 1987. Vulnerability mapping in Flanders, Belgium, Proceedings at ”Vulnerability of soil and groundwater to pollutants“. In: Duijvenbooden W van, Waegeningh GH van (Editors), TNO Committee on Hydrological Research, The Hague, Proceedings and Information, vol. 38, pp. 355-360.

Grath J., Scheidleder A., Uhlig S., Weber K., Kralik M., Keimel T., and Gruber D., 2001. The EU Water Framework Directive: Statistical aspects of the identification of groundwater pollution trends, and aggregation of monitoring results. Final Report. Austrian Federal Ministry of Agriculture and Forestry, Environment and Water Management (Ref.: 41.046/01-IV1/00 and GZ 16 2500/2-I/6/00), European Commission (Grant Agreement Ref.: Subv 99/130794), in kind contributions by project partners, Vienna.

Greene E.A., LaMotte A.E., and Cullinan K.A., 2005. Ground-water vulnerability to nitrate contamination at multiple thresholds in the Mid-Atlantic Region using spatial probability models. US Geological Survey Scientific Investigations Report 2004-5118, pp. 24.

Gritzner M.L., Marcus W.A., Aspinall R., and Custer S.G., 2001. Assessing landslide potential using GIS, soil wetness modeling and topographic attributes, Payette River, Idaho. Geomorphology, vol. 37, pp. 149-165.

Hamza M.H., Added A., Rodrıguez R., Abdeljaoued S., and Ben Mammou A., 2007. A GIS-based DRASTIC vulnerability and net recharge reassessment in an aquifer of a semi-arid region (Metline-Ras Jebel-Raf Raf aquifer, Northern Tunisia). Journal of Environmental Management, vol. 84, pp. 12-19.

Harris D.P., Zurcher L., Stanley M., Marlow J., and Pan G., 2003. A comparative analysis of favorability mappings by weights of evidence, probabilistic neural networks, discriminant analysis, and logistic regression. Natural Resources Research, vol. 12, pp. 241-255.

Helsel D.R., and Hirsch R.M., 1992. Statistical Methods in Water Resources. Elsevier, New York, pp. 522.

Holtschlag, D.J., and Luukkonen C.L., 1997. Vulnerability of ground water to atrazine leaching in Kent County, Michigan. U.S. Geological Survey Water-Resources Investigations Report 96-4198, pp.49.

Hosmer D.W., and Lemeshow S., 1989. Applied Logistic Regression. John Wiley and Sons, New York, NY, pp. 307.

Istat, 2001. Popolazione residente censita al 2001 (popolazione legale) e al 1991, differenze e densità abitativa, per comune. Censimento 2001. Available at: http://dawinci.istat.it/daWinci/jsp/dwDownload.jsp?tav=home

Kellogg R.L., Wallace S., Alt K., and Goss D.W., 1997. Potential priority watersheds for protection of water quality from nonpoint sources related to agriculture: Poster Presentation at the 52nd Annual SWCS Conference, July 22-25, Toronto, Ontario, Canada.

Kshirsagar A.M., 1972. In: Multivariate analysis, Marcel Dekker (Editor), New York, pp. 534.

Kulldorff M., Feuer E.J., Miller B.A., Freedman L.S., 1997. Breast Cancer Clusters in the Northeast United States: A Geographic Analysis. American Journal of Epidemiology, vol. 146, pp. 161-170.

LaMotte A.E., and Greene E.A., 2007. Spatial analysis of land use and shallow groundwater vulnerability in the watershed adjacent to Assateague Island National Seashore, Maryland and Virginia, USA. Environmental Geology, vol. 52, pp. 1413-1421.

Lee S., Choi J., and Min K., 2002. Landslide susceptibility analysis and verification usin the Bayesian probabilty model. Environmental Geology, vol. 43, no.1-2, pp. 120-131. doi: 10.1007/s00254-002-0616-x

Lee S., Ryu J.-H., and Kim I.-S., 2007. Landslide susceptibility analysis and its verification using likelihood ratio, logistic regression, and artificial neural network models: case study of Youngin, Korea. Landslides, vol. 4, pp. 327-338.

Lee S., Ryu J.-H., Lee M.-J., and Won J.-S., 2003a. Use of an artificial neural network for analysis of the susceptibility to landslides at Boun, Korea. Environmental Geology, vol. 44, pp. 820-833.

Lee S.M., Min K.D., Woo N.C., Kim Y.J., and Ahn C.H., 2003b. Statistical models for the assessment of nitrate contamination in urban groundwater using GIS. Environmental Geology, vol. 44, pp. 210-221.

Liggett J.E., and Talwar S., 2009. Groundwater Vulnerability Assessments and Integrated Water Resource Management. Streamline Watershed Management Bulletin, vol. 13, no. 1, pp. 18-29.

Lusted L.B., 1968. Introduction to medical decision making. Thomas C.C. (Editor), Springfield, IL.

Lynen G., Zeman P., Bakuname C., Di Giulio G., Mtui P., Sanka P., and Jongejan F., 2007. Cattle ticks of the genera Rhipicephalus and Amblyomma of economic importance in Tanzania:

distribution assessed with GIS based on an extensive Weld survey. Experimental and Applied Acarology, vol. 43, pp.303-319.

Margat J., 1968. Vulnérabilité des nappes d'eau souterraine à la pollution (Vulnerability of groundwater to pollution). BRGM Publication 68 SGL 198 HYD, Orléans, France.

Martinis B., and Mazzarella S., 1971. Prima ricerca idrica profonda nella pianura lombarda. Memorie dell'Istututo Geologico e Minerario, Università di Padova, XXVIII.

Masetti M., Poli S., and Sterlacchini S., 2007. The use of the weights-of-evidence modeling technique to estimate the vulnerability of groundwater to nitrate contamination. Natural Resources Research, vol. 16, no. 2, pp. 109-119. doi: 10.1007/s11053-007-9045-6

Masetti M., Poli S., Sterlacchini S., Beretta G.P., and Facchi A., 2008. Spatial and statistical assessment of factors influencing nitrate contamination in groundwater. Journal of Environmental Management, vol. 86, pp. 272-281. doi:10.1016/j.jenvman.2006.12.023

Masetti M., Sterlacchini S., Ballabio C., Sorichetta A., and Poli S., 2009. Influence of threshold value in the use of statistical methods for groundwater vulnerability assessment. Science of the Total Environment, vol. 407, pp. 3836-3846. doi:10.1016/j.scitotenv.2009.01.055

McCammon R.B., 1989. Prospector II – the redesign of Prospector. Al Systems in Government, Washington, D.C., pp. 88-92.

Mueller D.K., Ruddy B.C., and Battaglin W.A.,1997. Logistic model of nitrate in streams of the upper-midwestern United States. Journal of Environmental Quality, vol. 26, no. 5, pp. 1223-1230.

National Research Council (NRC), 1993. Ground water vulnerability assessment: Predictive relative contamination potential under conditions of uncertainty. National Academy Press, Washington D.C., pp. 224. ISBN: 978-0-309-04799-9

Nelson E.P, Connors K.A., and C. Suarez S., 2007. GIS-Based Slope Stability Analysis, Chuquicamata Open Pit Copper Mine, Chile. Natural Resources Research, vol. 16, no.2, pp. 171-190. doi: 10.1007/s11053-007-9044-7

Neuhäuser B., and Terhorst B., 2007. Landslide susceptibility assessment using "weights of evidence" applied to a study area at the Jurassic escarpment (SW-Germany), Geomorphology, vol. 86, pp. 12-24.

Nolan B.T., 1999. Nitrate behaviour in ground waters of south-western USA. Journal Of Environmental Quality, vol. 28, pp. 1518-1527.

Nolan BT, 2001. Relating Nitrogen Sources and Aquifer Susceptibility to Nitrate in Shallow Ground Waters of the United States. Ground Water, vol. 39, pp. 290-299.

Nolan B.T., Hitt K.J., and Ruddy B.C., 2002. Probability of Nitrate Contamination of Recently Recharged Groundwaters in the Conterminous United States. Environmental Science & Technology, vol. 36, no. 10, pp. 2138-2145.

Oh H.-J., and Lee S., 2010. Assessment of ground subsidence using GIS and the Weights-of Evidence model. Engineering Geology, vol. 115, no. 1-2, pp.36-48. doi: 10.1016/j.enggeo.2010.06.015

Panno S.V., Kelly W.R., Martinsek A.T., and Hackley K.C., 2006. Estimating Background and Threshold Nitrate Concentrations Using Probability Graph. Ground Water, vol. 44, pp. 697-709.

Poli S., and Sterlacchini S., 2007. Landslide Representation Strategies in Susceptibility Studies using Weights-of-Evidence Modeling Technique. Natural Resources Research, vol. 16, no. 2, pp. 121-134. doi: 10.1007/s11053-007-9043-8

Popescu I.C., Gardin N., Brouyére S., and Dassargues A., 2008. Groundwater vulnerability assessment using physically-based modelling: From challenges to pragmatic solutions. In: Refsgaard J.C., Kovar K., Haarder E., and Nygaard E. (Editors), ModelCARE 2007 Proceedings, Calibration and Reliability in Groundwater Modelling, IAHS Publication, No. 320, Denmark.

Postel S., 1993. Water and agriculture. In: Water in crisis: A guide to the world's freshwater resources, Gleick P.H. (Editor), Oxford University Press, New York, pp. 56-66.

Press S.J., 1972. In: Applied multivariate analysis, Holt, Rinehart and Winston (Editors), NewYork, pp. 521.

Provincia di Milano and Politecnico di Milano, 1995. Le risorse idriche sotterranee nella Provincia di Milano–Vol I: Lineamenti idrogeologici. Colombo F., Di Palma F. (Editors), SIF, Milan, pp.128.

Raines G.L., 1999. Evaluation of Weights of Evidence to Predict Epithermal-Gold Deposits in the Great Basin of the Western United States. Natural Resources Research, vol.8, no. 4, pp. 257-276.

Raines G.L., and Bonham-Carter G.F., 2007. Introduction to Special Issue on Spatial Modeling in GIS. Natural Resources Research, vol. 16, no. 2, pp. 81-84. doi: 10.1007/s11053-007-9041-x

Raines G.L., and Mihalasky M.J., 2002. A Reconnaissance Method for Delineation of Tracts for Regional-Scale Mineral-Resource Assessment Based on Geologic-Map Data. Natural Resources Research, vol. 11, pp. 241-248.

Regione Emilia-Romagna, 2006. Uso del suolo 2003, Edizione 2006. Stefano Corticelli (Project Leader).

Regione Emilia-Romagna and Eni Divisione Agip, 1998. Riserve idriche sotterranee della Regione Emilia-Romagna. Di Dio G. (Project Leader), S.EL.C.A., Firenze, pp.120.

Regione Emilia-Romagna, ARPA, and Provincia di Piacenza, 2004. Progetto Aquanet – Rapporto Finale. pp.136.

Regione Emilia-Romagna, ARPA, 2009. Implementazione della Direttiva 200/60/CE – Tipizzazione/caratterizzazione, e individuazione dei corpi idrici superficiali e sotterranei, prima individuazione delle reti di monitoraggio.

Regione Emilia-Romagna, ARPA Ingegneria Ambientale, 2003. Completamento del quadro conoscitivo sui carichi puntuali e diffuse e verifica ed aggiornamento del catasto degli scarichi. Bissoli R. (Editor), pp. 116.

Regone Emilia-Romagna, ARPA Servizio Idrometereologico, 2008. Annali Idrologici – Parte prima, pp. 267.

Regione Lombardia and Eni Divisione Agip, 2002. Geologia degli Aquiferi Padani della Regione Lombardia, Relazione tecnica. Carcano C., and Piccin A. (Project Leader), S.EL.C.A., Firenze, pp.130.

Reimann C., and Garrett R.G., 2005. Geochemical background-Concept and reality. Science of the Total Environment, vol. 350, pp. 12-27.

Reimann C., Filzmoser P., and Garrett R.G., 2005. Background and threshold. Critical comparison of methods of determination. Science of the Total Environment, vol. 346, pp.1-16.

Romero-Calcerrada R., and Luque S., 2006. Habitat quality assessment using Weights-of-Evidence based GIS modelling: The case of Picoides tridactylus as species indicator of the biodiversity value of the Finnish forest. Ecological Modelling, vol. 196, pp.62-76.

Romero-Calcerrada R., Novillo C.J., Millington J.D.A., and Gomez-Jimenez I., 2008. GIS analysis of spatial patterns of human-caused wildfire ignition risk in the SW of Madrid (Central Spain). Landscape Ecology, vol. 23, no. 3, pp. 341-354. doi: 10.1007/s10980-008-9190-2

Rosen L., 1994. A study of the DRASTIC methodology with emphasis on Swedish conditions. Ground Water, vol. 32, no. 2, pp. 278-285.

Rupert M.G., 1998. Probability of detecting atrazine/desethyl-atrazine and elevated concentrations of nitrate (NO2 + NO3-N) in groundwater in the Idaho part of the Upper Snake River Basin. U.S. Geological Survey Water-Resources Investigations Report 98-4203, pp. 32.

Rupert M.G., 2001, Calibration of the DRASTIC ground water vulnerability mapping method. Ground Water, vol. 39, no. 4, pp. 625-630.

Sawatzky D.L., Raines GL.., Bonham-Carter G.F., and Looney C.G., 2008. Spatial Data Modeler (SDM): ArcMAP geoprocessing tools for spatial data modelling using weights of evidence, logistic regression, fuzzy logic and neural network. Available at: www.ige.unicamp.br/sdm/default_e.htm (accessed Aug 01, 2010).

Schwab G.O., Fangmeier D.D., Elliot W.J., Frevert, R.K., 1993. Soil and Water Conservation Engineering, John Wiley & Sons, Inc., New York, NY, pp. 396.

Shiklomanov I.A., 1993. World freshwater resources. In: Water in crisis: A guide to the world's fresh water resources (Gleick P.H., Editor). Oxford University Press, New York, vol. 67, pp. 13-24.

Shiklomanov I.A., 1997. Assessment of water resources and water availability in the world. In: Comprehensive assessment of freshwater resources of the world (UN report). St. Petersburg.

Shiklomanov I.A., 1999. World water resources. A new appraisal and assessment for the 21st century. FAO, France: United Nations Educational, Scientific and Cultural Organization.

Shouyu C., and Guangtao F., 2003. A DRASTIC based fuzzy pattern recognition methodology for groundwater vulnerability evaluation. Hydrogeological Sciences, vol. 48, pp. 211-220.

Shukla S., Mostaghimi S., Shanholt V.O., Collins M.C., and Ross B.B., 2000, A county-level assessment of ground water contamination by pesticides. Ground Water Monitoring and Review, vol. 20, no. 1, pp. 104-119.

Sinclair A.J, 1974. Selection of threshold values in geochemical data using probability graphs. Journal of Geochemical Exploration, vol. 3, pp. 129-149.

Sinclair A.J., 1991. A fundamental approach to threshold estimation in exploration geochemistry: Probability plots revisited. Journal of Geochemical Exploration, vol. 41, pp. 1-22.

Spalding R.F., and Exner M.E., 1993. Occurrence of nitrate in groundwater–A review. Journal of Environmental Quality, vol. 22, pp. 392-402.

Spiegelhalter D.J., and Knill-Jones R.P., 1984. Statistical and Knowledge-Based Approaches to Clinical Decision-Support Systems, with an Application in Gastroenterology. Journal of the Royal Statistical Society, Series A (General), vol. 147, no. 1, pp. 35-77.

Sterlacchini S., Ballabio C., Blahut J., Masetti M., and Sorichetta A., 2011. Spatial agreement of predicted patterns in landslide susceptibility maps. Geomorphology, vol. 125, no. 1, pp. 51-61. doi: 10.1016/geomorph.2010.09.004

Stigter T.Y., Ribeiro L., and Carvalho Dill A.M.M., 2006. Evaluation of an intrinsic and a specific vulnerability assessment method in comparision with groundwater salinisation and nitrate contamination levels in two agricultural regions in the south of Portugal. Hydrogeology Journal, vol. 14, pp. 79-99. doi: 10.1007/s10040-004-0396-3

Stigter TY, and Carvalho Dill A.M.M., 2001. Limitations of the application of the DRASTIC vulnerability index to areas with irrigated agriculture, Algarve, Portugal. In: Proceedings 3rd International Conference on Future Groundwater Resources at Risk, Ribeiro L. (Editor), CVRM, Lisbon, pp. 105-112.

Stillwell W.G., Seaver D.A., and Edwards W. A Comparison of Weight Approximation Techniques in Multiattribute Utility Decision Making. Organizational Behavior and Human Performance, vol. 28, pp. 62-77.

Tesoriero A., and Voss F., 1997. Predicting the probability of elevated nitrate concentrations in the Puget sound basin: implications for aquifer susceptibility and vulnerability. Ground Water, vol. 35, no. 6, pp.1029-1039.

Tesoriero A.J., Inkpen E.L., and Voss F.D., 1998. Assessing groundwater vulnerability using logistic regression. In: Proceedings of the Source Water Assessment and Protection Conference, Dallas, TX, April 28-30.

Tucker K., Rushton S.R., Sanderson R.A., Martin E.B., and Blaiklock J., 1997. Modelling bird distributions - a combined GIS and Bayesian rule-based approach. Landscape Ecology, vol. 12, no. 2, pp. 77-93.

United Nations (UN), 2010a. General Assembly Press Release (GA/10967). Department of Public Information, News and Media Division, New York, NY. Available at: http://www.un.org/News/Press/docs/2010/ga10967.doc.htm (accessed Aug 01, 2010).

United Nations (UN), 2010b. UN Resolution 64/L.63/Rev.1 (The human right to water and sanitation). General Assembly, New York, NY. Available at: http://daccess-dds-ny.un.org/doc/UNDOC/LTD/N10/464/64/PDF/N1046464.pdf?OpenElement (accessed Aug 01, 2010).

United States Environmental Protection Agency (USEPA), 1990. Citizen's Guide To Ground-water Protection (EPA 440/6-90-004). U.S. States Environmental Protection Agency Office of Water, Washington, DC pp. 28.

United States Environmental Protection Agency (USEPA), 1993. A Review of Methods for Assessing Aquifer Sensitivity and Ground Water Vulnerability to Pesticide Contamination. USEPA, Office of Water, Washington, DC, pp. 147.

United States Soil Conservation Service (USSCS), 1964. National Engineering Handbook, Section 4, Hydrology, Washington D.C., pp. 30.

Van Stempvoort D., Evert L., and Wassenaar L., 1993. Aquifer vulnerability index: a GIS compatible method for groundwater vulnerability mapping. Water Quality Research Journal of Canada, vol. 18, pp. 25-37.

van Westen C.J., Rengers N., and Soeters R., 2003. Use of geomorphological information in indirect landslide susceptibility assessment, Natural Hazards, vol. 30, pp. 399-419.

Voigt H.-J., Heinkele T., Jahnke C., and Wolter R., 2004. Characterization of groundwater vulnerability of the water framework directive of the European Union. Geofisica Internacional, vol. 43, no. 4, pp. 567-574.

Vrba J., and Zaporozec A., 1994. Guidebook on mapping groundwater vulnerability. International Association of Hydrogeologists, International Contributions to Hydrogeology, no. 16. Verlag Heinz Heise, Hannover.

Welch A.H., Westjohn D.B., Helsel D.R., and Wanty R.B., 2000. Arsenic in ground water of the United States – Occurrence and geochemistry. Ground Water, vol. 38, no. 4, pp. 589.

World Health Organization (WHO), 2004. Guidelines for Drinking-Water Quality: Recommendations. 3rd Edition, vol. 1, WHO, Geneva.

World Health Organization (WHO), 2006. Protecting Groundwater for Health – Managing the quality of Drinking-water sources. Schmoll O., Howard G., Chilton J., and Chorus I. (Editors) (WHO Drinking-water Quality Series). ISBN: 9241546689 (WHO). Available at: http://www.who.int/water_sanitation_health/publications/protecting_groundwater/en/print.html (accessed Aug 01, 2010).

Worrall F., and Besien T., 2005. The vulnerability of groundwater to pesticide contamination estimated directly from observations of presence or absence in wells. Journal of Hydrology, vol. 303, pp. 92-107. doi:10.1016/j.jhydrol.2004.08.019

Worrall F., and Kolpin D.W., 2003. Direct assessment of groundwater vulnerability from single observations of multiple contaminants. Water Resources Research, vol. 39, no.1.

Appendix I
Articles on which the Ph.D. Thesis is based

Published peer-reviewed journal articles

Sorichetta A., Masetti M., Ballabio C., Sterlacchini S., and Beretta G.P., 2011 in press. Reliability of groundwater vulnerability maps obtained through statistical methods. Journal of Environmental Management.

Sterlacchini S., Ballabio C., Blahut J., Masetti M., and Sorichetta A., 2011. Spatial agreement of predicted patterns in landslide susceptibility maps. Geomorphology, 125, 51-61, doi:10.1016/j.geomorph.2010.09.004

Masetti M., Sterlacchini S., Ballabio C., Sorichetta A., and Poli S., 2009. Influence of threshold value in the use of statistical methods for groundwater vulnerability assessment. Science of Total Environment, 407, 3836-3846, doi:10.1016/j.scitotenv.2009.01.055

Articles in review in peer-reviewed journals

Sorichetta A., Masetti M., Ballabio C., Beretta G.P., and Sterlacchini S., in review. The use of positive and negative evidences of nitrate contamination to assess shallow groundwater vulnerability in the Province of Milan, Italy. Submitted to Environmental Earth Sciences on 21 May 2010.

Appendix II
Other scientific activities performed during the Ph.D. studies

Published peer-reviewed journal articles

Taramelli A., Melelli L., Pasqui M., and Sorichetta A., accepted for publication on 18 August 2010. Modelling hurricane element at risk in potentially affected areas by GIS system. Geomatics, Natural Hazards and Risk.

Sorichetta A., Seeber L., Taramelli A., McHugh C. M. G., and Cormier M.-H., 2010. Geomorphic evidence for tilting at a continental transform: the Karamursel Basin along the North Anatolian Fault (NAF), Turkey. Geomorphology, vol. 119, pp. 221-231. doi: 10.1016/j.geomorph.2010.03.035

Santini M., Taramelli A., Sorichetta A., 2010. ASPHAA: a GIS-based algorithm to calculate cell area on a latitude-longitude (geographic) regular grid. Transactions in GIS, 14(3), 351-377, doi: 10.1111/j.1467-9671.2010.01200.x

Nghiem S.V., Balk D., Rodriguez E., Neumann G., Sorichetta A., Small C., Elvidge C.D., 2009. Observations of urban and suburban environments with global satellite scatterometer data. ISPRS Journal of Photogrammetry and Remote Sensing, 64, 367-380, doi:10.1016/j.isprsjprs.2009.01.004

Invited book chapters

Taramelli A., Pasqui M., Melelli L., Santini M., and Sorichetta A., accepted for publication on 15 June 2010. Modelling hurricane related hazards and risk through GIS for early warning System (Chapter 23). Hurricane Research, Intech publisher.

Nghiem S. V., Sorichetta A., Elvidge C. D., Small C., Balk D., Deichmann U., and Neumann G., in review. Remote Sensing of Urban Environments – The Beijing Case Study. Encyclopedia of Remote Sensing, received by Springer publisher on 5 August 2010.

Conference proceedings

Sorichetta A., Masetti M., Sterlacchini S., Blahut J., 2009. Aquifer vulnerability assessment using positive and negative evidences of contamination. Rendiconti online Società Geologica Italiana, 3[a] Riunione Annuale del Gruppo GIT (Geology and Information Technology), Offida (AP), 3-5 June 2008, vol. 8, pp.144-147.

Sorichetta A., Ballabio C., Masetti M., Sterlacchini S., 2009. Aquifer vulnerability assessment using positive and negative evidences of contamination. In: IAMG 2009 Computational Methods for the Earth, Energy and Environmental Sciences, Electronic Conference Proceedings of the International Association for Mathematical Geosciences, 23-28 August 2009, Stanford University, USA, ISBN 978-0-615-33449-3, (available at: http://iamg09.stanford.edu/Rev_Program_IAMG.pdf)

Conference partecipations

Masetti M., Sorichetta A., Beretta G. P., Bonfanti M., Chahoud A., and Marcaccio M., 2010. Integration of vulnerability assessment and trend analysis to determine groundwater quality deterioration (ORAL PRESENTATION). International Association for Mathematical Geosciences 2010 - XIVth International Congress, 29 August – 02 September, Eötvös Lóránd University, Budapest, Hungary.

Sorichetta A., Masetti M., Sterlacchini S., and Ballabio C., 2009. Assessment of spatial agreement of groundwater vulnerability maps (ORAL PRESENTATION). 4[a] Riunione Annuale del Gruppo GIT (Geology and Information Technology), June 15-17, Cagli (PU).

Sorichetta A., Sterlacchini S., Poli S., Masetti M., and Blahut J., 2008. Groundwater vulnerability assessment using the Weights of Evidence model with positive and negative evidences of contamination (POSTER PRESENTATION). European Geosciences Union, General Assembly. April 13-18, Vienna. Geophysical Research Abstract, Vol. 10, abstract # 12310.

Sterlacchini S., Blahut J., Masetti M., and Sorichetta A., 2008 methodological approach for comparing predictive maps derived from statistic-probabilistic methods (POSTER PRESENTATION). European Geosciences Union, General Assembly. April 13-18, Vienna. Geophysical Research Abstract, Vol. 10, abstract # 06333.